Investigating the MeCP2 (E1/E2) Regulatory Network in the Human Control and Rett Syndrome Brain

by

Shervin Pejhan

A Thesis submitted to the Faculty of Graduate Studies of

The University of Manitoba

in partial fulfilment of the requirements of the degree of

MASTER OF SCIENCE

Department of Biochemistry and Medical Genetics

Max Rady College of Medicine, Rady Faculty of Health Sciences

University of Manitoba

Winnipeg, Manitoba, Canada

Abstract

Rett Syndrome (RTT) is a neurodevelopmental disorder characterized by neurological regression and autism spectrum features, usually in females with mutation in *MECP2*. Animal and cell models have contributed to our knowledge about RTT and MeCP2 function. However, many findings remain unverified in the human brain.

Based on a study on the rat brain, *miR132*, a neuronal microRNA that is highly conserved among vertebrates, is suggested to inhibit MeCP2. This microRNA is induced itself by Brain Derived Neurotrophic Factor (BDNF), a neurotrophin, which is controlled by MeCP2.

In an effort to study the possible translation of this suggested regulatory network from rat to human brain, and to evaluate the hypothesized changes of this network in the brain of RTT patients, I examined post-mortem brain samples of RTT patients and compared them with their age-, and sex-matched controls.

For the first aim of my project, I evaluated the transcript and protein levels of *MECP2*/MeCP2 isoforms, *BDNF*/BDNF, and the level of *miR132* by real time RT-PCR, Western blot, and ELISA in four brain regions of three human RTT brains and their age-, post-mortem delay-, and sex-matched controls.

The transcript level of the studied elements was significantly different in RTT patients; even though the change was not identical in all studied parts of the brain. The protein level of the studied elements did not follow the same pattern as the transcripts.

For the second aim of my project, I performed immunohistochemistry studies on three brain regions of four RTT patients and their age-, and sex-matched controls. My results showed significantly reduced immunoreactivity for MeCP2 protein, exclusively in

the glial cells of the white matter, but surprisingly, neurons did not show a noticeable decrease in MeCP2 staining. Immunolabeling of brain samples for BDNF revealed a dominant astroglial/endothelial pattern without noticeable difference between RTT and control tissues.

Furthermore, for the first time, the effect of post-mortem delay in fixation on MeCP2 and BDNF immunolabeling of human brain samples was studied in this project. MeCP2 protein appeared to be more sensitive to post-mortem delay than BDNF.

Despite challenges in evaluating autopsy samples, this project provides insight on RTT pathobiology, while highlighting the importance of studying human RTT brain in parallel with rapidly growing research on animal and cell models of the disease.

Acknowledgements

This work would not have been possible without the guidance and support of a fantastic team. First, I would like to thank my supervisor, Dr. Mojgan Rastegar for providing me the opportunity, guidance, and support throughout this project. Her patience, careful supervision, and persistence taught me a lot and will not be forgotten.

I would like to express the deepest appreciation to my advisory committee members, Dr. Marc Del Bigio, and Dr. Jeffry Wigle for their support, encouragement, and insightful advice for improving my project.

I am particularly thankful to Dr. Marc Del Bigio, who provided the opportunity for me to practice immunostaining in his lab and under his guidance. I would also like to thank Dr. Jessica Jarmasz, and Dr. Xiaoyan Mao, for their assistance while I was doing immunolabeling experiments.

I am grateful to Carl Olson, Dr. Rastegar's lab senior technician, for all I learned from him since my first steps in the lab. His patience and professional assistance will be always inspiring to me.

I am grateful to all of those whom I had the pleasure to work with during this project. Thanks to Shayan, Marjorie, Sandhini, Annan, David, previous labmates, and all the energetic summer students for their friendship and their inspirational assistance.

I am also using this opportunity to express my gratitude to the Regenerative Medicine family at the University of Manitoba who made this period more pleasant and productive for me.

I would like to acknowledge the funding agencies that supported my research activities and MSc project studies. The research that is reported in this thesis is supported by International Rett Syndrome Foundation (IRSF) Grant # 3212, Ontario Rett Syndrome Association (ORSA), and NSERC Discovery Grant 2016-06035 (conservation of

MeCP2E1-E2 network from mice to humans), and Graduate Enhancement of Tri-Council Stipends (GETS) from the University of Manitoba.

I would like to thank Dr. Victoria Siu and Dr. Lee Cyn Ang, Western University, for arrangement of the brain donation to Dr. Rastegar's lab for the T158M and A201V samples, and my supervisor, Dr. Mojgan Rastegar for arrangement of brain tissue donation for the P152H through direct consent of the patient's mother. I would like to acknowledge the NIH NeuroBioBank Program (neurobiobank.nih.gov) for frozen and fixed brain tissues of NIH case numbers: 4516, 5401, 5646, and 5287. For these NIH control and RTT samples, "human tissue was obtained from the University of Maryland Brain and Tissue Bank, which is a Brain and Tissue Repository of the NIH Biobank".

Finally, yet importantly, this project would not have been started without the support of family members who generously donated brain tissue of their loved ones for research in order to ease the pain of other patients.

Dedicated to my beloved family

my husband Ali, my parents Mehri and Ali, my siblings Shabnam and Khashayar

for their sacrifices and endless support.

Table of Contents

List of Figures

List of Tables

Abbreviations

AAV	Adeno-Associated Virus
BBB	Blood Brain Barrier
BDNF	Brain-Derived Neurotrophic Factor (protein)
BDNF	Brain-Derived Neurotrophic Factor (human gene)
Bdnf	Brain-Derived Neurotrophic Factor (non-human gene)
BiPAP	Bilevel Positive Airway Pressure
BSA	Bovine Serum Albumin
CRE	cAMP/Ca^{2+}-Response Element
CREB	cAMP Response Element-Binding Protein
CSF	Cerebrospinal Fluid
CTD	C-Terminal Domain
DAB	3, 3′-Diaminobenzidine
DAG	Diacylglycerol
DNMT	DNA Methyl Transferase
dNTP	deoxyribonucleotide Triphosphate
EDTA	Ethylenediaminetetraacetic Acid
ELISA	Enzyme-Linked Immunosorbent Assay
ERK	Extracellular signal-Regulated Kinase
GAPDH	Glyceraldehyde 3-Phosphate Dehydrogenase (protein)
GAPDH	Glyceraldehyde 3-Phosphate Dehydrogenase (human gene)
GFAP	Glial Fibrillary Acidic Protein
HDAC	Histone Deacetylase
HLA	Human Leukocyte Antigen
ID	Intervening Domain
IGF-1	Insulin-Like Growth Factor-1
IHC	Immunohistochemistry
iPSC	induced Pluripotent Stem Cell
LTP	Long-term Potentiation

MAPK	Mitogen-Activated Protein Kinase
mBDNF	mature Brain-Derived Neurotrophic Factor (protein)
MBP	Methyl Binding Protein
MDS	MECP2 Duplication Syndrome
MeCP2	Methyl CpG Binding Protein 2 (protein)
MECP2	Methyl CpG Binding Protein 2 (human gene)
Mecp2	Methyl CpG Binding Protein 2 (mouse gene)
miR132	microRNA132
MMP-7	Matrix Metalloprotease-7
MRE	MiRNA Resapons Elements
mTOR	mammalian Target of Rapamycin
ncRNAs	non-coding RNAs
NGF	Nerve Growth Factor
NIH	National Institute of Health (United States)
ND	N-Terminal Domain
NT	Neurotrophin
PBS	Phosphate-Buffered Saline
piRNAs	Piwi-interacting RNAs
PI3K	Phosphatidylinositol 3-Kinase
PKC	Protein Kinase C
PLCγ	Phospholipase Cγ
PMD	Post-Mortem Delay
PTM	Post-Translational Modifications
qRT-PCR	quantitative Reverse Transcription Polymerase Chain Reaction
RTT	Rett Syndrome
siRNA	small interfering RNA
SK-1	Subtilisin/Kexin-isoenzyme-1
SUDI	Sudden Unexpected Death in Infant
TET	Ten-Eleven Translocation
TRD	Transcription Repression Domain
Trk	Tropomyosin related kinase
WB	Western Blot

XCI	X-Chromosome Inactivation
5-mC	5-methylcytosine
5-hmC	5-hydroxymethylcytosine

1. Literature review

1.1 Rett Syndrome

1.1.1 History of Rett Syndrome (RTT)

It was in 1954 that Dr. Andreas Rett, a pediatrician from Austria noticed similar winding hand motions in two young girls waiting for a visit in his clinic. The clinical and developmental histories of these two patients were also similar. With further investigations, Dr. Rett found 6 other girls with the same disorder in his own practice, and 22 patients in his travels throughout Europe. Twelve years after that eye-catching coincidence in the waiting room of his clinic, Dr. Rett reported the clinical entity in the German medical literature [1]. Seventeen years later, Dr. Bengt Hagberg, a Swedish neurologist and his colleagues, attributed Rett's name to this syndrome, mainly overlooked because of the language of first report. The medical community recognized Rett syndrome (RTT) through an English report of 35 RTT cases from Dr. Hagberg in1983 [2].

In 1992, a protein called Methyl-CpG binding protein 2 (MeCP2) was identified by Dr. Adrian Bird's group [3]. Seven years later, this protein was discovered to be the underlying cause of RTT pathophysiology by Dr. Huda Zoghbi's team. They showed that mutations in *MECP2* gene are causative for the majority (over 90%) of RTT cases [4]. Soon after finding the genetic cause of RTT, in 2001, the first animal model of RTT became available [5], and since then several groups have worked to elucidate the pathophysiology of the disease, and running trials for therapeutic purposes [6].

1.1.2 Clinical features and diagnosis

Rett syndrome is a neurological disorder mainly affecting girls with a prevalence of 1 in 10,000 live female births [7]. While the neurodevelopmental process in RTT patients is apparently normal until 6-18 months of age, subtle symptoms such as muscle hypotonia, as well as deceleration of head growth are usually present earlier in their life but mostly ignored. Delay, stagnation, or regression in motor development is the most frequent complaint that brings patients to medical attention. General growth retardation, weight loss, and a weak posture caused by muscle hypotonia are other common findings at this stage [8, 9].

As RTT progresses, stereotypic hand wringing or washing movements replace purposeful use of hands. Abnormal gait with lack of coordinated movements of upper extremities in addition to social withdrawal and loss of verbal communications are other common findings in RTT patients. The autistic features such as poor response to environmental stimulations become less prominent and are replaced by signs of mental retardation as the child grows up [7]. RTT patients also suffer from autonomic perturbations including breathing abnormalities (e.g. breath holding, periods of hyperventilation, and apnea) [10], cardiac arrhythmias (prolonged QT syndrome) [11], and gastrointestinal dysfunction [12].

Seizures, ranging from easily controlled to intractable epilepsy are common in RTT (seen in more than 80% of cases in one study) [13]. Age of onset of seizures depends on the type of *MECP2* gene mutation, and its severity tends to decrease after teenage years and into adulthood [13].

Ataxia (gross lack of coordination in muscle movements), and gait apraxia (inability to perform learned movements) accompany mental detriment. Devastating motor dysfunction makes RTT patients wheelchair-bound during the teenage years, and as they enter adulthood, Parkinson-like features could be added to the clinical manifestations. The skeletal deformities such as scoliosis and osteopenia in RTT patients are partly caused by locomotor difficulties and sedentary state. Decreased muscle tone can be also responsible in this process [12].

Despite poor physical condition, RTT patients typically survive into adulthood (70% up to 45 years), and even up to 70 years of age. Cardio-respiratory compromise is the leading cause of death in RTT [14].

The diagnostic criteria for classic or typical RTT, revised in 2010, are shown in Table 1.1. Patients with some of RTT symptoms that do not fulfill the criteria mentioned in Table 1.1, might be categorized in the group of atypical or variant RTT. Preserved speech variant, early seizure variant, and congenital variant are three main atypical forms of RTT [7, 15]. These forms are defined in Figure 1.1.

Rett Syndrome is predominantly a female disorder. However, it can be seen in three groups of male patients. Patients in the first group have a mutation that causes typical RTT Syndrome in females. However, these boys have severe neonatal encephalopathy and a lifespan of less than one year. The diluting effect of X chromosome aneuploidy (Klinefelter syndrome) or somatic mosaicism can lead to a milder phenotype, similar to atypical RTT. The second group present mutations that are different from typical mutations in female patients, but are compatible with life into adulthood. The last group show mutations in genes other than *MECP2* such as *CDKL5* or *FOXG1* and are associated with RTT-like symptoms in males [16].

Table 1.1 Revised diagnostic criteria for RTT. Taken from Percy et al. [15]. By permission of John Wiley and Sons, Licence Number 4441360827758.

RTT Diagnostic Criteria 2010
Consider diagnosis when postnatal deceleration of head growth observed.
Required for typical or classic RTT
1. A period of regression followed by recovery or stabilization
2. 2 out of 4 main criteria
3. 5 out of 11 supportive criteria
Main Criteria
1. Partial or complete loss of acquired purposeful hand skills
2. Partial or complete loss of acquired spoken language
3. Gait abnormalities: Impaired (dyspraxic) or absence of ability
4. Stereotypic hand movements such as hand wringing/squeezing, clapping/tapping, mouthing and washing/rubbing automatisms
Exclusion Criteria for typical RTT
1. Brain injury secondary to trauma (peri- or postnatally), neurometabolic disease, or severe infection that causes neurological problems
2. Grossly abnormal psychomotor development in first 6 months of life
Supportive Criteria for atypical RTT
1. Breathing disturbances when awake
2. Bruxism when awake
3. Impaired sleep pattern
4. Abnormal muscle tone
5. Peripheral vasomotor disturbances
6. Scoliosis/kyphosis
7. Growth retardation
8. Small cold hands and feet
9. Inappropriate laughing/screaming spells
10. Diminished response to pain
11. Intense eye communication - “eye pointing”

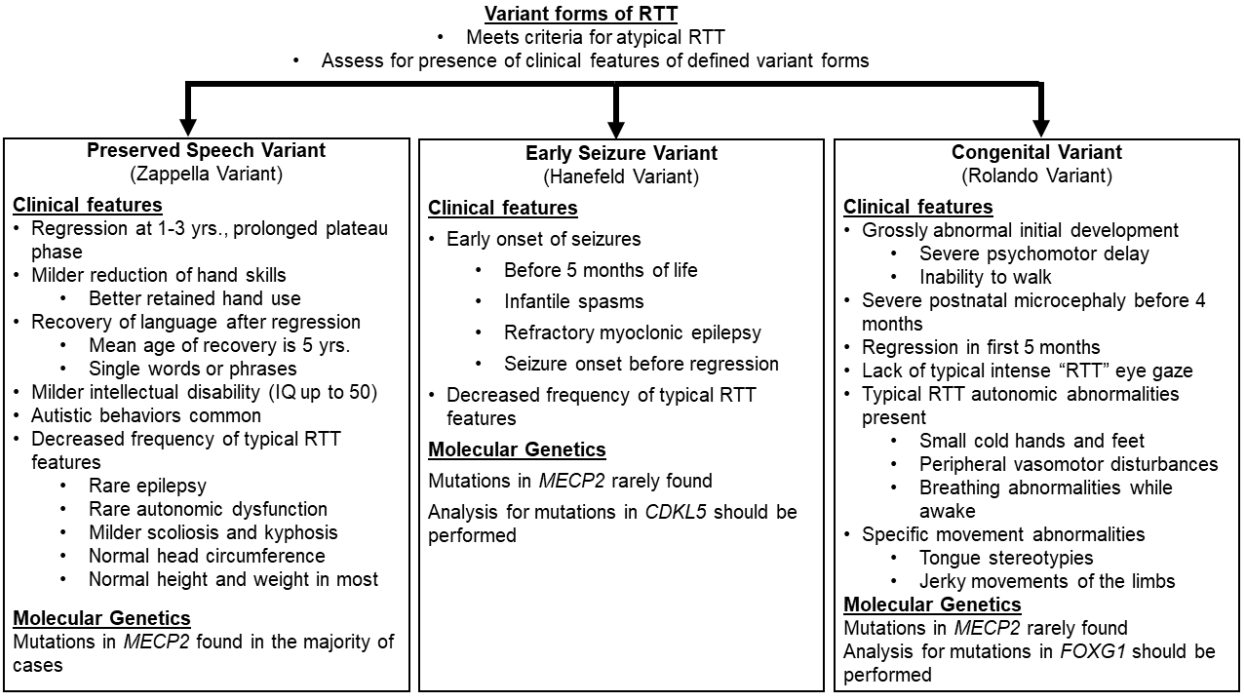

Figure 1.1 Main atypical forms of RTT. Taken from Neul et al. [7]. By permission of John Wiley and Sons, Licence Number 4441360951360.

1.1.3 Genetic basis of RTT

Mutations in *MECP2* gene located in Xq28 are the underlying cause of over 95% of typical and 75% of atypical cases of RTT [17]. The vast majority of these mutations happen *de novo* [18] mostly in the germline of the father [19]. This partially explains the female predominance for RTT. There are also rare familial cases of RTT that may happen due to skewing of X-chromosome inactivation (XCI) in the mother who can pass the mutation on to her male and female offspring as an asymptomatic carrier [20]. Having one copy of X-chromosome, most male patients present severe symptoms including infantile encephalopathy and die within 2 years of birth [20].

From more than 4600 identified variants in the *MECP2* gene, over 70% have association with RTT. However, the causative role of *MECP2* mutation has not been shown for all of them. Eight of these mutations account for about 47% of all mutations. These mutations in order of frequency are: T158M, R168X, R255X, R270X, R306C,

R294X, R133C, and R106W (Figure 1.2). As explained before, mutations in two other genes *FOXG1* and *CDKL5* can cause atypical forms of RTT syndrome birth [21].

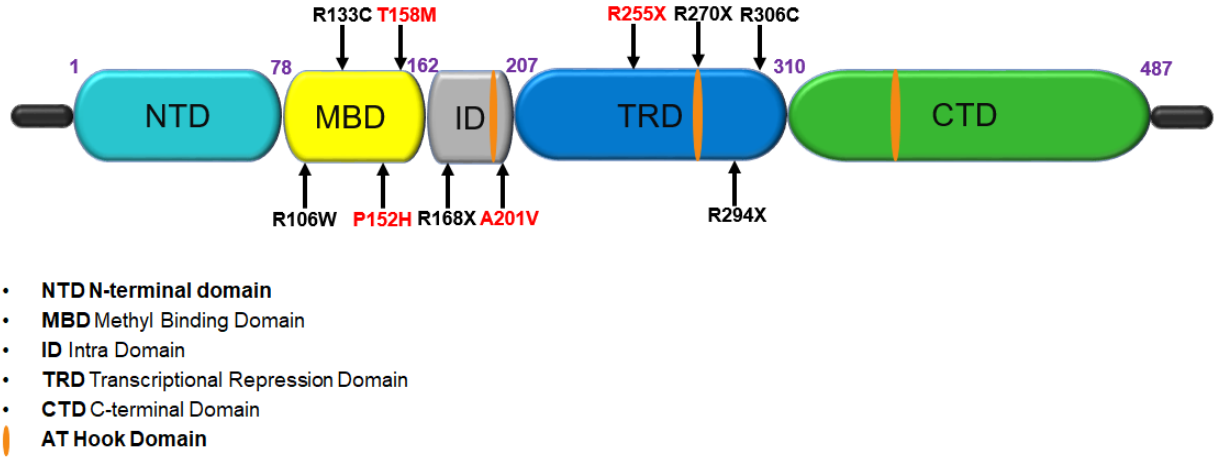

Figure 1.2 RTT- associated *MECP2* mutations affecting different regions of protein. Most common mutations are shown in black. Red arrows show the mutations in the RTT brain we examined in our study. Amino acid number at the beginning and the end of each domain are shown in purple.

1.1.4 Phenotypic variations in RTT

While dividing RTT into classical and atypical forms has decreased the differences within each category, there is still phenotypic variation in each group and even in one patient over time. X-chromosome inactivation is suggested as one of the main contributors of phenotypic variability [22]. Although the majority of classic cases of RTT have balanced XCI pattern in the brain tissue [23], non-random XCI or skewed pattern, has been reported in several cases [24]. Somatic mosaicism is another potential source of phenotypic variability [25]. Finally, specific types of *MECP2* mutation can also affect protein functions differently and lead to different severity of phenotypes. For instance, severe RTT caused by T158M mutation (affecting methyl binding domain of MeCP2) can be due to deficient binding to methylated DNA, and aberrant transcriptional control as a result [26, 27], whereas C-terminal deletions are associated with milder phenotypes [28].

1.1.5 Histopathology of RTT

1.1.5.1 Gross and microscopic features

Microcephaly is the main finding in gross pathology of RTT. Head circumference is normal at birth, and its growth begins to decelerate after 2-3 months. The reduction in the brain weight is not generalized, and cerebral hemispheres are relatively smaller than the cerebellum when compared to non-RTT conditions [29]. Prefrontal, posterior frontal, and anterior temporal regions show smaller volume in neuroimaging while posterior temporal and posterior occipital regions are relatively preserved [30, 31].

In general, microscopic evaluations of RTT brains have not recognized degeneration, demyelinating, or gross malformative processes. Reduction in gross brain volume is associated with abnormally small, densely packed neurons with reduced dendritic complexity and synaptic density in studies of the cerebral cortex [32]. Reduced melanin and tyrosine hydroxylase staining in the midbrain and substantia nigra, and altered contour and appendages in neurons of the globus pallidus are examples of findings in other regions of the brain in RTT Syndrome [33, 34]. Vagal tone abnormalities that have been found in functional studies of the vagus nerve are in line with the autonomic impairments in RTT. Abnormalities in serotonin receptors and substance P content have also been reported in brain stem studies [29]. Substance P is a neuropeptide acting as a neurotransmitter and neuromodulator. It is best known for its role in transmission of pain stimuli in the peripheral nervous system, but it participates in behavioural responses as well as neuronal survival in the central nervous system [35]. The altered sensitivity of RTT patients to pain can be related to the abnormality in substance P. There are also studies that suggest a role for MeCP2 in pain perception [36-38].

1.1.5.2 Immunohistochimistry (IHC) studies

The earliest MeCP2 expression in the normal human brain was reported in the cerebral sub-ventricular zone of the brain stem and the subcortical and Cajal-Retzius neurons of the cerebral cortex at 10 gestational weeks. MeCP2 will appear next in the

thalamus, midbrain, and basal ganglia. The hippocampus and cerebellum show less expression early in development. However, with maturation, most of neurons in these regions express MeCP2. That might explain the delay in the clinical manifestation of RTT in the course of development [23].

MeCP2 shows a mainly nuclear localization. However, slight cytoplasmic labeling of some neurons has also been recognized. Post-translationally modified protein has been suggested to be the source of this cytoplasmic fraction. Since the earliest IHC studies, the variable intensity of staining within the same type of neurons has made the interpretation of IHC studies for MeCP2 challenging [29]. Laser scanning cytometry has also confirmed the presence of cells with either low or high MeCP2 expression [39]. Difference in neuronal activity has been suggested as one of the reasons behind this variable labeling. However, the possibility of post-mortem degradation of protein has not been excluded [23, 29].

Regarding other protein labelling, some increase in glial fibrillary acidic protein (GFAP) has been reported in RTT brains. However, it is not clear whether this is a primary phenomenon or secondary to the main RTT pathology [29].

1.1.6 Biological systems to study RTT

The monogenic character of RTT, mainly caused by mutations in *MECP2* gene [4], has prompted several RTT animal [5, 40, 41], and cellular [42-44] models for the disease. Based on their genetic modifications, models can be categorized to: 1) *Mecp2*-deficient models such as *Mecp2* constitutive knockout mice [5, 41], or brain region/cell type-specific deletion of *Mecp2* [45, 46], and 2) *Mecp2* mutant models such as knock-in mouse models with specific *Mecp2* mutations [47, 48].

These animal models show different phenotypes and have different lifespans [49], and we need to be aware of some potential caveats in the interpretation of animal studies. First, while *Mecp2*-heterozygous female mice are more direct representative of RTT condition, male *Mecp2*-null mice are easier to work with and are more frequently used.

Second, mice present detectable symptoms of MeCP2-deficiency much later in the course of development as compared to humans [50].

Regarding the cell models of RTT, source of MeCP2-mutant cell lines can be neurons from human induced pluripotent stem cells (iPSCs), or human embryonic stem cells (patient-derived or produced by using transcription activator-like effector nucleases or TALENs to delete *MECP2*). Cell models can also originate from mouse embryonic stem cells. Examples of RTT mice models and cell lines with their phenotypes have been summarized in Table **1.2** taken from Lyst and Bird (2015) [50].

Table 1.2 Mouse and cell models of Rett syndrome and their phenotypes. Taken from Lyst and Bird (2015) [50]. By permission of Springer Nature, License Number 4441370487818. ESC: embryonic stem cell, GABA: γ-aminobutyric acid, iPSC: induced pluripotent stem cell, MeCP2: methyl-CpG-binding protein 2, POMC: pro-opiomelanocortin, TALEN: transcription activator-like effector nuclease.

MeCP2 status	Phenotype	References
Mouse models		
Deletion from SIM1-expressing neurons in the hypothalamus	Heightened stress response, increased aggressive behaviour, hyperphagia and obesity	[51]
Deletion from the POMC neurons in the arcuate nucleus of the hypothalamus	Over-eating and obesity	[52]
Removal from dopaminergic and noradrenergic neurons	Motor abnormalities	[53]
Removal from serotonergic neurons	Aggressive behaviour	[53]
Removal from forebrain GABAergic neurons	Seizures	[54, 55]
Deletion in the brainstem and spinal cord	Abnormal breathing responses and early lethality	[56]
Viral-mediated deletion in the basolateral amygdala	Defects in cue-dependent fear conditioning	[57]
Removal from GABA-releasing neurons	Repetitive behaviours, progressive motor dysfunction, breathing defects and early lethality	[58]
Deletion in postnatal forebrain neurons	Similar to MeCP2-null animals but milder and delayed	[41, 59]
Cell lines		
Neurons from human iPSCs, and human ESCs (patient-derived or using TALENs to delete MeCP2)	Reduced nuclear size, transcription and translation; impaired mitochondrial function, fewer synapses and reduced spine density	[42, 43]
Neurons from mouse ESCs	Reduced nuclear size and transcription	[44]

1.1.7 Therapeutic strategies for RTT

The monogenic character of RTT and the reversibility of its symptoms in preclinical models have brought optimism to the field of therapeutic research for this devastating disease. Availability of rodent models showing quantifiable symptoms such as abnormal breathing makes evaluations of therapies more translatable when compared to the behavioral disorders of more common conditions such as non-symptomatic autism [60].

Our knowledge about the biology of MeCP2 and the consequences of its loss on the function of neuronal circuit and behavior is the basis of potential therapeutic strategies. These strategies include: 1) molecular approaches ranging from gene and protein replacement therapy to reactivating the wild-type allele on the inactive X chromosome, 2) pharmacologic approaches, which target MeCP2 downstream target genes/mechanisms to restore their role in neuronal circuits [61].

1.1.7.1 Molecular treatments and gene dosage concerns

An excess of MeCP2, a condition similar to what happens in boys with *MECP2* Duplication Syndrome (MDS), leads to RTT-like neurological dysfunction presenting with seizure and hypoactivity [62, 63]. Therefore, any molecular therapy that targets *MECP2* directly to normalize the protein, must keep the level of protein within its narrow acceptable limits by avoiding *MECP2* overdosage [60].

1.1.7.2 Activating *MECP2* on the inactive X chromosome

This novel method has been already studied in another neurodevelopmental disorder (Angelman syndrome), and the *Mecp2-GFP* fluorescent reporter mouse is a useful tool for high throughput, small molecule screening. Other than the cost and stability concerns for this procedure, availability of active and safe compounds that diffuse across the blood- brain barrier (BBB) is another limitation in restoring MeCP2 levels across the relevant cell types. Furthermore, targeting *MECP2* specifically or the entire inactive X is another concern in this method [60, 64, 65].

1.1.7.3 Gene editing strategies

The first attempt to study a gene therapy for Rett Syndrome, was reported by Dr. Mojgan Rastegar et al. (2009). They showed that *Mecp2* promoter vectors could be effective for gene therapy by recapitulating the endogenous expression of MeCP2 in neurons and glia [66]. Editing or replacement of an abnormal gene has become available through adeno-associated virus (AAV) vector designs such as AAV9. Intravenous delivery of an AAV9/*Mecp2* vector has partially normalized phenotypes of male and female RTT mice [60, 67]. Delivering *Mecp2* expression homogenously and within the narrow normal range is one of the main challenges for gene therapy [60].

About 35% of RTT patients with in-frame premature stop codons might benefit from compounds that allow the read through of the nonsense mutations [68]. It has been shown to be effective in cultured R168X (most common RTT causing truncated mutation) mouse fibroblasts [69, 70].

1.1.7.4 Challenges of protein replacement

Homogenous and continuous delivery of appropriate level of MeCP2 across the BBB is the major challenge for protein replacement. Ensuring the adequate penetration of protein at cellular and sub-cellular level up to the nucleus, and making sure that post-translational modifications are happening in a regular manner are other obstacles to overcome in this method [60].

1.1.7.5 Targeting downstream signalling pathways of MeCP2

Classical neurotransmitter and neuromodulator signaling, growth factor signaling including Brain Derived Neurotrophic Factor (BDNF) or Insulin-like growth factor 1 (IGF-1), and metabolic signaling including cholesterol biosynthesis and mitochondrial function are main targeted pathways [71, 72].

A drug prepared for one pathway might not treat the full spectrum of RTT symptoms. However, ameliorating one main symptom such as breathing abnormality may have a considerable impact on the quality of life for RTT patients [60].

1.1.7.6 Clinical trials

There are several challenges in a clinical trial for a rare disease like RTT. A vast number of RTT- associated mutations and a limited pool of participants are two of the obstacles. From several ongoing or completed trials listed in Figure 1.3, only rare ones are parallel, randomized, double blind, and placebo-controlled, and none has reached to the level to be used in practice [6, 60].

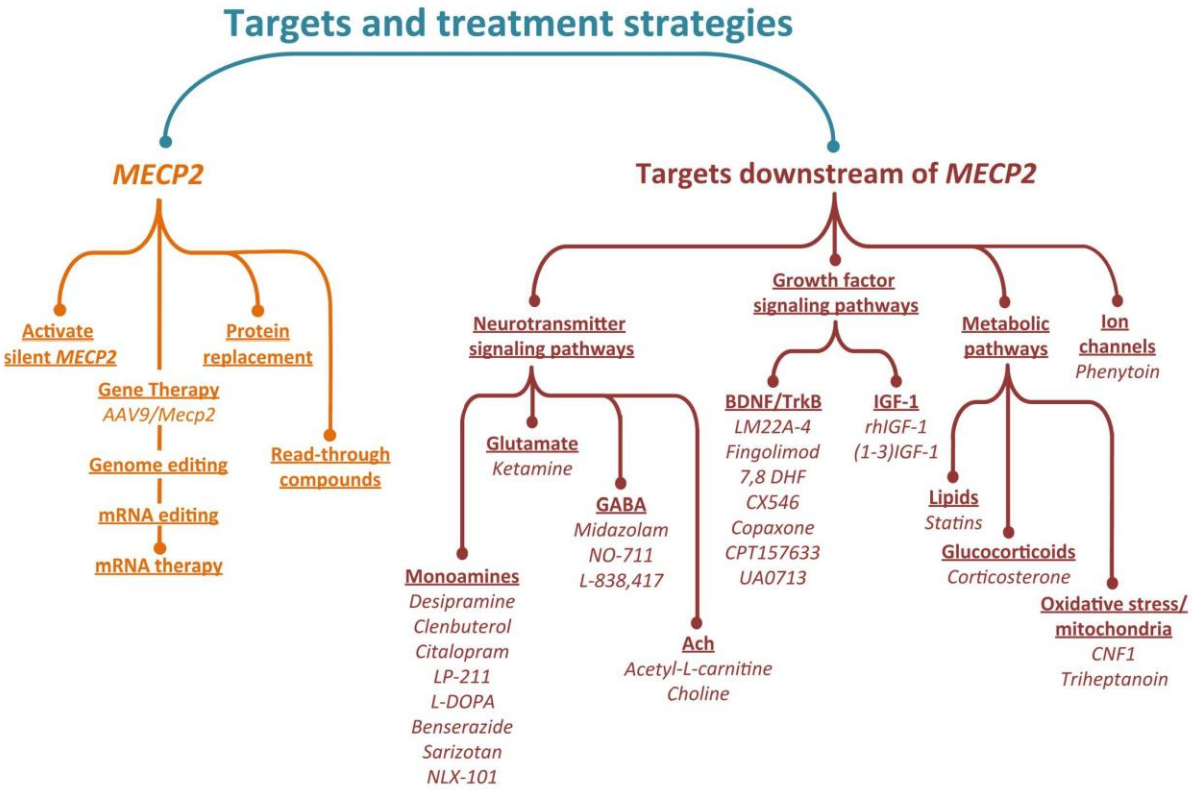

Figure 1.3 Therapeutic strategies for Rett Syndrome. Targets of treatment have been underlined. Compounds investigated *in vivo* have been shown in italics. IGF-1, insulin-like growth factor 1; MeCP2/*MECP2*, methyl-CpG-binding protein 2/gene. Taken from Katz et al. publication [60]. With permission from Elsevier, Licence Number 4443310878154.

1.2 Epigenetic mechanisms

Epigenetic mechanisms including chromatin remodelling, DNA methylation, histone post-translational modifications (PTM), and non-coding RNAs, regulate gene expression without any change in the underlying DNA sequences [73]. It has been shown that these mechanisms have a major impact in several processes including development, aging, and in disease condition [73, 74].

1.2.1 Chromatin remodeling

The genome material in eukaryotic cells is composed of DNA, and DNA-bound proteins (mainly histones), and is called “chromatin”. A 147-bp stretch of DNA wrapped around a histone octamer (two copies of H2A-H2B dimers, as well as H3, and H4 histones) make up the basic unit of DNA packaging, which is called “nucleosome”. Linker DNA connects nucleosomes and is more accessible to DNA binding proteins. Nucleosome structure on the other hand prevents the interaction of genes with transcription factors, acting as negative regulators of transcription. It has been shown that a group of proteins can modulate gene expression through repositioning of nucleosomes, and remodeling of the chromatin in the promoter of specific genes [75]. This process has been shown during neurodevelopment [76-78].

1.2.2 Histone PTM

The N-terminal tail of histones mainly includes the amino acids that are subjected to various PTM. Specific amino acids such as lysine is commonly the target for acetylation, phosphorylation, methylation, somoylation, and ubiquitination, whereas arginine can be methylated or ADP-ribosylated [79, 80].

These histone marks can change the overall charge of basic histone proteins and interfere with histone-DNA interactions, affecting the nucleosome stability [78, 81]. They can also affect transcriptional activity of the genes by recruiting co-activator or co-repressor complexes [82]. Various histone PTM play role in important processes such as demarcating euchromatin and heterochromatin regions. For example, facultative

heterochromatin, which contains selectively silenced genes, is enriched for H3K27me3, whereas the constitutive heterochromatin with permanently repressed genes (like centromere), contains abundant H3K9me3 [83-86].

1.2.3 Non-coding RNAs

While the number of protein-coding genes in the human genome (~21,000) is similar to less complex species, tens of thousands of non-coding RNAs (ncRNAs) can play a role in physiological complexity of humans as well as other mammals [87].

Small RNAs (~20-30 nucleotides in length) include small interfering RNA (siRNA), microRNAs (miRNAs), and Piwi-interacting RNAs (piRNAs) that modulate gene expression in a sequence-specific manner. Long ncRNAs (typically > 200nt) are also active in epigenetic regulation of gene expression in transcription level by targeting transcription activator and repressor, and during mRNA translation [78, 81, 88].

1.2.4 DNA methylation

DNA methylation is one of the most studied epigenetic modifications primarily characterized as covalent binding of a methyl group to the fifth carbon of a cytosine nucleotide, 5-methyl cytosine (5-mC), in the context of cytosine guanine dinucleotide (CpG). Now we know that methylation can also happen in non-CpG context, targeting other nucleotides (adenine, guanine, and thymine) [85]. While DNA methylation first was recognized as a marker for gene inactivation, later it became clear that in 5-hydroxy methyl cytosine (5-hmC), it could activate gene expression [85, 89].

Epigenetic modifications are mediated by specific enzymes known as writers, recognized by effector proteins known as readers, and the reversible marks can be removed by another set of enzymes called erasers [73].

1.2.4.1 Writers of DNA methylation

The process of DNA methylation is mediated by DNA methyl transferases (DNMTs) such as DNMT3A, and DNMT3B which induce *de novo* methylation, and DNMT1, which copies the pre-existing methylation profiles from one cell division to the

next DNA methylation in a reversible process [90, 91]. These enzymes are important for proper development and their impairments are reported in different diseases. For instance, DNMT1 mutation is associated with ‘’hereditary sensory neuropathy with hearing loss and dementia type IE’’ [91].

1.2.4.2 Erasers of DNA methylation

DNA demethylation can occur in a passive way when methylation marks dilute and fade from one cell division to the next. This happens in early stages of development that production of DNMTs has not stated yet and DNMT1 originated from oocyte is getting diluted by cell divisions. There is also an active demethylation catalyzed by Ten-eleven translocation (TET) family of proteins that transform a 5-methylcytosine (5-mC) to a 5-hydroxymethylcytosine (5-hmC), which takes a series of steps to return to an unmethylated cytosine [73, 85, 90].

1.2.4.3 Readers of DNA methylation

Methylation of DNA is read and interpreted by different families of proteins that recognize this epigenetic modification and bind to it. Methyl-binding protein (MBP) family including their prototype member, MeCP2, Kaiso family proteins and the SET and RING finger associated (SRA) domain family proteins are examples of these DNA methylation readers [74, 92].

1.2.4.3.1 Methyl binding protein family

This family of DNA methyl readers is characterized by methyl binding domain (MBD) that facilitates protein binding to methylated DNA. From its 11 members, MeCP2, MBD2, and MBD3 are preferably associated with methylation of the promoters and generally supress gene transcription. MBD1 mostly functions through histone modification and heterochromatin formation, and MBD4 takes part in DNA repair. Dysregulation or mutations of MBD proteins are present in a variety of cancers as well as neurologic disorders such as RTT [74, 93, 94].

1.3 Methyl CpG Binding Protein 2 (MeCP2)

MeCP2 is the second member of a family of proteins that bind to methylated CpG DNA templates without sequence specificity. While the first member of this group (MeCP1) needs at least 12 symmetrical methylated CpG, the second and most abundant protein of this group (MeCP2) is able to bind a single methylated CpG pair [95, 96].

1.3.1 *MECP2*/*Mecp2* gene structure

The *MECP2/Mecp2* gene is located on the long arm of the X-chromosome at Xq28 in human and XqA7.3 in mouse. It is composed of four coding exons and three introns. Three polyadenylation sites in its 3'UTR result in mRNA transcripts with varying lengths. The two translational start sites at exon one and two give rise to the common splice variants of the protein that differ only at their N-termini. The MeCP2E1 isoform is encoded by exons 1, 3, and 4, and its transcripts are reported to be the main isoform in the brain. The MeCP2E2 isoform is encoded by exons 2, 3, and 4 and its transcript level has been reported to be higher than *MECP2E1* in the liver, placenta, prostate gland, and skeletal muscles (Figure **1.4**) [97].

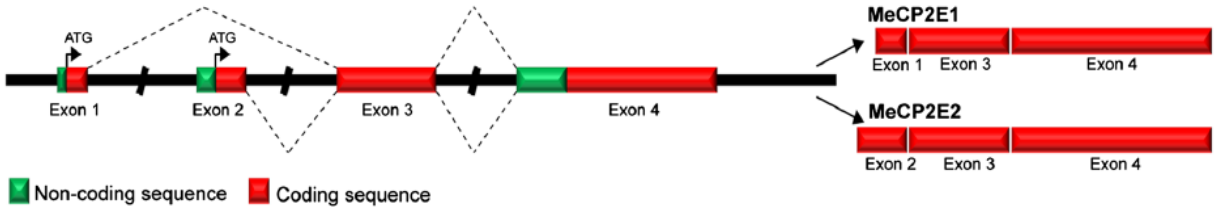

Figure 1.4 The structure of *MECP2*/*Mecp2* gene and generation of two MeCP2 isoforms. Taken from Liyanage and Rastegar paper [74]. By permission from Springer Nature, Licence Number 4441081356553.

1.3.2 MeCP2 protein

MeCP2 is a protein with a calculated mass of ~53 kDa (but it is usually detected at ~75 kDa), and is composed of five major domains: The N-terminal Domain (NTD), Methyl Binding Domain (MBD), Intervening Domain (ID), Transcription Repression Domain

(TRD), and C-terminal Domain (CTD). Three AT hook domains, which exist within ID, TRD, and CTD make binding to AT-rich DNA possible [98].

MeCP2 is considered an intrinsically disordered protein due to its major unstructured format (~60%) [99]. From the two MeCP2 isoforms, MeCP2E1 (previously called MeCP2B or MeCP2α) has 21 unique residues at its N-terminal region and an acidic isoelectric point (pI) of 4.24. The other isoform that was discovered first, MeCP2E2 (previously called MeCP2A or MeCP2β) has 9 unique residues at the N-terminal region and a basic pI of 9.5.

Dr. Bird's team suggested that the presence of upstream open reading frame in *MECP2E2* could have an inhibitory effect on the protein translation and result in more abundant MeCP2E1 [100]. However, the lack of MeCP2 isoform-specific antibodies limited the studies until 2012 that our lab reported the generation of MeCP2 isoform specific antibodies [101] and the differential expression of the two isoforms in the mouse brain [70]. Based on their study MeCP2E1 has a relatively uniform distribution across different brain regions such as cortex, hippocampus, thalamus, brain stem and cerebellum, while MeCP2E2 isoform is differentially enriched in various brain regions of mouse [70]. Expression of these isoforms in the human brain is still one of the least-studied areas of this field.

1.3.3 MeCP2 expression

Even though brain-specific expression of MeCP2 has been extensively studied in the context of neurological phenotypes of RTT, this protein has been found in different organs from lung and spleen with high expression level to liver, heart, and small intestine with lower expression levels [23]. In the brain, MeCP2 is expressed not only in neurons but also in other cell types such as astrocytes [66, 102], and microglia [103]. Selective MeCP2-deficiency in both of these cell types has caused neuronal abnormalities, which could be then resolved by re-expression of MeCP2 in these cells [104, 105].

1.3.4 MeCP2 function

MeCP2 was first described as a repressor of methylated DNA through interaction with a co-repressor complex composed of mSin3A, a transcriptional repressor, and histone deacetylases (HDACs), which can cause compaction of chromatin structure and gene silencing as a result [106, 107]. NCoR/SMRT is another, more recently found, co-repressor complex that has a specific binding domain in TRD region of MeCP2 [108].

In contrast to primary findings, more recent studies have shown that MeCP2 can also play the role of a transcriptional activator by recruiting activating factors such as CREB (cAMP response element-binding protein) [109]. It has been also suggested that MeCP2 can play the role of transcription activator when it binds to 5-hydroxymethylcytosine, which is a common modification of DNA in the brain and is enriched in active genes [110].

Other studies suggest that MeCP2 can play the role of a global regulator of chromatin. Its level in neuron is almost similar to histones. In addition, it can bind to non-methylated DNA [111], and compact nucleosomes in a manner similar to histone H1 [112]. MeCP2 may also affect its targets such as *DLX5* by making a loop in DNA [113] (Figure 1.5).

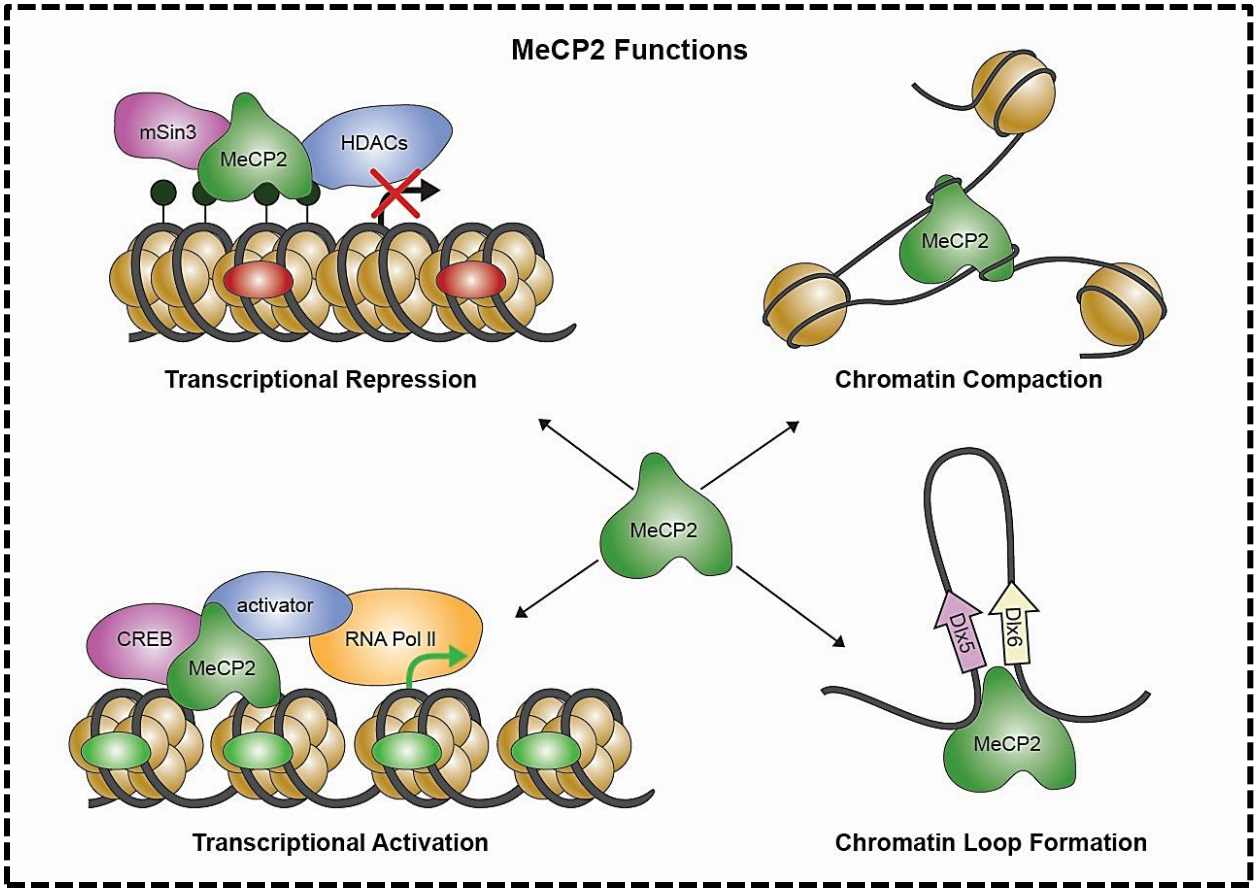

Figure 1.5 MeCP2 functions in gene regulation and chromatin organization. Taken from Zachariah and Rastegar publication [114]. Open access article under the Creative Commons Attribution Licence.

1.3.5 MeCP2 regulation

MeCP2 is regulated transcriptionally and post-transcriptionally by multiple mechanisms. Positive and negative regulatory factors upstream of the *MECP2* promoter region can regulate its expression. There are also silencers and enhancers in the region that can act as cis-regulatory elements for *MECP2* gene [115, 116]. In addition, there are polyadenylation sites at 3'UTR of *MECP2*/*Mecp2* gene, which are responsible for different length of transcripts in a tissue specific manner. Trans-acting factors involved in polyadenylation can bind to these sites [117, 118]. Similar to other genes, epigenetic factors such as microRNAs and histone PTMs can also affect MeCP2 regulation [74]. Our lab has already shown how DNA methylation can affect expression of *Mecp2* isoforms during *in vitro* neural stem cell differentiation [116]. Furthermore, we have reported how

an environmental insult such as ethanol exposure can cause misexpression of *Mecp2*/MeCP2 in differentiating brain cells through deregulation of 5-mC and 5-hmC DNA methylation [119].

1.3.6 RTT-causing *MECP2* mutations

N-terminal domain: From the hundreds of *MECP2* mutations found in RTT patients, less than 1% target exon 1, which means MeCP2E1 dysfunction is sufficient to cause Rett Syndrome [97, 120, 121]. While MeCP2E2-specific mutations have not been described in RTT, it has been shown that expression of MeCP2E2 can improve some of the RTT phenotypes in *Mecp2*-null mice. Isoform-specific MeCP2 transgenic lines were used in this study to rescue neurophenotypes exhibited by Mecp2-null mice (*Mecp2*$^{-/Y}$) [122]. Mutations affecting parts of NTD region, which are shared by both MeCP2 isoforms, have been described in RTT patients [21].

Methyl binding domain: Thr158, Arg133, and Pro152, within the MeCP2 MBD region, are three common spots for RTT-related mutations. T158M located in MBD region of the protein, is the most frequent mutation that can cause RTT (~9%). R133C and R106W from MBD region are the 7th and the 10th in the list of RTT-causing mutations [21]. P152H is another mutation within MBD region, already reported in a male individual with intellectual disabilities [123], whose brain sample is part of the current study.

Intervening domain: ID is the region that links MBD and TRD, and is the location for R168X, a truncating mutation that is the second most common mutation in RTT patients [21]. A few mutations in ID region of MeCP2 such as R190H, and R190C have been also associated with Schizophrenia [124, 125]. One of the RTT brain samples in our study has been shown to have A201V mutation. This is the 21st most common *MECP2* mutation found in 0.61% of RTT patients. However, it is unclear if it has a cause effect in this syndrome or it is just a polymorphism found in association with RTT [21].

Transcriptional repression domain: TRD binds with partner proteins such as co-repressor Sin3a, HDACs [126], and NCoR/SMRT co-repressor [108]. R255X, R270X, and R294X, three most common truncating mutations after R168X (from ID), are located

within TRD. Moreover, R306C, which is the second most common missense mutation after T158M (from MBD), is located in TRD [21]. Because of the R306C mutation, MeCP2 loses its interaction with NCoR/SMRT [108].

C-terminal domain: The MeCP2 CTD might play a role in binding to histones [127]. This domain also contains S421, a serine residue that can become phosphorylated during neural activity [128], resulting in transcriptional activation of the Brain derived neurotrophic factor (*Bdnf*) [129]. L386fs, the most common frameshift mutation in RTT patients, is located in CTD. E397K, which is the sixth most common RTT-associated substitution, is also located in CTD.

A list of the 21 most common *MECP2* mutations and their prevalence in RTT patients has been shown in Table 1.3. This comes from 680 recognized *MECP2* mutations or group of mutations reported in RTT patients [21].

Table 1.3 Common RTT- associated mutations in *MECP2* gene. Adapted from RettBASE database [21]. Open access database last assessed in 2017.

	Mutation	**Reported Cases**	**% Frequency**
1	p.T158M	419	8.81
2	p.R168X	365	7.67
3	p.R255X	313	6.58
4	p.R270X	276	5.80
5	p.R306C	245	5.15
6	p.R294X	237	4.98
7	p.R133C	217	4.56
8	intronic variation	192	4.04
9	3'UTR variation	174	3.66
10	p.R106W	132	2.77
11	p.L386fs	106	2.23
12	p.P152R	71	1.49
13	p.G269fs	63	1.32
14	p.R9fs	61	1.28
15	p.P389X	47	0.99
16	p.E397K	46	0.97
17	p.T299T	38	0.80
18	p.S194S	38	0.80
19	p.M1?	38	0.80
20	p.S411S	30	0.63
21	p.A201V	29	0.61

1.3.7 MeCP2 target genes

Studies on MeCP2 target genes show little overlap, and association of these target genes with RTT has not been established in most cases [114]. MeCP2 is capable of having either an activator or a repressor effect on these studied targets not only as a transcriptional regulator but also as an epigenetic modulator that can affect RNA splicing and chromatin structure as explained earlier [74]. Genes such as *Dlx5*, *Fgf2-5*, *Fut8*, and *Nf1* have shown alterations in splicing observed in an RTT mouse-model (*Mecp2* $^{308/y}$) [130]. A list of target genes studied in human samples or cell lines is adapted from Zachariah and Rastegar 2012 [114] and presented as Table 1.4.

BDNF is an important and perhaps the most studied target of MeCP2. Its cross-talk with MeCP2 has been studied mainly in animal models [129, 131]. MicroRNAs (miRNAs) are other important targets for MeCP2 and its regulations. Several miRNAs have shown altered expressions in RTT mouse models [89, 132]. BDNF and miRNAs interactions with MeCP2 will be discussed in next parts of this chapter.

Table 1.4 Known target genes of MeCP2 in studies on human samples. Adapted from Zachariah and Rastegar paper [114]. Open access article under the Creative Commons Attribution Licence.

Gene target	Function	Cell/tissue type studied	Direct association with MeCP2	Reference
PCDHB1	Cell adhesion	Oral cancer cell lines (ZA, KOSC2, HSC5, NA)	Yes (SH-SY5Y)	[133]
PCDH7				
APBP3	Intracellular signal transduction			
CLU	Extracellular molecular chaperone	RTT patient brain (frontal cortex)	No (SH-SY5Y)	[134]
CRMP1	Component of semaphoring signal transduction pathway		Yes (SH-SY5Y)	
DNMI	Vesicular trafficking, production of microtubule bundles, hydrolyzes GTP		Yes (SH-SY5Y)	
GNBI	Integrates signals between receptor and effector proteins		Yes (SH-SY5Y)	
APLP1	Enhancer of neuronal apoptosis		No (SH-SY5Y)	
CO1	Mitochondrial respiratory chain		No (SH-SY5Y)	
GDI1	Regulates GDP/GTP exchange		No (SH-SY5Y)	
ID1-ID4	Regulation of neuronal differentiation	SH-SY5Y	Yes (SH-SY5Y)	[135]
UBE3A	Ubiquitin ligase	Brain cerebral samples of RTT, Angelman Syndrome, and autism patients	No (adult mouse cerebellum samples)	[136]
GABRB3	GABA-A receptor			

1.4 Brain-derived neurotrophic factor

Brain-derived neurotrophic factor is a well-known member of the neurotrophin family of growth factors. Nerve growth factor (NGF), Neurotrophin-3 (NT-3), NT (4/5), and NT-6 are other members of this family. Neurotrophins together with tropomyosin receptor kinases (TRKs), and low affinity nerve growth factor receptor (p75) regulate survival, maturation, and differentiation of neurons and participate in synaptic development and neural plasticity [137-139].

1.4.1 *BDNF/Bdnf* gene structure

All neurotrophin genes consist of multiple 5' exons linked to promoters that initiate transcription of distinct mRNAs. A 3' exon that is common among all transcripts includes an open reading frame encoding the precursor peptide, pre-pro neurotrophin. Despite similarities among the gene structures of different neurotrophin family members, the *BDNF*/*Bdnf* gene has one of the most complex structures, which is closely conserved between humans and rodents. Mice, rats, and humans have at least eight homologous exons in common, which are regulated by alternative upstream promoters. The multi-promoter character of *BDNF*/*Bdnf* is suggestive for additional flexibility of BDNF expression in response to a diverse range of stimuli [140].

The human *BDNF* gene spans about 70kb on the chromosome 11, region p13-14, and has 11 exons (I-IX plus Vh and VIIIh). Some exons have different subsets that are labeled as a, b, c, and d. The protein coding sequence is located within exon IX, and different upstream promoters of alternatively spliced exons yield several *Bdnf*/*BDNF* transcripts. There are two polyadenylation sites for exon IX that double the number of transcripts by generating short and long splicing variants (Figure 1.6). Despite the existence of different transcripts, all the mRNAs encode for a single protein. The apparently redundant generation of transcripts controls the requirements of context- and cell type-specific demands [141]. For example, while exons I, IV, V, VII, and IX in mouse are activated by DNA methylation, a different group of exons (III, VIII, IX), are induced by inhibitors of histone deacetylase (HDAC) [142]. In addition, it has been shown that transcript variants with short 3'UTR stay in the soma and regulate neuronal survival, while

transcripts containing the long 3'UTR are preferentially localized in the dendrites to modulate synaptic plasticity [143-145].

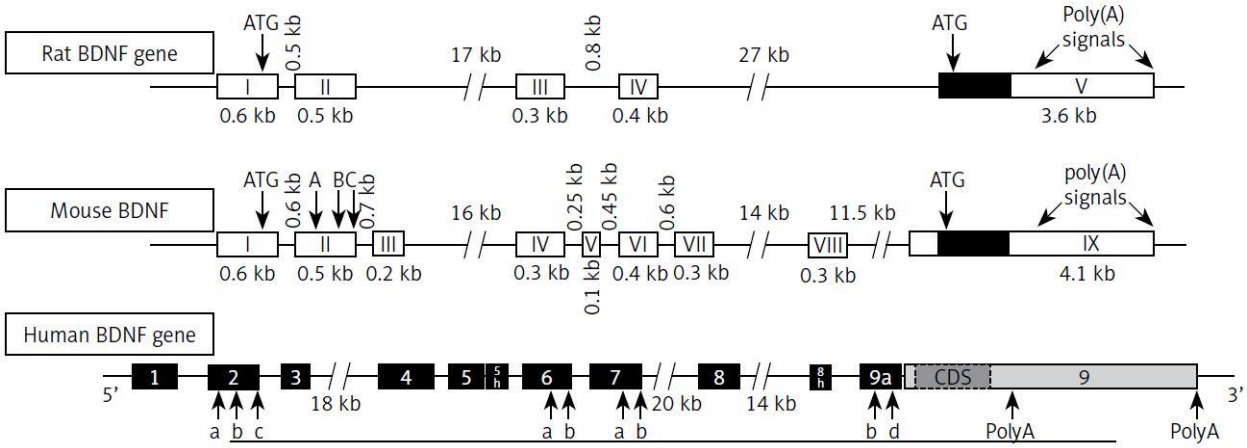

Figure 1.6 Mouse, rat, and human *BDNF* gene structures. There are four promoters in rat and 9 promoters in mouse. Transcripts of *BDNF* mRNAs contain one of the four 5′ non-coding exons (I, II, III, IV) spliced to the common 3′ protein coding exon. Eleven exons of human *BDNF* are shown in black with arrows indicating alternative polyadenylation sites (PolyA) in the 3′-UTR and internal alternative splice sites in exons 2, 6, 7 and 9a (letters a, b, c and d). Taken from Bathina and Das paper [141]. Open access article under the international CCBY-NC-SA 4.0 license.

1.4.2 BDNF protein

BDNF, first isolated in the 1980s, was initially purified from the pig brain. Having an isoelectric point around 9-10, BDNF is stable during biochemical purification. However, because of its extremely low concentration in the brain, 1.5 kg of starting material was needed to yield 1 µg of the purified protein [137, 146]. BDNF has about 50% of its amino acids in common with other members of neurotrophin family, and similar to the rest of neurotrophic factors, it consists of two pairs of anti-parallel β-stands. Three disulfide bonds stabilize this structure, which is called a cysteine knot as a whole [147].

1.4.2.1 Biosynthesis, processing, and secretion

Pre-proBDNF is the precursor form of the BDNF protein with approximately 270 amino acids and it is produced in the endoplasmic reticulum. After translocation to the Golgi apparatus, the "pre" region of the translated protein is removed, resulting in the generation of proBDNF, which is yet another form of the immature protein. The proBDNF

has a molecular weight of 32kDa, consisting of 129 amino acids as the pro-domain and 118 amino acids of the mature BDNF [148]. The proteolytic cleavage of the proBDNF by subtilisin/kexin-isoenzyme-1 (SK-1) protease can produce a truncated form of BDNF with a molecular weight of ~28kDa. This truncated BDNF protein is a final product without the capacity for further processing. The mature BDNF (mBDNF) has a molecular weight of ~14kDa and is generated by three different proteases; furin, matrix metalloprotease-7 (MMP-7), and plasmin [149-151]. Colocalization of both proBDNF and mBDNF in the secretory granules has been shown in different studies on cultured mouse hippocampal neurons [152, 153] as well as sections of adult mouse hippocampus [154]. Therefore, it has been suggested that cleavage of proBDNF by endoproteases occurs in these secretory granules. The final processing of the mature BDNF may also happen after secretion in the extracellular space near active synapses [155].

It has been shown that the ratio of proBDNF to mBDNF may vary in the course of development with predominance of mBDNF in adulthood [156]. In non-neuronal cells, BDNF is constitutively secreted. However, in neurons, BDNF has an activity-regulated secretion in addition to a constitutive mode of secretion. Moreover, previously secreted BDNF can be endocytosed at the primary sites of protein release, which can then be recycled for additional rounds of secretion even at far distant sites within the same neuron [157, 158].

While previous studies have detected *BDNF* mRNA, and BDNF protein throughout the CNS, with highest expression levels in the hippocampal formation (the dentate gyrus, the hippocampus proper, and the subicular cortex) and the cerebral cortex, there are conflicting results about protein expression observed by different research groups [159]. Technical issues such as the sensitivity and/or specificity of anti-BDNF antibodies could be the source of these different results. In addition, different factors such as enriched environment, dietary restriction, light, stress, and circadian rhythm can also impact BDNF expression [160]. At the subcellular level, BDNF secretion is not limited to somatic sites. Both dendritic and axonal secretion of BDNF has been noticed by different groups [153, 161]. In addition to neuronal BDNF secretion, uptake and re-exocytosis of BDNF by astrocytes and neurons has also been reported [162]. In addition to astrocytes,

endothelial cells, platelets, and microglia are of non-neuronal sources for BDNF secretion [159].

1.4.2.2 BDNF Signaling

BDNF binds the tropomyosin-related kinase B (TrkB) with specific/high affinity. This leads to TrkB dimerization and auto-phosphorylation, leading to the activation of several downstream signal transduction cascades. That includes the mitogen-activated protein kinase (MAPK) which promotes neural differentiation, the phosphatidylinositol 3-kinase (PI3K) that promotes growth and survival of neurons, and the phospholipase Cγ (PLCγ) pathway that promotes synaptic plasticity [163]. Similar to other neurotrophins, BDNF can also bind to the p75 neurotrophin receptor (p75NTR). P75NTR is a member of the tumor necrosis family of proteins that can activate several signaling pathways including programmed cell death, when p75NTR is activated in the absence of TrkB signaling [164].

Cooperation of p75NTR and TrkB receptors increases the affinity of mBDNF for the complex and the pro-survival, growth-related signaling will be enhanced [147, 165]. On the contrary, when p75NTR forms a heterodimer with sortilin (a transmembrane protein that regulates neurotrophin sorting), the resulted complex acquires a higher affinity for ProBDNF. The cell death-signalling pathway will then be activated through the induction of several proapoptotic pathways [166]. Therefore, the biological role of pro-peptide is beyond the traditional assistance in folding of the mature protein. It has been shown that the BDNF pro-peptide is biologically active as a synaptic modulator, that facilitates long-term depression when directly binds p75NTR receptor [167]. From different downstream signaling cascades, the PLCγ pathway has been suggested to mediate rapid BDNF-related effects that happen within seconds to minutes, while the other two (MAPK, and PI3K) work more slowly through changes in gene transcription [147].

1.4.2.2.1 MAP kinase pathway

When TrkB becomes phosphorylated at Tyr^{490} and Tyr^{515}, its affinity for Src homology 2 domain containing adaptor protein (Shc) increases. Upon binding to the specific phosphorylated sites, the growth factor receptor bound protein 2 (Grb2) will be recruited. Grb2 makes a complex with SOS, which is an exchange factor for Ras. Ras acts upstream of ERK (extra cellular signal-regulated kinase1/2) in the MAK cascade, activating Raf protein Ser/Thr kinase. That in turn leads to the activation of MEK (MAP kinase/ERK kinase), which can activate ERK1/2. Active ERK can then transfer to the nucleus, activating transcription factors such as CREB. The phosphorylated CREB can bind to the *Bdnf*/*BDNF* promoter inducing its transcription. BDNF-ERK-CREB signaling pathway plays a major role in cell survival, synaptic structure, and plasticity [168-171].

1.4.2.2.2 PLCγ pathway

TrkB Phosphorylation at Tyr^{816} generates inositol 1, 4, 5-triphospahte (IP3) and diacylglycerol (DAG). IP3 is responsible for Ca^{2+} release from internal sources, leading to the activation of Ca^{2+}/calmodulin-dependent protein kinases. This results in CREB phosphorylation and a cascade is initiated that continues similar to MAPK pathway [172, 173]. DAG on the other hand, stimulates protein kinase C (PKC), phosphorylation of which can activate different proteins including ERK1/2 (Figure 1.7) [173].

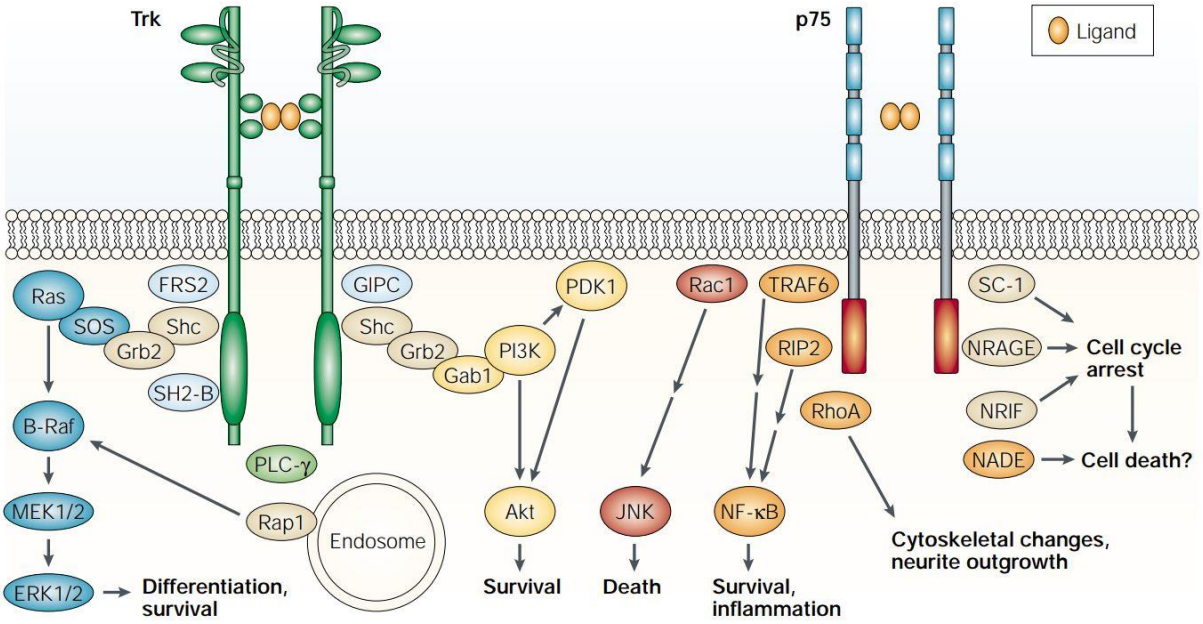

Figure 1.7 Schematic representation of the neurotrophin receptor signalling pathways. Binding of a neurotrophin to its Trk and/or p75 receptor activates several downstream pathways with different, and sometimes opposing functions. Taken from Moses v. Chao's publication [163]. By permi**s**sion of Springer Nature, License Number 4444860490039.

1.4.2.2.3 PI3K pathway

Activation of PI3K by BDNF can be associated with the combined action of RAS [174] that can also activate AKT, an important kinase that phosphorylates mTOR (mammalian Target of Rapamycin). The signal transduction cascades that activate mTOR pathway is involved in the regulation of protein translation and that is where BDNF may become involved in local protein synthesis [175, 176].

1.4.3 *BDNF*/*Bdnf* regulation

Membrane depolarization in neurons could be induced by sensory stimuli [177-179], activation of glutamate receptors [180-182], or seizure [183] with a positive regulatory role on *BDNF* transcription. It has been shown that binding of cAMP response element-binding protein (CREB) to cAMP/Ca^{2+}-response element (CRE) in the promoter IV of human *BDNF* gene is critical for activity-dependent transcription from this promoter. Human promoter IX can be also induced by neuronal activity. CRE and PasRE (basic

helix-loop-helix-PAS transcription factor response element) contribute to the induction of this promoter [184]. *BDNF/Bdnf* transcription is reported to be regulated at least partly by epigenetic factors. Decreased methylation of cytosine residues in CpG dinucleotides at the *BDNF/Bdnf* promoter IV has been shown in transcription induction of the gene by neuronal activity. That is where MeCP2 can play its role as a transcriptional regulator by binding to methylated DNA in the region of *BDNF/Bdnf* promoter IV [129].

A few studies have examined histone modifications as another epigenetic regulator of *BDNF* transcription. For instance, an increase in histone methyl transferase H3K4 tri-methylation, a marker of active chromatin, has been shown at the *BDNF* promoters I and IV during the BDNF upregulation in the course of transition from fetal to childhood and/or young adult stages [185].

MicroRNAs (discussed in next section), are among epigenetic regulators that can modulate *BDNF* expression. Several microRNAs have been studied in this regard. It has been shown that *miR-1*, *miR-106*, *miR-155*, and *miR191* can supress *BDNF* gene expression by binding to the *BDNF* 3'UTR [186]. There is a long list of miRNAs predicted to target *BDNF*, and *miR132*, as part of my study that is explained in the next section, has been reported to regulate BDNF [187].

1.4.3.1 Role of MeCP2 in BDNF regulation

There is still controversy about BDNF regulation by MeCP2. Earlier studies were more in favor of a repression model. It was reported that membrane depolarization could release MeCP2 from its binding site at the *Bdnf* promoter IV, resulting in *Bdnf* transcriptional activation [129, 188]. MeCP2 phosphorylation at Ser^{421} [128], and decreased methylation of CpG sites within the *Bdnf* promoter IV [131], induced by neuronal depolarization were thought to cause dissociation of MeCP2 and its co-repressors (i.e. Sin3a and HDAC1) from the *Bdnf* promoter IV. Other studies showed decreased *Bdnf* mRNA and protein in the *Mecp2*-null mice (hemizygous $Mecp2^{tm1.1Jae}$ mutant males of the Jaenisch strain, and cre93 $Mecp2^{-/y}$), suggesting of an activatory role for MeCP2 in *Bdnf* transcription [189, 190].

There are other models that suggest a dual role for MeCP2 in BDNF regulation, explains these discrepancies [191]. Based on a model studied in SH-SY5Y neuroblastoma cells, MeCP2 remains bound to its target genes and the regulatory complexes, which are recruited by its phosphorylation, may activate or repress expression of these target genes [192]. MeCP2 phosphorylation is not the only contributing factor in this dual operating model. Other epigenetic modifications can also play a role. For instance, it has been shown that transcription of some of the microRNAs that target the 3'UTR of *Bdnf* transcripts are controlled by MeCP2 [89]. Furthermore, changes in MeCP2 might affect not only the expression of *BDNF*/*Bdnf* at the transcription level, but it might also affect the translation or stability of BDNF protein. That might explain some of the discrepancies between the different models that have studied BDNF in transcript or protein level [193].

1.4.4 BDNF and pathophysiology of RTT

Studies on RTT mouse models have shown reductions in BDNF expression after the first 3-4 postnatal weeks at the same time that RTT-like features start to appear. The decrease manifests first in caudal parts of the brain (brainstem and cerebellum), and gradually the entire brain is involved [191].

There are controversial results about BDNF impairment in the brain of RTT patients. While two reports show that the level of BDNF protein in cerebrospinal fluid (CSF) and blood serum of RTT patients is comparable with unaffected controls [194, 195], there are other studies that describe lower transcript level of *BDNF* in RTT brain samples compared to controls. Technical limitations especially for the assessment of protein levels might be the reason behind the disparities [196, 197].

In addition to the above-mentioned controversies, the functional consequences of reduced BDNF are not fully clear. Animal models with *Bdnf* loss-of-function mutations show features similar to *Mecp2*-null mutants or models with RTT causing MeCP2 mutations. Smaller brains and neurons with reduced dendritic arborisation, impaired hippocampal LTP (Long-term potentiation) in *Bdnf* $^{-/-}$, or *Trkb* $^{-/-}$ mice [198], as well as irregular breathing and impaired locomotion [199, 200] are a few examples. Moreover,

overexpression of *Bdnf* in *Mecp2*-null mice (cre93 *Mecp2*$^{-/y}$) has improved survival as well as locomotor function in this model [189].

1.5 MicroRNAs

MicroRNA (miRNAs) are members of non-coding RNA family with a length of ~22-23 nucleotides that can regulate a vast number of biological events through gene silencing. In the genome, miRNA genes can be localized within the introns of coding genes (host genes) or in areas without known coding activity either as a single gene or as clusters of genes [201]. The process of miRNA biogenesis is tightly controlled in a temporal and spatial manner, and its deregulation has been shown to be associated with several human diseases [202].

1.5.1 miRNAs maturation pathways and function

RNA poll II transcribes miRNA genes under the influence of different transcription factors (such as p53 or MYC) and epigenetic controls (such as DNA methylation or histone modification). The primary transcripts (pri-miRNA) are typically over 1 kb in length and consist of a stem-loop with 33-35 nucleotides and two single-stranded RNA segments at 5' and 3' ends [203]. The maturation process starts in the nucleus with the nuclear RNase III, Drosha, and its cofactor, Pasha (DGCR8). They form a complex called microprocessor crops the stem-loop and releases the pre-miRNA, a hairpin-shaped RNA of 65 nucleotides. In the next step, pre-miRNA is exported to the cytoplasm by a transport complex made of exportin5 and GTP-binding nuclear protein (RAN.GTP). In the cytoplasm, the RNase Dicer in complex with double stranded RNA-binding protein TRBP cleaves the pre-miRNA hairpin to its mature length. The functional strand of the mature miRNA, guide strand, is loaded together with Argonaute (Ago2) proteins to make RNA-induced silencing complex (RISC). This functional strand guides RISC to silence target mRNAs with partially complementary binding sites within their 3'UTRs called microRNA response elements (MRE). The guide strand acts through mRNA cleavage, translational repression or de-adenylation, whereas the other strand (passenger or miRNA*) is usually degraded after release (Figure 1.8). Depending on the context, miRNAs might be more involved in mRNA degradation or local regulation of mRNA

translation [202, 203]. It is worth mentioning that in addition to their initially described function, miRNAs can also bind to the other regions of mRNA rather that 3'UTR and can have a positive effect on gene expression *via* binding to target gene promoter(s) [204, 205].

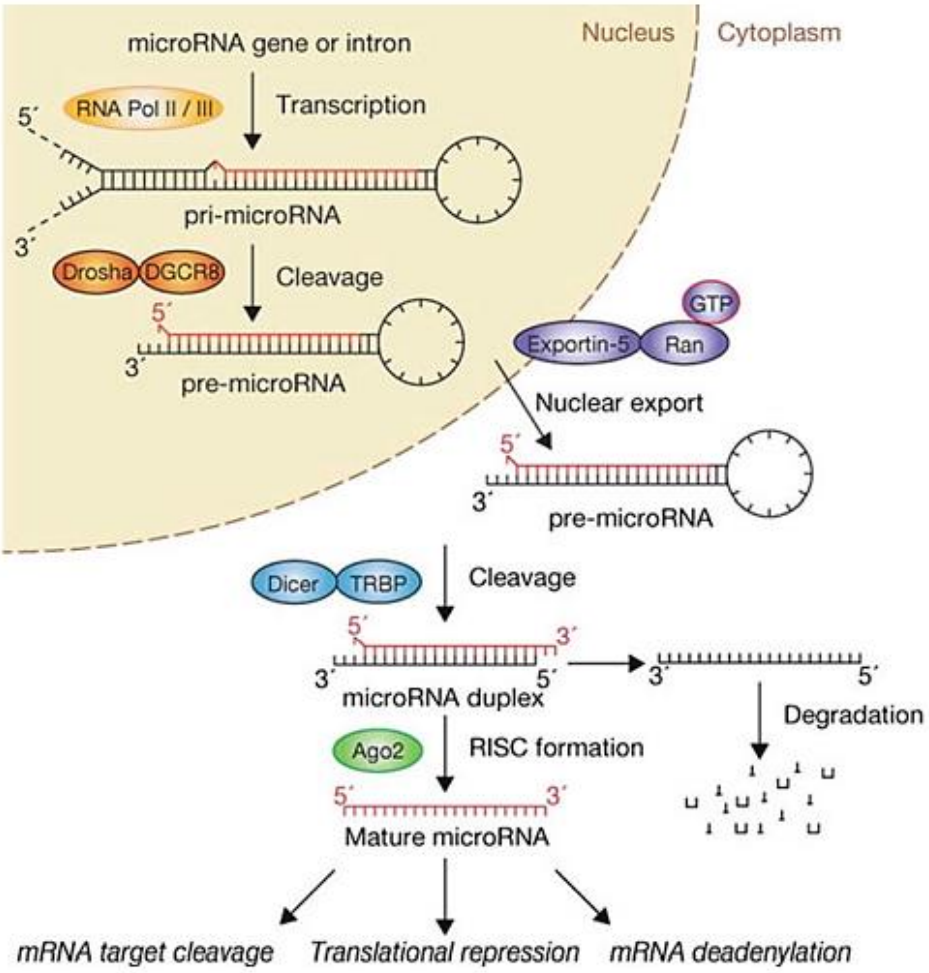

Figure 1.8 miRNA processing pathway. Taken from Winter et al paper [203]. By permission of Springer Nature, License Number 4441380946316.

1.5.2 Role of miRNAs in CNS development

There is still many points to be clarified about how miRNAs regulate their target genes. However, we know that miRNAs affect the process of nervous system development during the embryonic patterning and into neural differentiation, and plasticity

[206]. More recent studies have also shown important role of miRNAs in the adult synaptic plasticity and cognition [201].

Time-specific spatially restricted or cell type-specific miRNAs can play roles in cell fate determination of neuronal precursor cells toward neurons or glial cells. This happens mainly during embryonic development for neurons and continues in early post-natal, for glial differentiation. miRNAs are also associated with adult neurogenesis in localized parts of the adult brain such as subgranular zone of the hippocampus, which is important in learning and memory. In addition, miRNAs have been shown to be involved in more specific glial or neural cell type determination. miRNAs also play role in migration of newborn neurons to their specific locations as well as neuronal polarization, which refers to functional separation of neuron processes to the axonal and dendritic compartments. Axonal branching and dendritogenesis are another area that neuronal miRNAs may regulate. They also affect maturation of neurons that happens through connection with proper targets. The dynamic structure and function of synapses give them the ability to respond to external stimuli. This process known as synaptic plasticity is also affected by miRNAs reaction to activity dependent pre- and post-synaptic physiology [206].

In summary, several studies have highlighted the regulatory role of miRNAs in every aspect of neural development, and their impairments have been observed in several neurologic disorders such as schizophrenia, autism, and RTT [201].

1.5.3 *miR132* and its effects on neural structure and function

Among the many miRNAs that are present in the CNS, *miR132* is expressed in an activity-dependent manner. This microRNA has a highly conserved sequence among vertebrates and is regulated by CREB as the transcription factor [207].

miR132 not only affects neuronal morphology, but it also controls neuronal function. One supporting evidence for such an activity comes from a study that shows BDNF-induced axonal branching in mouse retina can be promoted by *miR132* [208]. This activity-regulated miRNA also regulates dendritogenesis in mice and chicks [209, 210].

miR132 also plays a role in dendritic spine morphogenesis, affecting synaptic plasticity [211, 212].

Deregulation of *miR132* has been shown to be associated with different neurological disorders as expected from its role in neuronal development and function. Downregulation of *miR132* in the brain of patients with Huntington's disease, schizophrenia, and bipolar disorder are a few examples [213, 214].

The location and function of *miR132* is not limited to neurons. Its level changes in immune-related contexts and there is increasing evidence for *miR132* involvement in inflammatory processes. For example, inflammatory conditions induce *miR132* level in different cell types such as monocytes, mast cells, and lymphatic endothelial cells. There are also reports suggesting that hormone and nutrition condition can regulate *miR132* [215]. Furthermore, the function of *miR132* encompasses areas like tumorigenesis. For instance, *miR132* level has been shown to decrease in pancreatic cancer or increase in chronic lymphoblastic leukemia when compared to non-cancerous condition [216, 217].

1.5.4 Homeostatic regulation of MeCP2 by *miR132*

Multiple polyadenylation sites of *MECP2*/*Mecp2* result in transcription with short (~1.8 kb) or long (~10 kb) 3'UTRs. The main transcript in the brain is the longer form with highly conserved MRE for several miRNAs including *miR132*. The shorter transcript does not have these sites [218]. While the basal level of *miR132* is low before birth, it has been shown that this microRNA contributes to the BDNF-mediated neurite outgrowth in rat neonatal neurons. On the other hand, *miR132* introduction into rat primary cortical neurons negatively affects the protein level of MeCP2 [219]. Forskolin and KCl treatment both induce *miR132* through CREB pathway, leading to decreased MeCP2 level. The unchanged level of mRNA in this study is in favor of a post-transcriptional effect [187]. The authors also showed that MeCP2 overexpression as well as *miR132* blocking could increase *BDNF III* transcript while *BDNF I* without binding site for MeCP2 or *miR132* MRE did not change. In addition, in Jaenisch *Mecp2*- knockout mice both *Bdnf IV* and *miR132* were decreased. Findings from the same authors that show MeCP2 increases *BDNF* expression, together with reports that BDNF induces *miR132* leads to the suggested

homeostasis network that MeCP2 induces BDNF, which itself induces *miR132* that represses MeCP2 protein. From several studied miRNAs that can bind 3'UTR of *Mecp2*, *miR132* is the only one, which is enriched in the brain [187].

Another study has shown that during fetal stages, miRNAs other than *miR132* (for example *miR483*) can suppress MeCP2 protein. However, *miR132* can fine-tune MeCP2 level in post-natal stages [220].

MeCP2 regulation by *miR132* through binding to the evolutionary conserved binding sites has been studied in animal models in different contexts from RTT [187] to drug abuse [221], and pain transmission [222]. However, the limited number of studies on human cells or brain samples are not consistent with the results from animal models [220].

1.6 Rationale, hypothesis, and specific research aims

The two main isoforms of MeCP2 are identical in 96% of their amino acids. The MeCP2E1 isoform is slightly longer (498 amino acids in human) with 21 unique N-terminal amino acids. The MeCP2E2 isoform, which is 12 amino acid shorter, has 9 unique N-terminal amino acids [97, 100]. While MeCP2E1 isoform is present in all vertebrates, the MeCP2E2 isoform is only found in mammals [223]. Predominance of MeCP2E1 isoform in the brain and the brain region-specific expression of the two isoforms have already been shown in mice brain by independent groups including us [23, 70, 100]. In addition, the half- lives of the two isoforms have been predicted to be very different, ~4 hours for MeCP2E1, and ~100 hours for MeCP2E2 [224].

The fact that two isoforms of MeCP2 are highly similar, and observations such as the capacity of MeCP2E2 overexpression in preventing key RTT-like phenotypes in RTT mice models [122], point towards a functional overlap between the two isoforms. However, the fact that mutations that only affect *MECP2E1* can cause RTT, and *Mecp2e1*-specific knockout can generate RTT mouse models [225, 226], suggests that MeCP2E2 is not capable of compensating for the lack of MeCP2E1 *in vivo*.

It is not clear if the lower level of MeCP2E2 isoform, the specific function of each isoform, or regional distribution of these isoforms in the brain are responsible for their different functionality [225].

Due to limited availability of the human brain samples, and technical difficulties in controlled assessments of these samples, distribution and level of the two MeCP2 isoforms has remained largely unexplored in the human brain. Moreover, research into MeCP2 regulatory systems has mainly targeted animal models. A regulatory loop composed of MeCP2, BDNF, and *miR132* has been suggested to exist in the rat brain. *miR132*, as a neuronal-specific microRNA (highly conserved among vertebrates [215]) inhibits MeCP2. Expression of this microRNA is induced by BDNF, which is controlled itself by MeCP2 [187] as shown in Figure 1.9. Although a well-received study in the field, the conservation of this regulatory loop has not been studied in the human brain to date.

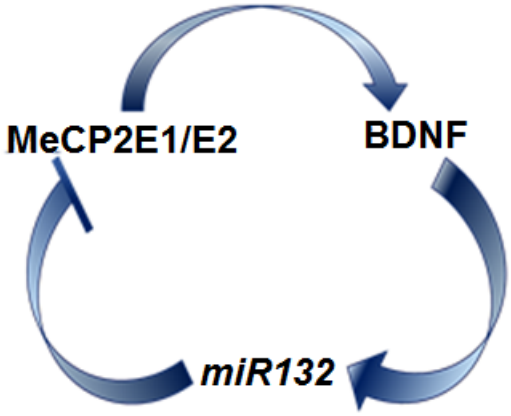

Figure 1.9 Hypothetical MeCP2E1/E2-BDNF-*miR132* regulatory network in the human brain. This regulatory loop, studied in my thesis, is proposed based on the study in rat neurons [187].

1.6.1 Rationale

Currently, there are limited studies on how MeCP2 isoforms are regulated in the brain, and how this regulation is impacted by different RTT-associated *MECP2* mutations. Furthermore, the role of BDNF deregulation in RTT pathophysiology is controversial. On the other hand, due to challenges in research on post-mortem human brain tissues and

limited access to human brain samples of this rare disease, many of our findings from animal or cellular models have not been verified in the human brain. By studying MeCP2E1/E2-BDNF-*miR132* regulatory network in human brain tissues, this research is aimed to address two fundamental questions on MeCP2 regulatory network:

1) Is MeCP2 regulatory network (MeCP2E1/E2-BDNF-*miR132)* conserved from rodents to humans?

2) What are the impacts of RTT-associated *MECP2* mutations on this regulatory network?

1.6.2 Hypothesis

I hypothesize that MeCP2 isoforms are controlled by MeCP2E1/E2-BDNF-*miR132* regulatory network in the human brain, and that *MECP2* mutation causes molecular deregulation of this network.

1.6.3 Research Aims

To address our hypothesis, two specific aims are proposed:

- Aim1: To study the components of the MeCP2E1/E2 regulatory network in the frozen lysates of control and RTT human brain tissues.
- Aim2: To study MeCP2 and BDNF at the histologic level in formalin-fixed control and RTT human brain samples, and verifying the impact of post-mortem delay on their detection.

2. Material and Methods

2.1 Ethics Statement

Our research on human brain tissues has been peer-reviewed and approved by the University of Manitoba Bannatyne Campus research ethics board and Health Research Ethical Board (REB) # HS20095 H2016: 337 for Dr. Mojgan Rastegar.

2.2 Frozen and formalin-fixed human brain tissue

Autopsy brain samples of four RTT patients, three females and one male, were analyzed in this study, and compared with the brain samples of appropriate age- and sex-matched controls**.** Table 2.1 summarizes the information about these brain samples.

T158M and R255X mutations in two of the studied RTT patients are the first and third most common RTT-causing mutations. They affect main MeCP2 functional domains, MBD and TRD, respectively [21]. The other two patients with the clinical diagnosis of RTT had P152H (male RTT patient with a missense substitution) [123] and A201V (female RTT patient with a polymorphism known to be associated with RTT) [21] mutations. The formalin-fixed brain tissue of the male patient was used along with three female RTT brain samples for Immunohistochemistry (IHC) studies. As the brain with P152H mutation did not have optimal freezing condition (embalmed prior to freezing), only the brain tissues of the three female patients were used for Aim 1. From the age- and sex-matched controls used in this study, only the NIH sample # 5646 had both frozen and fixed tissues. The rest of human brain samples were used for either molecular or IHC studies as shown in Table 2.1. Based on the potential link to cognitive, behavioral, and locomotor impairments in RTT, four brain regions (namely; the cortex, hippocampus, amygdala, and cerebellum) were selected for molecular analysis of extracted RNA and protein. However, IHC studies on formalin-fixed samples did not include amygdala, as it was not available for all cases.

The slides of control human brain tissues including the tissue array of brain samples with different PMDs, and slides of operative samples of brain and appendix were provided by our collaborator, Dr. Marc Del Bigio, at the University of Manitoba for the IHC studies (under his REB).

Table 2.1 Human brain samples used in present study. All patients and controls are Caucasian. Three RTT brain samples were donated directly to our lab for research (*), two of brain donations were coordinated through collaboration with Dr. Victoria Siu (Western University) and obtaining proper consent for research (T158M and A201V). Donation of the brain for the P152H (male RTT) was coordinated with direct contact (and consent) of the family members with Dr. Mojgan Rastegar and further coordination with Dr. Marc Del Bigio. Three fixed brain samples were provided by HSC pathology lab, Winnipeg, MB (¤). Post-mortem delay (PMD) shows the interval between death and tissue preservation. Samples from NIH neuoBiobank were obtained by Dr. Mojgan Rastegar and signed Material Transfer Agreement (MTA); Y(Years), M(Months).

NIH#	RTT/Control	Age (years)	Sex	PMD	Storage in Fixative	Frozen/Fixed Tissue
*	T158M	13	F	< 6 h	> 3.5Y	Frozen/Fixed
*	A201V	19	F	24 h	> 3.5Y	Frozen/Fixed
4516	R255X	21	F	9 h	> 14Y	Frozen/Fixed
*	P152H	44	M	72 h	> 6M	Fixed
¤	Control	14	F	24 h	< 1M	Fixed
¤	Control	18	F	48 h	< 1M	Fixed
5401	Control	19	F	22 h	> 7.5Y	Frozen
5646	Control	20	F	23 h	> 5Y	Frozen/Fixed
5287	Control	23	F	15 h	> 9Y	Frozen
¤	Control	44	M	48h	< 1M	Fixed

2.3 Transcript Analysis

RNA was extracted from the cortex, hippocampus, amygdala, and cerebellum of frozen brain samples by using TRIzole (Life Technologies Inc. 15596-062) as per manufacturer's guidelines. The frozen tissues were grinded by another lab member (Mr. Carl Olson) and aliquots of brain tissues from each region were provided for protein/RNA extraction required for this study.

2.3.1 RNA extraction

RNA extraction was done as previously reported [77]. Briefly, in a clean and RNase-free condition, 0.5 mL of TRIzol was added to the frozen brain powders of about 50 mg in each tube. The mixture was then homogenized by pipetting up and down. After incubation at room temperature for 5 minutes, 0.1 mL of chloroform per 0.5 mL of TRIzol used for lysis, was added to each tube. After 3 minutes incubation at room temperature, the tubes were centrifuged for 15 minutes at 12,000xg at 4°C. The colorless upper aqueous phase was then collected and transferred to the new tube. Five microgram of RNase-free glycogen was then added to the solution in addition to 0.25 mL of isopropanol per 0.5 mL TRIzol used at the beginning. After incubating the mixture for 10 minutes at room temperature, the tubes were centrifuged for 10 minutes at 12,000xg at 4°C. The supernatant was then discarded and the pellet was washed with 0.5 mL of 75% ethanol per 0.5 mL of starting TRIzol. The samples were then centrifuged for 5 minutes at 12,000xg at 4°C, the supernatant was discarded, and the RNA pellet was air-dried before I re-suspend it in 30µl of RNase free water. It was then gently mixed and quantified by NanoDrop 2000 micro-volume spectrophotometer, and stored in -80°C for further usage.

2.3.2 DNase treatment of extracted RNA

Ambion TURBO DNA-free™ kit was used to remove genomic DNA contamination. One and a half microliter of the 10x TURBO DNase Buffer was added to 1 µl of TURBO DNase enzyme and 1 µg of RNA. The total volume was reached to 10.5 µl by using sterile RNase-free water. After being gently mixed, the tube was kept in 37°C water bath for 30 minutes. Then 2 µl of DNase inactivating reagent was added to the tube, mixed gently,

and kept at room temperature for 5 minutes while it was flicked every one minute. Then the tube was centrifuged at 13,000 rpm for 1.5 minutes and the supernatant was transferred to a new tube and quantified again.

2.3.3 cDNA synthesis

One microliter of dNTPs, 0.1 µl of Random primers, and 500ng of DNase treated RNA were diluted to 13 µl in sterile water. After mixing gently, the tube was incubated on a hot plate of 65°C for 5 minutes. Then it was moved to an ice where it was incubated for 2 minutes. After a brief spin, 4 µl of 5x First Strand Buffer, 1 µl of 0.1 M DTT, 1 µl of RNaseOut, and 1 µl of Superscript III Reverse Transcriptase (from Invitrogen) was added to 13 µl of the cDNA synthesis mix. Then the tube was incubated at room temperature for 5 minutes followed by 60 minutes incubation at 50°C and 15 minutes incubation at 70°C on hotplate. The tube containing the synthetized cDNA was then transferred onto ice and stored in -20 until being used.

2.3.4 Quantitative real time polymerase chain reaction (qRT-PCR)

Quantitative RT-PCR performed in a Fast 7500 Real-Time PCR machine (Applied Biosystems) by using SYBR Green-based RT-PCR Master Mix (Applied Biosystems). Transcripts levels of *MECP2* isoforms and *BDNF* were assessed using the primers listed in Table 2.2.

The qRT-PCR reaction mix was made of 1 µl primer mix, 10 ng template, 10 µl SYBR Green, and ultra pure water (Invitrogen) up to 21 µl of volume. Ten microliter of the reaction mix was added to each well in duplicate. The condition of qRT-PCR for the used primers (*MECP2E1*, *MECP2E2*, *BDNF*, and *Glyceraldehyde 3-phosphate dehydrogenase, GAPDH)* was already optimized in Dr. Rastegar's lab and the running method was 95°C (10 minutes), 35 cycles of 95°C (15 secnds), 60°C (1 minutes), 72°C (45 seconds), and 72°C (10 minutes), followed by a melt curve of 95°C (15 seconds), 60°C (1 minutes), 95°C (30 seconds), and 60°C (15 seconds).

The $\Delta\Delta C_T$ method was used to measure relative expression of target genes, and results were normalized to *GAPDH* as the housekeeping gene. Microsoft Excel 2.10 and GraphPad Prism 7 were used for the analysis of the results**.**

Table 2.2 List of primers used for qRT-PCR in this project.

Gene	Forward (5' to 3')	Reverse (5' to 3')	Ref
MECP2E1	AGGAGAGACTGGAGGAAAAGTC	CTTGAGGGGTTTGTCCTTGA	[97]
MECP2E2	CTCACCAGTTCCTGCTTTGATGT	CTTGAGGGGTTTGTCCTTGA	[97]
BDNF	TAACGGCGGCAGACAAAAAGA	GAAGTATTGCTTCAGTTGGCCT	[227]
GAPDH	CCACTCCTCCACCTTTGAC	ACCCTGTTGCTGTAGCCA	[228]

2.3.5 TaqMan assay for *miR*132 detection

The TaqMan®MicroRNA assay kit from ThermoFisher was used to analyse and quantify *miR132.* First cDNA was reverse transcribed from DNase-treated RNA by TaqMan®MicroRNA reverse transcription kit (ThermoFisher Cat. No. 4366596). First, 5ng of DNase-treated RNA from a 1 ng/µl diluted solution was added to a master mix composed of 0.15 µL of dNTPs, 1 µl of MultiScribe™ Reverse Transcriptase, 1.5 µL of 10x Reverse Transcription Buffer, 0.095 µL of RNase Inhibitor (Invitrogen Cat. No. 10777019), 4.255 µL of Nuclease-free water, and 3 µl of 5x RT primer. After mixing gently and spinning briefly, the tubes were put in the thermocycler (Eppendorf® Mastercycler® pro S) at 16°c (30'), 42°c (30'), 85°c (5'). The tubes were then incubated on ice until RT-PCR reaction. The RT reaction mix was prepared from adding 1µL of TaqMan® MicroRNA Assay (20x) in a light protection condition (as it is sensitive to light), to 10 µl of TaqMan® Universal PCR Master Mix (2x) from ThermoFisher with Cat. No. 4304437, 7.67 µL of Nuclease-free water and 1.33 µL from primary cDNA product. The final volume of 20 µL was then divided into 2 wells of RT-PCR plate in two technical replicates and

RT-PCR was performed. The running method for *miR132-3p*, *miR132-5p*, and *U6* was 95°C (20 minutes), 40 cycles of 95°C (3 seconds), 60°C (30 seconds).

The TaqMan primers from ThermoFisher (hsa-*miR132-3p*, Cat. No. 000457 and hsa-*miR132-5p*, Cat. No. 002132) were used for the two strands of *miR132* and the results were normalized to *U6* snRNA (endogenous control for human and mouse #001973), with the same analysis method as the other studied genes.

2.4 Western Blot (WB)

2.4.1 Extraction and quantification of nuclear and cytoplasmic protein fractions

Nuclear and cytoplasmic protein fractions were isolated from the cortex, hippocampus, amygdala, and cerebellum of frozen brain samples by NE-PER Extraction Kit [Thermo Scientific, Cat. No. 78833]. Based on previous studies in our lab [70], and according to the manufacturer's instruction the ice-cold Cytoplasmic Extraction Reagent that I mixed with Roche Protease Inhibitor (PI), Cat No. 11 836 153 001, was added to the frozen tissue powder (200 µl for 20 mg of tissue + 4 µl of PI). After 15 seconds of vigorous vortex, it was incubated on ice for 10 minutes. At the next step, Cytoplasmic Extraction Reagent II was added to the mixture (11 µl for 20 mg of tissue), then it was mixed for 5 seconds before incubation on ice for 1 minute and then centrifugation at 16,000x g for 5 minutes at 4°C. The supernatant containing the cytoplasmic fraction of protein was transferred to pre-chilled tubes and kept on ice for aliquoting and later storage at -80°C. The pellet in the first tube was resuspended in ice-cold Nuclear Extraction Reagent mixed with Roche PI (100 µl for 20 mg of tissue + 2.5 µl of PI). Then it was mixed vigorously for four rounds of 15 seconds every 10 minutes. Subsequently, the mixture was centrifuged at 16,000x g for 10 minutes at 4°C. The supernatant which contained the nuclear fragment of protein extraction was aliquoted in pre-chilled tubes and stored at -80°C.

Bradford assay using Bio-Rad Protein Assay Dye Reagents (#5000006) was used for protein quantification according to the manufacturer's instructions. Using a spectrophotometer (SpectraMax M2e, Molecular Devices), the absorbance value of the

mixture of samples and dye was assessed in comparison with a standard curve of Bovine Serum Albumin dilution series. The Softmax Pro 5.3 was used for calculating the protein concentrations.

2.4.2 Western Blot

Polyacrylamide gel of 12-15% containing Sodium dodecyl sulfate was used for electrophoresis (SDS-PAGE). After denaturing for 5 minutes in boiling water, 20-30 µg of nuclear and/or cytoplasmic protein extracts were loaded on to the gel for assessment of MeCP2 and BDNF, respectively. Electrophoresis was performed at 100V in the cold room at 4°C. Separated proteins were then transferred to nitrocellulose membrane (for MeCP2E1 and MeCP2E2) or polyvinylidene difluoride membranes (for BDNF) and blocked in 3-5% skim milk in Tris-buffered saline with 0.2% Tween 20 (TBST) for 3h at room temperature. All primary antibody incubations were done overnight at 4°C. The primary antibodies used in this project are listed in Table 2.3. This was followed by three washes with TBST. Subsequently, membranes were incubated with peroxidase-conjugated secondary antibody at room temperature for 1h. After three times washing (each for 20 minutes) with TBST, an enhanced chemiluminescence method was used to develop the membranes (EMD Millipore). After that, the membranes were exposed to X-ray films and the developed films were scanned. Detected bands for WB on films were quantified by AlphaEase software (6.0.0). GAPDH (Glyceraldehyde 3-phosphate dehydrogenase) was checked on all membranes as the loading control and results for each antibody was normalized to GAPDH. Primary and secondary antibodies used for WB are listed in Table 2.3 and Table 2.4, respectively.

Table 2.3 List of primary antibodies.

Primary Antibody	Application and Dilution	Description	Source
BDNF (within aa 150 to the C-terminus)	WB 1:500 IHC 1:2000	Rabbit monoclonal	Abcam, Toronto, ON, Canada, ab108319
BDNF (within aa 128-247)	ELISA Capture and Detection	Mouse monoclonal	Millipore, Billerica, MA, USA,RAB0026
GAPDH	WB 1:3000	Rabbit polyclonal	Santa Cruz, Dallas, TX, USA, sc25778
MeCP2E1	WB 2 µg/ml	Chicken polyclonal	Home-made [70, 101]
MeCP2E2	WB 2 µg/ml	Chicken polyclonal	Home-made [101]
MeCP2 (C-terminus)	IHC 1:100	Rabbit polyclonal	Millipore, Billerica, MA, USA, 07-013

Table 2.4 List of secondary antibodies.

Secondary Antibody	Application and Dilution	Source
Peroxidase-AffiniPure donkey anti-rabbit IgG	WB 1:7500	Jackson ImmunoResearch 711-035-152
Biotin-Streptavidin conjugated goat anti-rabbit	IHC 1:300	Jackson ImmunoResearch 111-665-144

2.5 Enzyme-Linked Immunosorbent Assay (ELISA)

ELISA method was used to quantify BDNF protein because many regions had very low expression for BDNF in Western blots. Human BDNF ELISA kit from Sigma-Aldrich (RAB0026) was used according to the manufacturer's instructions. Intra and inter-assay coefficients of variation were <10% and <12% respectively, and the sensitivity was determined to be 80 pg/ml. BDNF level was checked in the cytoplasmic protein extract of brain samples.

First, we brought all reagents and samples to room temperature. Then, we added 100 µL of each standard or sample to the capture antibody pre-coated wells. We next covered the plate and incubated it for 2.5h at room temperature with gentle shaking. At the next step, we discarded the solution and washed the wells 4 times with 300 µl of 1x Wash Buffer by using a multi-channel pipettor. The wash solution was removed completely at each step, and after the last wash, the plate was inverted and tapped gently against clean paper towels. Hundred microliter of 1x prepared detection antibody solution was then added to each well. The plate was covered and incubated for 1h at room temperature with gentle shaking. After discarding the solution and repeating wash procedure, 100 µL of prepared Streptavidin solution was added to each well. Covered plates were incubated for 45 minutes at room temperature with gentle shaking. Next, the solution was discarded and followed by 4 times wash. After that, 100 µL of TMB One-Step Substrate Reagent was added to the wells and incubated for 30 minutes at room temperature in the dark and with gentle shaking. Finally, 50 µL of Stop Solution was added to each well and the absorbance was measured on a SpectraMax M2e plate reader (Molecular Devices) at 450 nm. The concentrations were calculated based on a standard curve that was generated by the Softmax Pro 5.3. BDNF level was calculated as ng/mg of total protein in the extract. The information about BDNF antibody in ELISA kit is presented in Table 2.3.

2.6 Immunohistochemistry (IHC) by 3, 3'-diaminobenzidine (DAB)-labeling

Formalin-fixed paraffin-embedded sections of human brain samples (5μm thick), prepared in HSC pathology lab, were deparaffinized by placing the slides in a glass rack and putting it in the oven for 30 minutes in 60-65 °C and then in four jars of xylene (4 minutes in each jar). At next step decreasing concentrations of ethanol (100%, 95%, 70%, H_2O) were used for tissue rehydration. Then, the heat-induced antigen retrieval process was performed in Tris-EDTA buffer at PH=9 except for the over-fixed brain samples that hydrogen chloride at pH=3 showed the best results. For each condition, one litter of the buffer was added to the rice cooker and the slides, transferred to metal rack, were placed in the boiling buffer for 20 minutes. The slides were incubated in the buffer for another 5 minutes while the rice cooker was turned off and its lid was open. Then they were transferred to a glass rack and put in the water for another 5 minutes and then to a jar of 3% peroxidase (Fisher Chemicals, Cat. No. 7722-84-1) in methanol for 10 minutes in order to quench the endogenous peroxidase. After that, a 10% blocking serum with 1% BSA/PBS was used to reduce non-specific bindings of the antibodies. Sections were then incubated for 2h at room temperature with 400 microliter per slide of either 1/100 diluted rabbit polyclonal MeCP2 antibody (Millipore, 07-013), or 1/2000 diluted rabbit monoclonal BDNF antibody (Abcam, 108319). The antibody diluent used in all steps was a solution made from 1x Phosphate-buffered saline (PBS) and 0.5% Bovine Serum Albumin (BSA). The Biotin-Streptavidin conjugated goat anti-rabbit antibody (Jackson Immuno Research 111-665-144) and Peroxidase-Conjugated Streptavidin were both used with 1/300 dilution as secondary and tertiary antibodies. The 3, 3'-Diaminobenzidine (DAB) in H2O2 (10/1) was the chromogen solution for visualising the proteins. The chromogen solution (400 μL for each slide) was added to the slides while they were protected from light. After incubating with DAB solution for 8 minutes in order to detect MeC2, and 5 minutes in order to detect BDNF, the slides were dipped into water. After 5 minutes, all sections were counterstained with Hematoxylin (Fisher Chemical Cat. No. 28-600-99). In order to do that, the slides were immersed in hematoxylin for 30 minutes, then rinsed under the tap water, and next dipped 3 times in acid alcohol (10 mL of concentrated HCl in 1L of 70%

ethanol), once in water, and 3 times in ammonia water (7.5 ml of concentrated ammonia in 1L H_2O). Finally the stained slides were dehydrated by dipping in the increasing concentrations of ethanol (70%, 95%, 100%), and Xylene. Coverslips were mounted to the slides by Permount Medium from Fisher Chemical (Cat No. SP15-100).

IHC slides were examined by an Axio Observer Z1 inverted microscope (Carl Zeiss Canada Ltd). Images were obtained and analyzed using Zen software (Carl Zeiss Canada Ltd.), and assembled into figures using Adobe Photoshop C5 and Adobe Illustrator C5. The information about antibodies used for IHC are presented in Table 2.3.

2.7 Statistical Analysis

GraphPad Prism software was used for statistical analysis and generating the graphs. Statistical significance was determined by one-way ANOVA with multiple pairwise comparisons among different brain regions for transcript assessments and protein quantifications by ELISA. Student's t-test was used to compare controls and RTT samples for these parametric data. Western blot non-parametric results were analysed by Kruskal-Wallis, and Mann-Whitney tests. The significance level was determined at *$P<0.05$, **$P< 0.01$, ***$P< 0.001$, and ****$P< 0.0001$.

3. Results

Autopsy brain samples of four patients with a diagnosis of RTT and with four different *MECP2* mutations were compared in this study with their age and sex-matched controls. A summary of the information about these RTT samples in addition to the control brain tissues used in this project is provided in Table 2.1. Frozen brain samples of four different brain regions (cortex, hippocampus, amygdala, and cerebellum) from three female RTT patients and their age and sex-matched controls was used to study transcript and protein level of *MECP2*/MeCP2 isoforms, *BDNF*/BDNF, as well as *miR132-3P,* and *miR132-5P*. Formalin-fixed parts of all four RTT brains (three female and one male) were available for three regions (cortex, hippocampus, and cerebellum), and were used for histological studies of the total MeCP2 and BDNF proteins. The male RTT brain was not used for the first aim of our project as it had not been frozen properly. In addition, the amygdala was not included in histological studies as it was not available for all fixed brain samples. Our plan for the experiments was adapted with these conditions.

The limited IHC studies on RTT brain samples for total MeCP2 go back to 2002 [23, 229]. After 16 years, we tried to reopen the discussion about the challenges in MeCP2 immunolabeling of human brain samples. In order to do that, we studied the total MeCP2 in different regions of human brain, and for the first time we have targeted Post- Mortem Delay (PMD), as one of the potential factors that affect IHC staining. Furthermore, as the unpublished data from our lab had shown similar pattern among human brain tissues stained by antibodies against total MeCP2 and MeCP2E1, and in order to have a point of reference in the literature, the focus of my IHC studies was total MeCP2 in addition to BDNF.

3.1 Clinical history of studied RTT patients and the pathological findings in post-mortem brain samples

The clinical history of RTT patients and the macroscopic description of autopsy brain samples presented below are based on the information we received from London Health Sciences Centre Genetics Clinic (for cases #1 and #2), NIH NeuroBioBank (for case #3), and Ontario Forensic Pathology Service (for case #4). Reports of macroscopic examination for the three non-NIH brain samples used in this study was provided by Dr. Marc Del Bigio, neuropathologist and our collaborator in this research. Histopathologic studies of three brain regions (cortex, hippocampus and cerebellum) in three RTT patients and their sex- and age-matched controls were performed on Hematoxylin and Eosin (H&E) stained slides prepared by Pathology, and Human Anatomy and Cell Science Departments at the University of Manitoba as a paid service.

3.1.1 Case I (T158M)[a]

The first patient was a 12.5-year-old girl from Ontario, Canada who was born apparently normal without any remarkable medical condition before or after birth. She started showing gradual regression and delay in developmental milestones after 6 months with a further advancement at 18 month, when she stopped walking and purposeful hand movement, and became nonverbal. Repetitive abnormal hand movements, autonomic abnormalities (such as cardiac arrhythmia, and respiratory problems), and seizure disorder were later added to the clinical picture of the disease. She had generalized polyspiking waves (grade-four dysrhythmia) in electroencephalography, and mild brain atrophy was reported by Magnetic Resonance Imaging of the head. She was labeled as a Rett Syndrome patient clinically when she was 3 year old, and the genetic testing showed a mutation in exon 3 of the *MECP2* gene designated as 473C>T (non-conservative amino acid substitution pThr158Met). Her seizure disorder was treated

[a] Additional information about this case is presented in Olson CO, Pejhan S, Kroft D, Sheikholeslami K, Fuss D, Buist M, Sher AA, Del Bigio MR, Sztainberg Y, Siu V, Ang LC, Sabourin-Felix M, Moss T, and Rastegar M: MECP2 mutation interrupts Nucleolin-mTOR-P70S6K signaling in Rett Syndrome Patients. Frontiers in Genetics. doi: 10.3389/fgene.2018.00635 (accepted manuscript).

initially with Phenytoin and later with Valproic acid. Following her gradual neurological decline, she became dependent on gastrostomy tube for feeding and positive pressure airway support (BiPAP) nightly. She succumbed to respiratory failure before turning 13. Her family donated her brain to our lab for research purposes through arrangements by Dr. Victoria Siu from Western University, London, Ontario, and in collaboration with Dr. Mojgan Rastegar. We received the brain with its right half frozen, and the left half formalin-fixed.

The brain was small (797g in weight before fixation) with bilateral patchy orange discoloration on the internal surface of the dura and adjacent to the falx cerebri, due to partially resolved subdural hemorrhage. Slightly thinner corpus callosum in posterior area, and mildly enlarged lateral ventricles were the only findings in gross examination of the brain (Figure 3.1 A). No focal abnormalities were seen in the cerebellum.

Microscopic examination of H&E stained slides did not reveal eosinophilic neurons or inflammation in the studied regions of the brain. Congested areas were present in different studied regions including hippocampus. Our collaborator, Dr. Marc Del Bigio performed neuropathological examination on the brain slides and reported subjectively, increased cell density and smaller pyramidal neurons in comparison to an age and sex-matched control (Figure 3.1 B, C).

Specific staining and IHC studies were performed in the Pathology Department for markers other than what we looked for in this project. They showed diffuse mild microglial activation in the white matter and leptomeninges through immunostaining for the Human Leukocyte Antigen (HLA)-DR. However, there were no microglial nodules in gray matter structures (which would have been suggestive of neuronal death). Immunohistochemistry studies for Neurofilament showed no abnormalities in the cerebellum. In addition, the dura exhibited hemosiderin-containing macrophages on the inner surface, which, stained with Perls Prussian blue method.

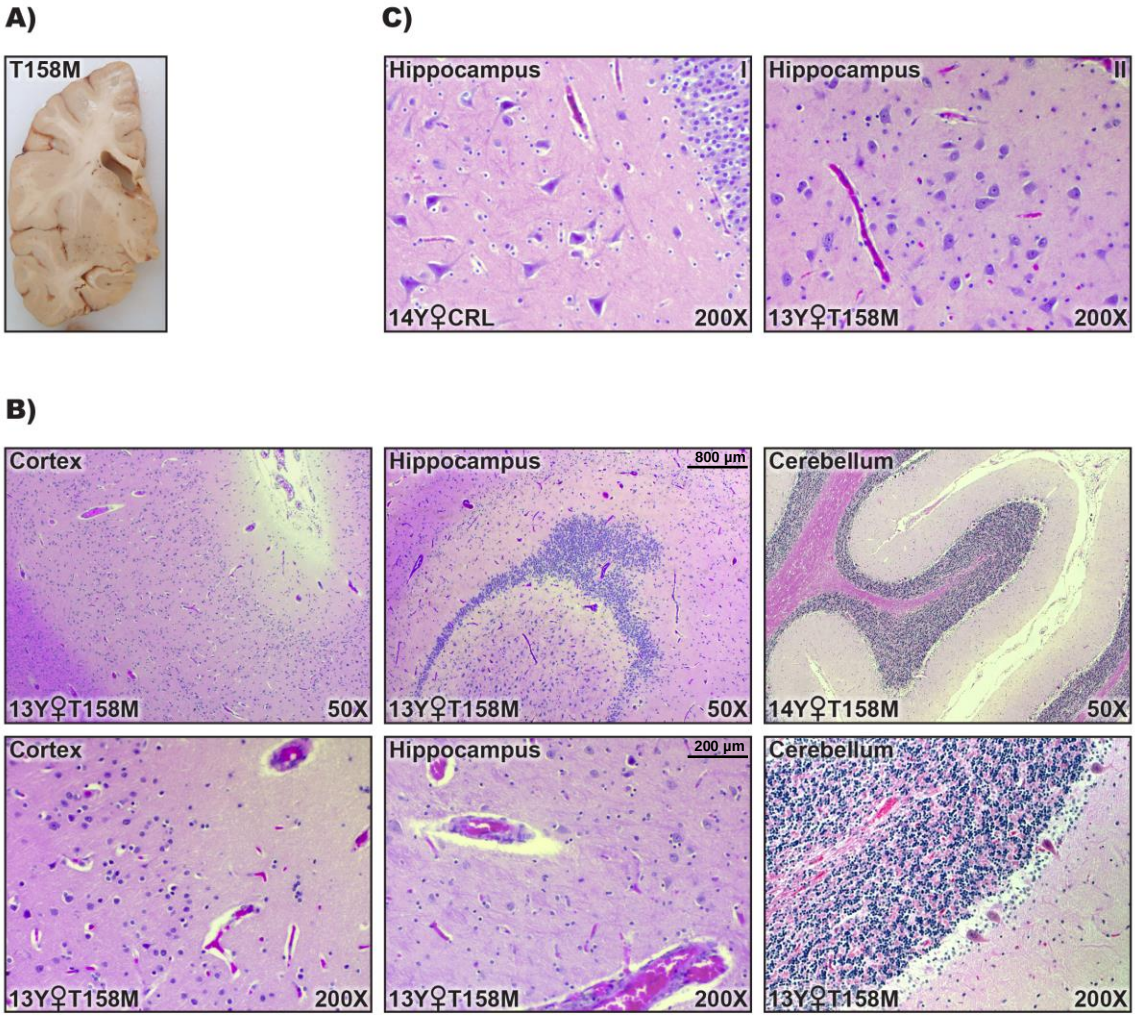

Figure 3.1 Gross and microscopic examination of 13 year-old RTT patient with T158M mutation in MeCP2 protein. A) Left half of the hemisphere in coronal section of formalin-fixed brain from RTT patient with T158M mutation shows mildly enlarged ventricle. B) Vascular congestion is observed in H&E stained slides of T158M brain tissue, especially in the hippocampus. C) Smaller pyramidal neurons and increased cell density are observed in hippocampal region of T158M brain (II) compared to age and sex matched control (I); Control (CRL). Scale bars shown in two middle figures of part B are similar in all identical magnifications.

3.1.2 Case II (A201V)

The second patient was an 18.5-year-old girl without any known risk factor or remarkable family history who was apparently normal up to 4 months of age. She was referred to the Neurology clinic at the age of 7 months because of the delay in motor development, which became more serious during the next two years. She developed seizure episodes, which were treated with Lamotrigine. She was unable to talk, but despite decreased central muscle tone, she could walk with support by a wide-based, stiff-legged gait. With a height of 75th percentile, her head circumference was at 25th percentile. She showed non-specific changes in EEG, but the rest of paraclinical tests including magnetic resonance imaging of the head were reported as normal. In addition to motor and cognitive features, the spontaneous laugh episodes she had led to the clinical diagnosis of Angelman Syndrome eventhough it was not supported by the genetic testing of chromosome 15q region. The diagnosis was then shifted toward Rett Syndrome, and the sequencing of *MECP2* gene showed an amino acid substitution (c602C>T; pAla201V). The A201V sequence variant had been interpreted as clinical neutral by the testing lab. According to Rett BASE, this is the 21st most commonly reported amino acid substitution in RTT [21]. Some reports in the database suggest that this is a polymorphism that does not cause the disease. She died when she had less than 19 years old. Her family donated her brain to our lab for research purposes through arrangements by Dr. Victoria Siu from Western University, London, Ontario, and in collaboration with Dr. Mojgan Rastegar. We received the brain while its right half was formalin-fixed and the left half was frozen.

The brain was small (1179 g in weight before fixation). No obvious abnormalities were found in gross examination or sectioning of different parts of the brain including the cerebellum (Figure 3.2 A).

Microscopic evaluation of the H&E stained slides did not show evidence of neuron death or inflammation. The dentate gyrus of the hippocampal formation was slightly thin towards the end and focally hypocellular (Figure 3.2 B, C). The rest of studied sections including the sections from the cerebellum were unremarkable.

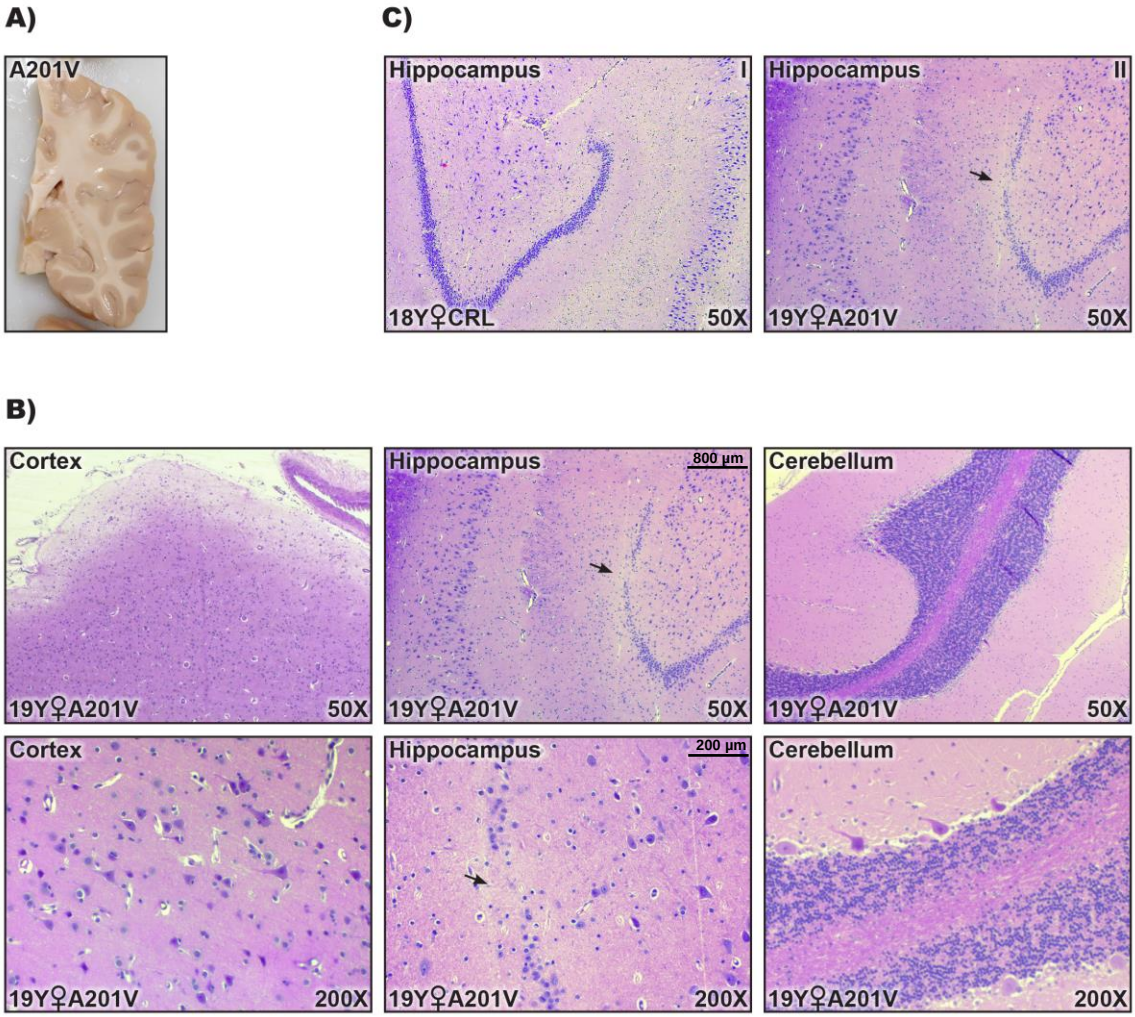

Figure 3.2 Gross and microscopic examination of 19 year-old RTT patient with A201V mutation in MeCP2 protein. A) Right half of the hemisphere in the coronal section of formalin-fixed brain from RTT patient with A201V mutation is macroscopically unremarkable. B) H&E stained slides of brain tissue are not showing any remarkable change. C) Thin and slightly hypocellular dentate gyrus is observed in the hippocampus of A201V brain (II) versus control (I); Black arrows (hypocellular area of dentate gyrus); Control (CRL). Scale bars shown in two middle figures of part B are similar in all identical magnifications.

As mentioned for the previous case, specific staining and IHC studies were performed in the Pathology Department for markers other than what we looked for in this project. They showed a negative labeling in the cortex for NeuN (a neuron differentiation marker), which could be the result of overfixation artifacts. Cortical lamination was identified as normal with regular distribution of calretinin-immunoreactive inhibitory interneurons. HLA-DR immunoreactivity showed microglial activation throughout temporal and cerebellar white matter; which could be related to a premortem illness. Immunostaining for Neurofilament showed the bodies of stellate cells in the molecular layer of the cerebellum. Calretinin labeled brush cells in the granular layer.There were no abnormal axonal varicosities.

3.1.3 Case III (R255X)

The third patient was a 21-year-old girl who was clinically diagnosed with Rett Syndrome at the age of three. She showed regression in developmental achievements at about 16 months of age by arrest in speech development, difficulties in purposeful hand movements, and losing her ability to potty train. Recurrent seizures, mostly complex partial with consciousness alterations, started at the age of two. She lost her life nine days before turning 21. Parts of her brain tissue were received by Dr. Mojgan Rastegar from NIH NeuroBioBank, under a signed & approved Material Transfer Agreement (MTA) between the University of Manitoba and NIH NeuroBioBank.

NIH NeuroBioBank reported slight cerebral atrophy and mild degenerative changes in the cerebellum and substantia nigra. Post-mortem genetic analysis showed a heterozygous C>T transition at nucleotide 763, which substitutes a stop codon for an arginine at amino acid 255 of the MeCP2 protein (c.763>T, p. R255X).

Microscopic evaluation of H&E slides was unremarkable in different studied regions except for less neuropil compared to age- and sex-matched control, which was suggested subjectively by our collaborator, Dr. Marc Del Bigio, based on his experience in Neuropathology. Artifacts apparently caused by fixative were also observed in different brain regions (Figure 3.3 A, B).

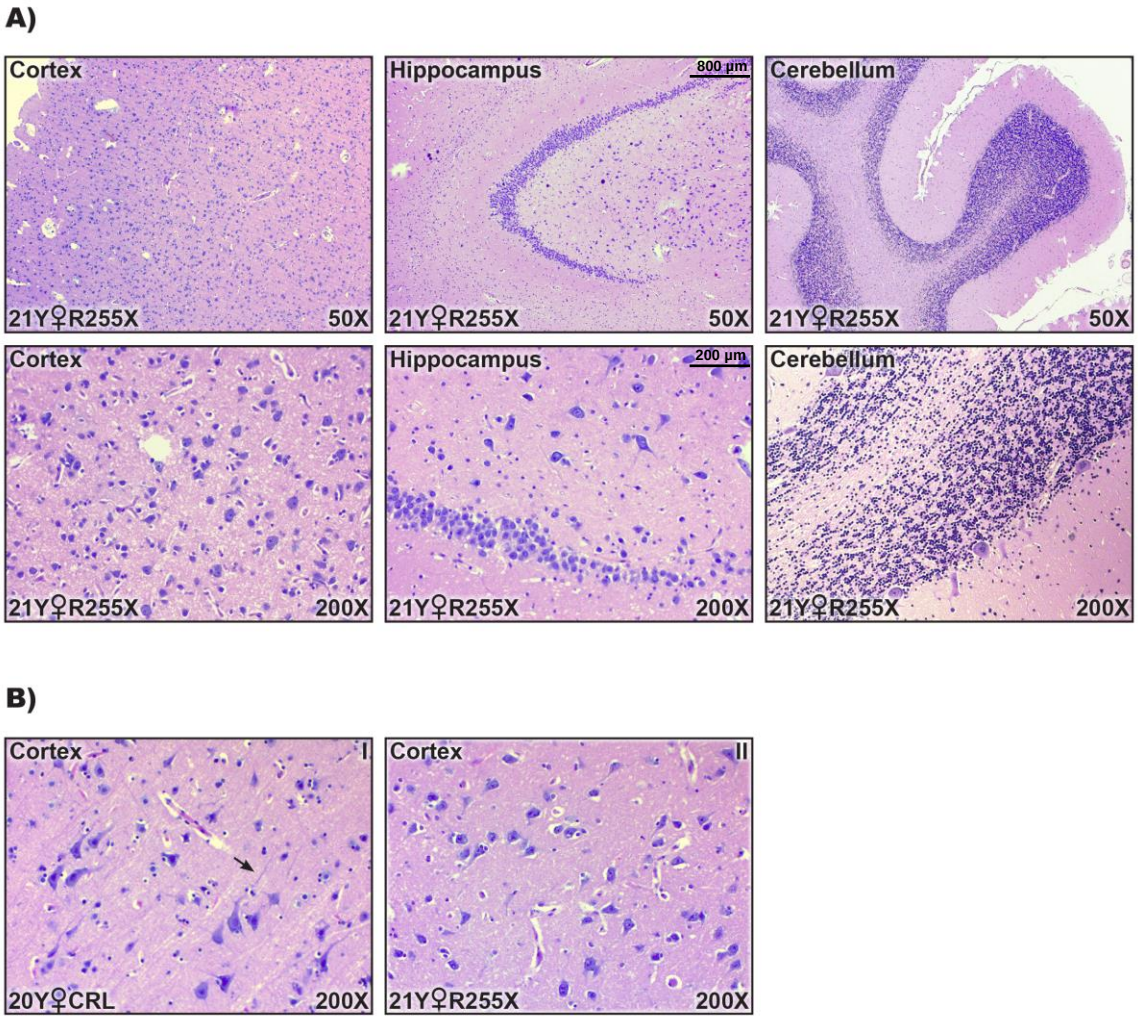

Figure 3.3 Gross and microscopic examination of 21 year-old RTT patient with R255X mutation in MeCP2 protein. A) H&E stained slides of brain tissue are not showing remarkable changes. B) Less neuropil is observed in cortical region of RTT brain with R255X mutation (II) compared to age- and sex-matched control (I); Black Arrow (neuropil); Control (CRL). Scale bars shown in two middle figures of part A are similar in all identical magnifications.

3.1.4 Case IV (P152H)

The last patient was a 44-year-old man with a history of significant developmental delay, who had been diagnosed at birth with cerebral palsy. He had scoliosis, sleep apnea, and tremor.

Cytogenetic analysis was performed in 2011. Microarray analysis on peripheral blood specimen showed a 0.313Mb deletion in chromosome region 1q32.1, which resulted in the loss of one copy of RefSeq genes *TMEM9*, *IGFN1*, *LAD1*, and three OMIM Morbid Map genes *CACNA1S*, *PKP1*, *TNNT2*. The clinical significance of these findings was considered unknown.

In 2012, Next Generation Sequencing Panel for X-Linked Intellectual Disabilities (XLMR) showed a P152H mutation of MeCP2 caused by a suspected pathogenic variant of *MECP2* gene (exon 4, c.455C>A). In 2016, this mutation was reported in a male individual with intellectual disabilities, which is the 4th patient in our study [123]. This mutation has not been reported in RettBASE (database for Rett Syndrome) [21] yet. Based on the authors of the report from 2016, the patient with P152H had muscle weakness, regression of motor skills, spoke several words, and had a Clinical Severity Score of 18. Experimental transfection of the mutant DNA into cultured cells had shown a moderate effect on heterochromatin clustering.

In July 2017, he was diagnosed with squamous cell carcinoma that was identified after drainage of a chronic "cyst" on his right lower chest/upper abdomen. Less than one month after a surgical procedure on the skin lesion, he died suddenly and unexpectedly in his sleep. Initially, his body was sent to the School of Anatomy at the University of Toronto, where he was embalmed. Upon the request of his mother, a limited autopsy was performed there and evidence of embalming was reported without any evidence of trauma or meningitis. The brain samples were donated for research to Dr. Rastegar's lab. Donation was coordinated by direct contact of the patient's mother with Dr. Mojgan Rastegar, and consent for research in our lab. According to the guidance from our lab, the brain was removed; a portion of the left frontal lobe was frozen (-80ºC), and the remainder was fixed before being sent to the University of Manitoba.

Based on autopsy reports, the brain weight (1310 g) was within the normal range for a male of his age [230]. Macroscopic evaluation performed by our neuropathologist collaborator, Dr. Marc Del Bigio, showed an unremarkable dura with pale vessels. That pallor was also observed in the right frontal lobe, right temporal lobe, left temporal lobe, brainstem, and anterior aspects of the cerebellum, most probably as a consequence of the embalming perfusion. The left parietal lobe, both occipital lobes, and the posterior cerebellum apparently had not been perfused well. The anterior falx cerebri was partially calcified. There were no obvious abnormalities in the gyral pattern. The cerebellum had a normal size. Coronal sections through the cerebral hemispheres and horizontal sections through the brainstem and cerebellum demonstrated no focal abnormalities (Figure 3.4).

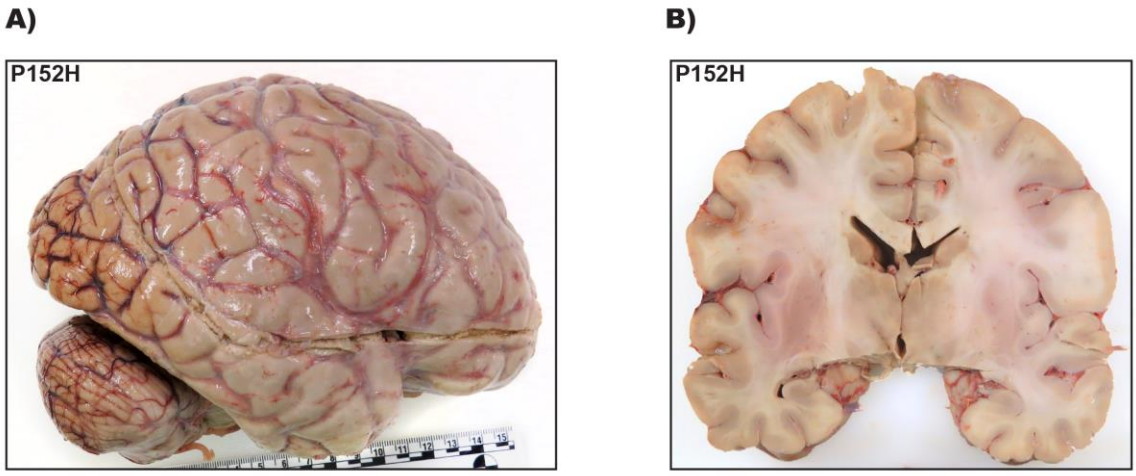

Figure 3.4 Macroscopic examination of 44 year-old male RTT patient with P152H mutation in MeCP2 protein. A) Unremarkable outer surface of right hemisphere of cortex and cerebellum. The pallor, better seen close to the ruler, is due to the embalming perfusion. B) Unremarkable coronal sections through the cerebral hemispheres except for the pallor caused by embalmment.

Microscopic evaluation of H&E slides as well as specific staining and IHC studies were performed in the Pathology Department for markers other than what we looked for in this project. The microscopic examination was reported as unremarkable without features of dead neurons or inflammation. The only reported abnormality was in the left

and right hippocampi at the level of the lateral geniculate nucleus where there were considerable irregularities of the dentate gyrus. The posterior right hippocampus exhibited rare slightly eosinophilic and pyknotic neurons in the CA1 sector. The dentate gyrus was reported to be somewhat sparse and convoluted. Immunostaining of the frontal, temporal, and parietal cortices performed for NeuN was reported to be variable, perhaps as a consequence of the embalming fixation. The laminar pattern of cortical neurons was reported as apparently preserved on the NeuN, non-phosphorylated neurofilament, and calretinin (calbindin 2) immunostainings. No abnormal immunostaining for hyperphosphorylated tau protein (AT8 antibody) was reported. Immunostaining of inhibitory interneurons in the frontal lobe with calretinin was reported as reduced; which could be also a consequence of the embalming perfusion. Immunolabeling for neurofilament revealed a few distended cell processes in the internal granular layer; the significance of which is unclear. Perivascular spaces in the lateral temporal white matter were seen in this report as slightly enlarged. Structural features of the brainstem and organization of the cerebellar cortex were reported as normal.

Figure 3.5 shows the comparison between H&E stained slides of the three female RTT and their age- and sex- matched controls. H&E stained slides were prepared in the Pathology and Human Anatomy and Cell Science Departments as a paid service.

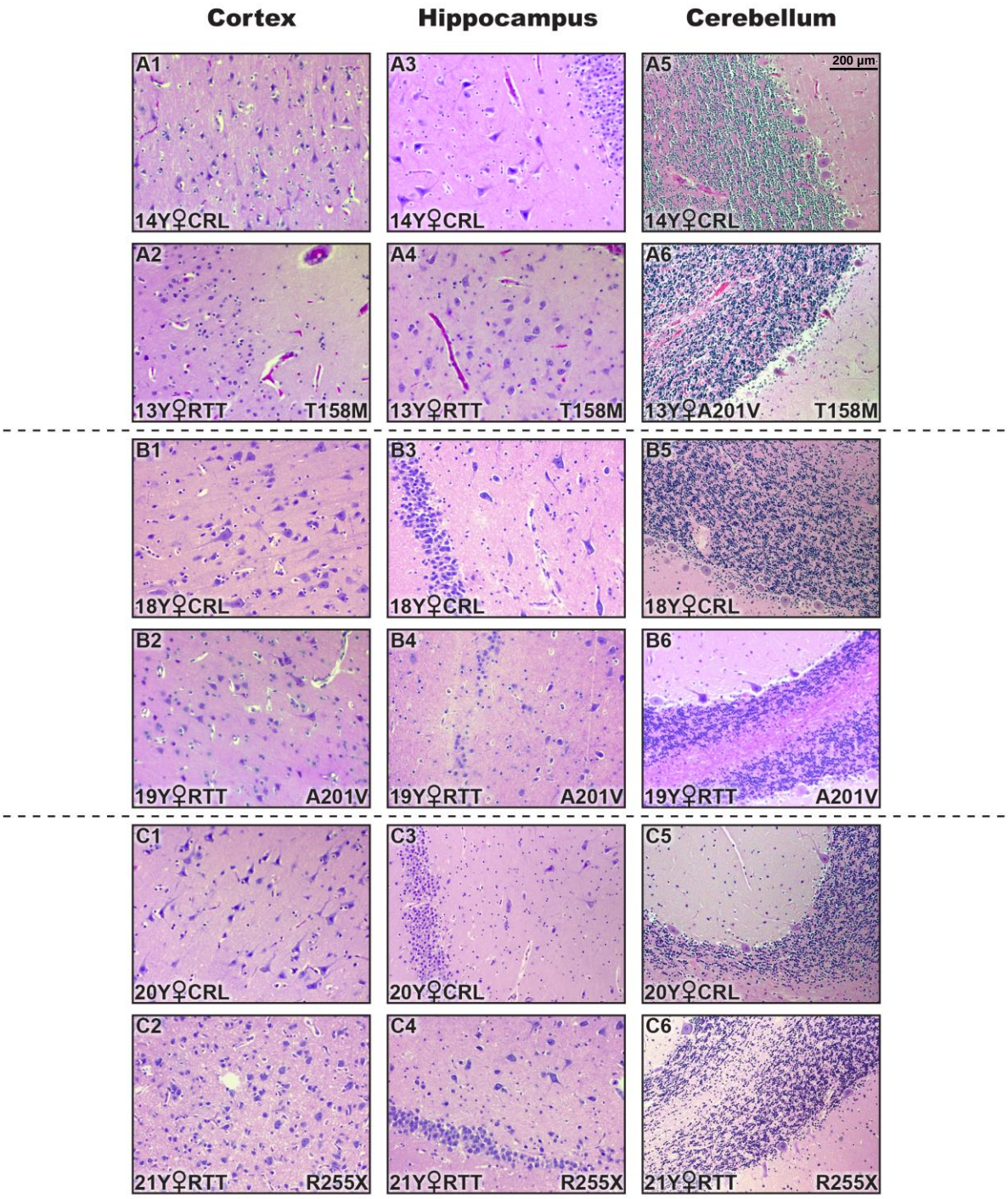

Figure 3.5 Histopathologic studies of three brain regions (cortex, hippocampus and cerebellum) in three RTT patients and their sex-, and age-matched controls stained by Hematoxylin and Eosin (H&E). There were not noticeable findings at microscopic level. Three subtle changes are shown here: small pyramidal neurons and increased cell density in hippocampal region of T158M brain (A4) compared to the control (A3); Thin and hypocellular dentate gyrus in the hippocampus of A201V brain (B4) compared to the control (B3); Less neuropil in RTT cortex with R255X mutation (C2) versus control (C1); Control (CRL); Year old (Y); 200x Magnification. Scale bar shown in A5 is identical for the whole figure.

3.2 Variations at the transcript level of *MECP2* isoforms, *BDNF*, and *miR132*

In order to evaluate the predicted regulatory network including *MECP2* isoforms, *BDNF*, and *miR132* (Figure 1.8) at the transcript level, we extracted RNA from human brain samples, and performed qRT-PCR and TaqMan assay as explained in chapter 2. The results from different regions of the brain were compared. In addition, the results from RTT samples were compared with their age-, and sex matched controls.

3.2.1 Transcript level of *MECP2* isoforms in the brain of RTT patients and controls

The expression level of *MECP2* isoforms in four different brain regions (cortex, hippocampus, amygdala, and cerebellum) was determined by qRT-PCR in both control and RTT brain samples. These four regions were selected based on their potential link to cognitive, behavioral, and locomotor impairments observed in RTT patients. Quantitative data were normalized to *GAPDH* as an internal housekeeping gene. Comparison studies of the two isoforms indicated that *MECP2E1* is the main isoform at the transcript level in all of the studied brain regions in the control and RTT patients (Figure 3.6 A, B). The transcript level of *MECP2* isoforms varied between different brain regions, with cerebellum showing significantly higher level for both *MECP2E1* and *MECP2E2* transcripts compared to the other tested regions. Only *MECP2E1* level in cortex of controls was roughly comparable with cerebellum and was significantly higher than the level of *MECP2E1* in the hippocampus.

As presented in Figure 3.6 C, both *MECP2* isoforms showed significantly lower transcript level when the average of all three RTT patients was compared to the mean of controls (considered to be 100%). There was also a difference between the four studied brain regions in this regard in a way that in the cortex, *MECP2E1* transcript had the minimum RTT/Control ratio of around 40% that was significant ($P<0.001$), while in the hippocampus the RTT/Control ratio was around 80% without any statistical significance (Figure 3.6 C).

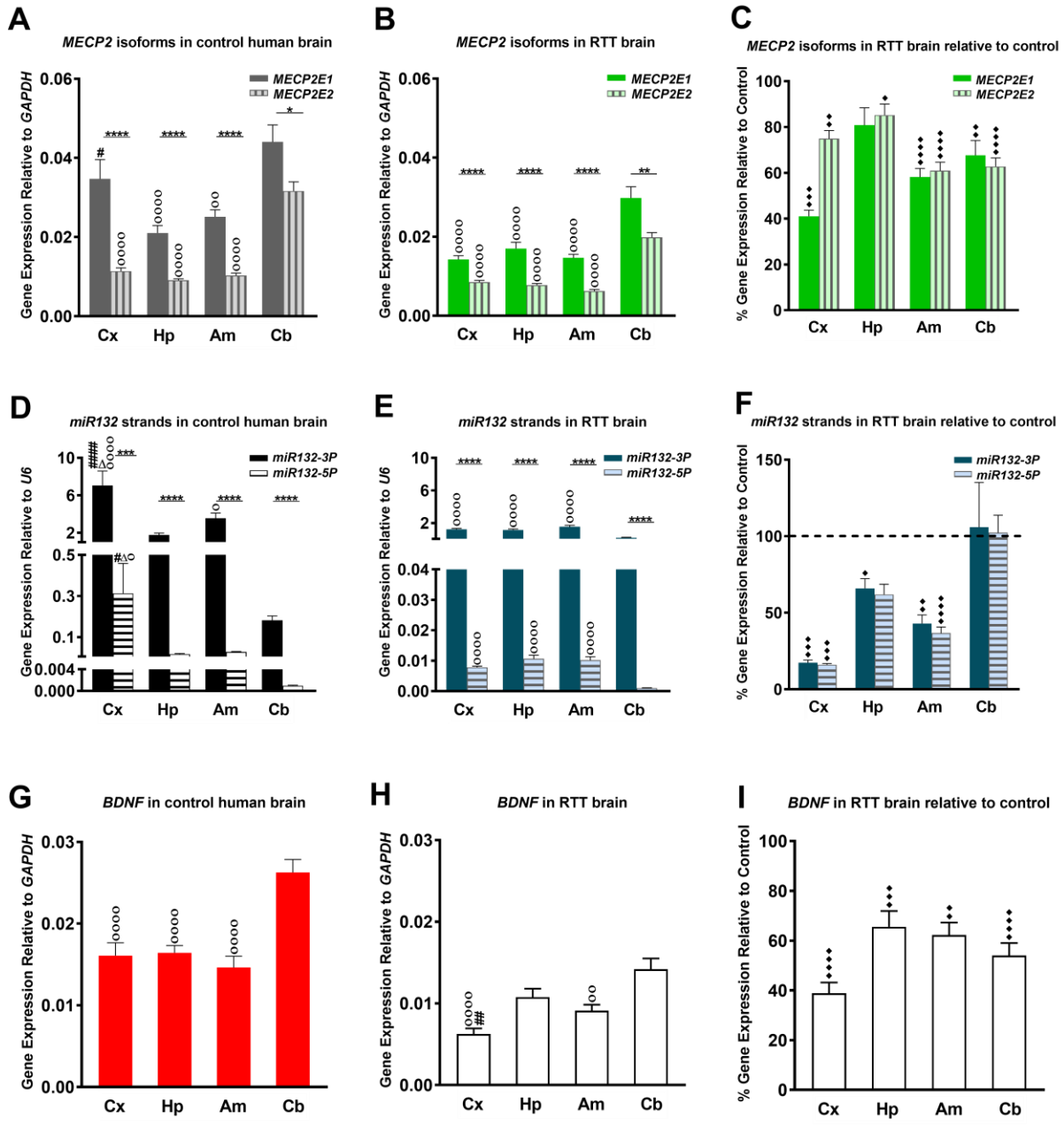
A
MECP2 isoforms in control human brain
Gene Expression Relative to GAPDH
MECP2E1
MECP2E2
Cx Hp Am Cb
B
MECP2 isoforms in RTT brain
C
MECP2 isoforms in RTT brain relative to control
% Gene Expression Relative to Control
D
miR132 strands in control human brain
Gene Expression Relative to U6
miR132-3P
miR132-5P
E
miR132 strands in RTT brain
F
miR132 strands in RTT brain relative to control
G
BDNF in control human brain
H
BDNF in RTT brain
I
BDNF in RTT brain relative to control
★ Difference of Isoforms and Strands; # Difference from Hippocampus; ◆ Difference from Controls
Δ Difference from Amygdala; O Difference from Cerebellum

Figure 3.6 Transcript levels of *MECP2E1*, *MECP2E2*, *BDNF*, and *miR132*. In all studied brain regions of three RTT (B, E) and controls (A, D), *MECP2E1* and *miR132-3P* are significantly higher than *MECP2E2* and *miR132-5P*, respectively. Cerebellum in comparison with the other three regions shows the highest level for all the studied transcripts except for microRNA132 (A, B, D, E, G, and H). RTT patients are showing lower transcript levels of *MECP2E1*, *MECP2E2*, *BDNF*, *miR132-3P*, and *5P* in four studied brain regions compared to their age-, and sex- matched controls (C, F, I). Cerebellum has exceptionally similar level of miRNAs in RTT and controls (F). Cortex (Cx), Hippocampus (Hp), Amygdala (Am), Cerebellum (Cb); N=3±Standard Error of the Mean (SEM); One-way ANOVA with multiple pairwise comparisons used among different brain regions. Student's t-test was used to compare controls and RTT samples for each parameter. The significance level was determined at *P<0.05, **P< 0.01, ***P< 0.001, and ****P< 0.0001.

3.2.2 Transcript detection of *miR132* and *BDNF* in the brain of RTT patients and controls

To evaluate the level of *miR132* in RTT and control human brain, we performed TaqMan real time PCR assay for both *3P* and *5P* strands. My data indicated that *miR132-3p* was the dominant transcript with statistical significance (P< 0.0001) in all four studied regions of brain and not only in the controls, but also in RTT patients (Figure 3.6 D, E). While *miR132-5P* strand was detected at very low levels, it still followed the same pattern as the *miR132-3P* strand.

Previous studies on the role of *miR132* in MeCP2 regulation focused on the guide strand of this microRNA (*3P*) [187, 215, 222]. However, it was shown that the passenger strand of *miR132* (*5P*), can also be stimulated by neurotrophins, and it has been suggested that it can regulate different mRNA target based on its different sequence (Figure 3.7) [231].

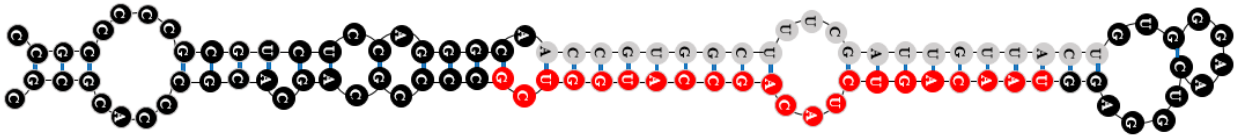

Figure 3.7 Predicted structure of human *pre-miR132*. The sequence of guide strand of *miR132* is shown in red, the passenger strand sequence is indicated in grey and hydrogen bounds are shown in blue. Adapted from Wanet et al paper [215]. By permission of Oxford University Press, License Number 4441120461177.

Noticeably, and in contrast to *MECP2*E1/E2 transcripts, the lowest level of *miR132* was detected in the cerebellum. The fact that the highest transcript level of *MECP2* isoforms was found in the cerebellum while it showed the lowest level for *miR132*, was in line with the negative regulatory role of this microRNA on MeCP2 expression in rat brain [187]. The other three brain regions showed quite similar levels of *miR132* among RTT patients. However, in control samples, cortex had a higher level of *miR132* when compared to hippocampus and amygdala (Figure 3.6 D, E). Finally, the RTT samples had significantly lower level of *miR132-3P* in all studied brain regions except for the cerebellum that showed a reverse ratio in a way that *miR132-3P* levels were similar in the cerebellum of RTT samples when compared to the controls (Figure 3.6 F).

Next, we studied the transcript level of *BDNF*, the third element of MeCP2 regulatory loop suggested in rat brain (Figure 1.8). qRT-PCR results showed that in the control brains, *BDNF* transcript had significantly higher levels in the cerebellum when compared to the other regions (Figure 3.6 G). In RTT patients, *BDNF* levels in the cerebellum were significantly higher than the cortex or amygdala. Hippocampus was not significantly different from cerebellum, but showed higher levels of *BDNF* when compared to the cortex (Figure 3.6 H). Lastly, I showed that all the four tested regions of RTT brains had significantly lower level of *BDNF* when compared to the counterpart controls (Figure 3.6 I).

Taken together, in all studied RTT brain samples *MECP2* isoforms and *BDNF* were found to be lower than controls. The decrease in these two elements of studied regulatory network showed a change in similar direction, which was expected based on the suggested model (Figure 1.8). However, only in the cerebellum the unchanged level of *miR132* in RTT brains was not against the findings in rat brain model [187]. For the other three regions, the decreased level of this microRNA was against the suppressive role of *miR132* suggested by studies on rat brain (Figure 1.8) [187].

3.3 Variations in protein level of MeCP2 isoforms, and BDNF in the brain of RTT patients and controls

At this step, we evaluated the elements of the suggested regulatory network including MeCP2 isoforms, and BDNF at the protein level. In order to do that, we extracted nuclear and cytoplasmic protein from human brain samples, and performed Western Blot, and ELISA experiments as explained in Materials and Methods. The results from different regions of the brain were compared. In addition, the results from RTT samples were compared with their age-, and sex- matched controls.

3.3.1 Expression analysis of MeCP2 isoforms in RTT and control human brain tissues

In order to evaluate the protein level of MeCP2 isoforms in the human brain samples, we performed WB experiments of isolated nuclear extracts, using the reported anti-MeCP2E1 and MeCP2E2 antibodies from our lab [70, 101, 116]. Both MeCP2E1 and E2 proteins were detected in RTT patients and control brain tissues at ~75kDa (Figure 3.8 A). Semi-quantitative analysis of WB signals (normalized to GAPDH) showed noticeable variation for both MeCP2 isoforms among the controls and RTT samples. For example, the 20 year-old control brain (NIH# 5646) showed lower levels of both isoforms in some of the studied brain regions when compared with other controls (Figure 3.8 A). Different peri-mortem factors could possibly play a role in this regard. It is also possible that different gene mutations in RTT patients led to change in MeCP2E1 and MeCP2E2 levels. For example, brain samples of the RTT patient with the R255X nonsense mutation showed lower level of MeCP2 isoforms in most brain regions. The smaller size or degradation of the truncated MeCP2 in R255X mutation may play a role in the lower amount of the protein that was quantified at ~75kDa.

We did not detect any significant difference in MeCP2 isoforms from each other in most studied brain regions, except for the cerebellum of the RTT samples; where MeCP2E1 showed a significantly higher level compared to MeCP2E2. On average, the level of MeCP2E1 in the cerebellum of RTT brain samples was significantly higher than

the cortex and hippocampus. MeCP2E1 level in the hippocampus of RTT patients was also significantly lower than amygdala (Figure 3.8 B and C). WB studies also showed that average protein level of MeCP2E1 and E2 in RTT brain was not significantly different from the controls (Figure 3.8 D), and that was not in concordance with transcript analysis studies. The storage time of the control samples was longer than RTT samples, except for the R255X (Table 2.1). That might affect the quality of proteins used in this study, and might explain the lower level of MeCP2 isoforms in controls. The different half-lives of the two isoforms of MeCP2, and the potential impact of MeCP2 mutation on these half-lives might play a role in higher MeCP2E2 level (with longer half-life) in the cortex of controls and RTTs, as well as hippocampus of RTTs, whereas *MECP2E1* was the dominant transcript in all studied samples (Figure 3.6 A and B).

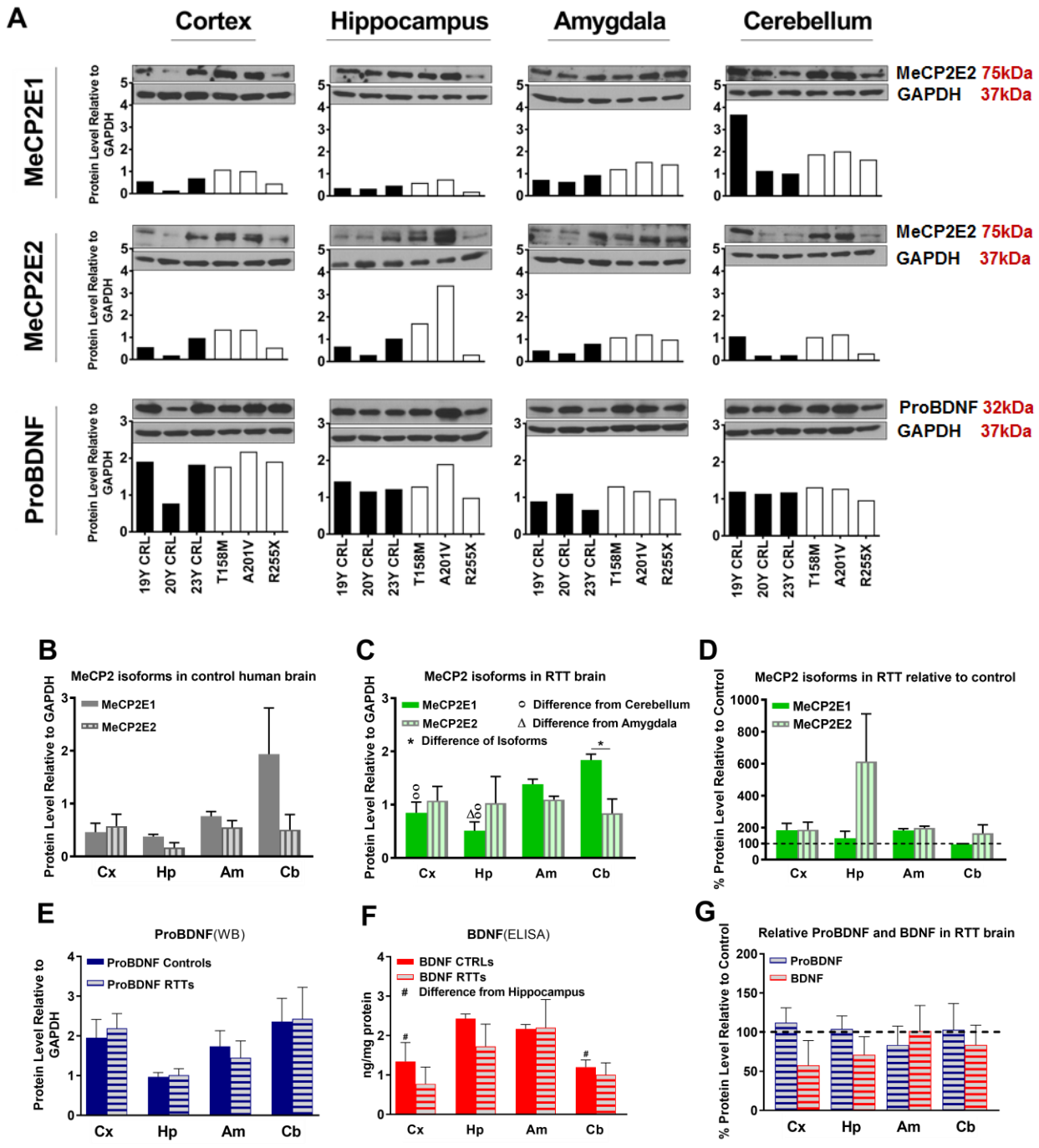
A
Cortex
Hippocampus
Amygdala
Cerebellum
MeCP2E1
MeCP2E2
ProBDNF
Protein Level Relative to GAPDH
MeCP2E2 75kDa
GAPDH 37kDa
ProBDNF 32kDa
19Y CRL
20Y CRL
23Y CRL
T158M
A201V
R255X
B
MeCP2 isoforms in control human brain
MeCP2E1
MeCP2E2
Protein Level Relative to GAPDH
Cx
Hp
Am
Cb
C
MeCP2 isoforms in RTT brain
Difference from Cerebellum
Difference from Amygdala
Difference of Isoforms
D
MeCP2 isoforms in RTT relative to control
% Protein Level Relative to Control
E
ProBDNF(WB)
ProBDNF Controls
ProBDNF RTTs
F
BDNF(ELISA)
BDNF CTRLs
BDNF RTTs
Difference from Hippocampus
ng/mg protein
G
Relative ProBDNF and BDNF in RTT brain
ProBDNF
BDNF

Figure 3.8 Protein levels of MeCP2E1, MeCP2E2, ProBDNF, and BDNF in RTT and control brain tissues. (A) Western Blot results for MeCP2 isoforms and ProBDNF normalized to GAPDH in three RTT patients and their age-, and sex-matched controls show inter-regional variations as well as variable amount of proteins among controls and RTTs. (B) Western blot results for MeCP2 isoforms quantified and analyzed in four brain regions for mean of controls show non-significant variations between the regions. (C) Western blot results for MeCP2 isoforms quantified and analyzed in four brain regions for mean of RTTs show higher level of MeCP2E1 isoform in the cerebellum compared to the cortex or hippocampus. (D) Mean of MeCP2 isoforms in RTT and controls are not significantly different in relative RTT/control analysis. (E) Western blot results for ProBDNF quantified and analyzed in four brain regions for mean of controls and RTTs show non-significant inter-regional variations without significant difference between RTT and controls. (F) ELISA results for BDNF quantified and analyzed in four brain regions for mean of controls and RTTs show significantly higher levels in Hippocampus compared to Cortex and Cerebellum of the controls. (G) Mean of ProBDNF and BDNF in RTT and controls are not significantly different in relative RTT/Control analysis. Control (CRL); Year old (Y); Cortex (Cx); Hippocampus (Hp); Amygdala (Am); Cerebellum (Cb); Kilo Dalton (kDa); N=3± Standard Error of the Mean (SEM); One-way ANOVA (ELISA)/Kruskal-Wallis test (WB) with multiple pairwise comparisons used among different brain regions. Student's t-test (ELISA)/Mann-Whiney test (WB) was used to compare controls and RTT samples for each parameter. The significance level was determined at *P<0.05, **P< 0.01, ***P< 0.001, and ****P< 0.0001. 18Y CRL (NIH # 5401); 20Y CRL (NIH # 5646); 23Y CRL (NIH #5287); R255X (NIH # 4516).

3.3.2 BDNF and ProBDNF levels in the brain of RTT patients and controls

In order to detect BDNF as a mainly cytoplasmic protein [232, 233], we performed WB with cytoplasmic extracts of frozen brain tissues of the four tested brain regions. My results showed the presence of the mature BDNF at around 14 kDa, and pro-BDNF at 32 kDa (Figure 3.9). A 28-kDa band, suggested to be truncated protein [149], is visible in our blot and has been reported in other studies. There was no significant difference between RTTs and controls for proBDNF (Figure 3.8 A and E). All results were normalized against GAPDH signals. Surprisingly, the mature BDNF was found at very low levels in the cerebellum of both RTT and control tissues (Figure 3.9). To ensure about the WB results of BDNF, we also studied BDNF levels by ELISA (Sigma-Aldrich, RAB0026), capable to quantify BDNF as low as 80 pg/ml.

Based on ELISA results, hippocampus had a higher level of BDNF in comparison with cortex and cerebellum of control brain tissue. Inter-regional differences among RTT samples were not statistically significant (Figure 3.8 F). In addition, we did not detect any

significant difference between the controls and RTT samples for either proBDNF or mature BDNF protein (Figure 3.8 G).

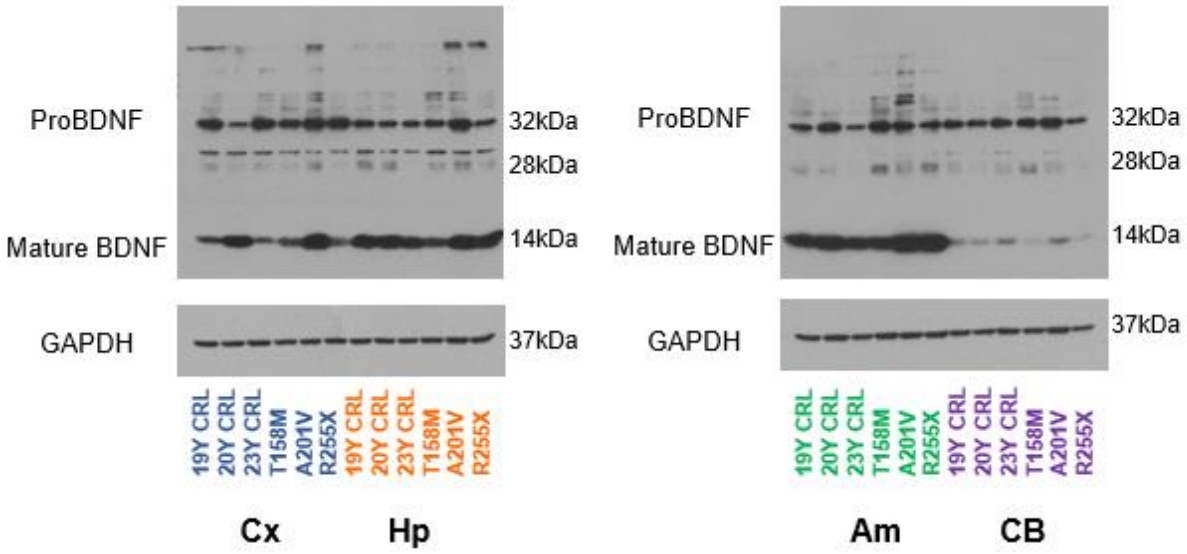

Figure 3.9 Western blot analysis of ProBDNF and mature BDNF in RTT and control brain tissues. ProBDNF is detected around 32kDa while the mature BDNF is detected around 14 kDa. The bands detected around 28 kDa have been observed by other groups and are suggested to be truncated protein [149]. Mature BDNF has a significantly lower level in cerebellar tissues of both controls and RTTs compared to the other three studied brain regions (cortex, hippocampus and amygdala). However, the level of ProBDNF in the cerebellum is comparable to the other regions. The results are normalized with GAPDH as the housekeeping protein. Control (CRL); Year old (Y); Cortex (Cx); Hippocampus (Hp); Amygdala (Am); Cerebellum (Cb); Kilodaton (kDa).

3.4 IHC studies for MeCP2 and BDNF on formalin-fixed brain samples

At this step, we studied MeCP2 and BDNF, two protein elements of the suggested MeCP2 regulatory network (Figure 1.8), in sections of three brain regions (Cortex, Hippocampus, and Cerebellum) of four RTT patients and their age- and sex- matched controls. As the second aim of this project, studying the cellular distribution of MeCP2 and BDNF in RTT and control human brain was the main goal of our IHC studies. In addition, for the first time, we studied the impact of post-mortem delay on immunostaining for these two proteins in human brain samples. DAB labeling was the method used for immunohistochemistry studies as explained in chapter two.

3.4.1 MeCP2 detection in the human operative brain samples and study of post-mortem delays

To have a good understanding of MeCP2 in a histological context, next we performed IHC studies on human operative brain samples provided as unstained slides by our collaborator, Dr. Marc Del Bigio. In order to perform DAB labeling technique, we used a commercial anti-MeCP2 antibody that recognizes both MeCP2 isoforms and has been successfully used for both IHC and WB experiments in the previous studies of our lab [70, 101]. IHC studies on operative surgical brain samples of the hippocampus from epilepsy patients were used to study MeCP2 immunoreactivity in rapidly fixed brain tissues. Here, we tried to eliminate post-mortem delay as one potential interfering factor in my study, which is based on human autopsy samples. We showed that almost all brain cells including granular cells of the dentate gyrus were positive for MeCP2 in operative samples. Endothelial cells were mainly negative in these slides (Figure 3.10 A1-C2). Further, we showed that comparable age ranges of the two sexes were similar for MeCP2-labeling (Figure 3.10 A1-C2).

Hippocampus is one of the rare regions of the human brain that we have access to its optimally preserved tissue through the surgery of epileptic patients. In order to investigate another region of the brain, we performed IHC on the cerebellar operative samples excised for decompression purpose in cerebellar infarct, or as part of surgeries for tumors. As expected, theses tissues were not intact histologically because of the cause of surgery and the surgical procedure itself. However, they showed that the majority of cells in the molecular layer were MeCP2 positive. The white matter showed a similar distribution of MeCP2 positive cells, while the Purkinje and granular cells showed sparse and weak immunoreactivity for MeCP2 (Figure 3.11). Differences in age and pre-operative conditions such as hypoxia and compression might cause the variability in immunolabeling for MeCP2 in similar cells of different specimens. Immunolabeling was performed with a single antibody at a time and different types of cells were identified based on their microscopic morphology.

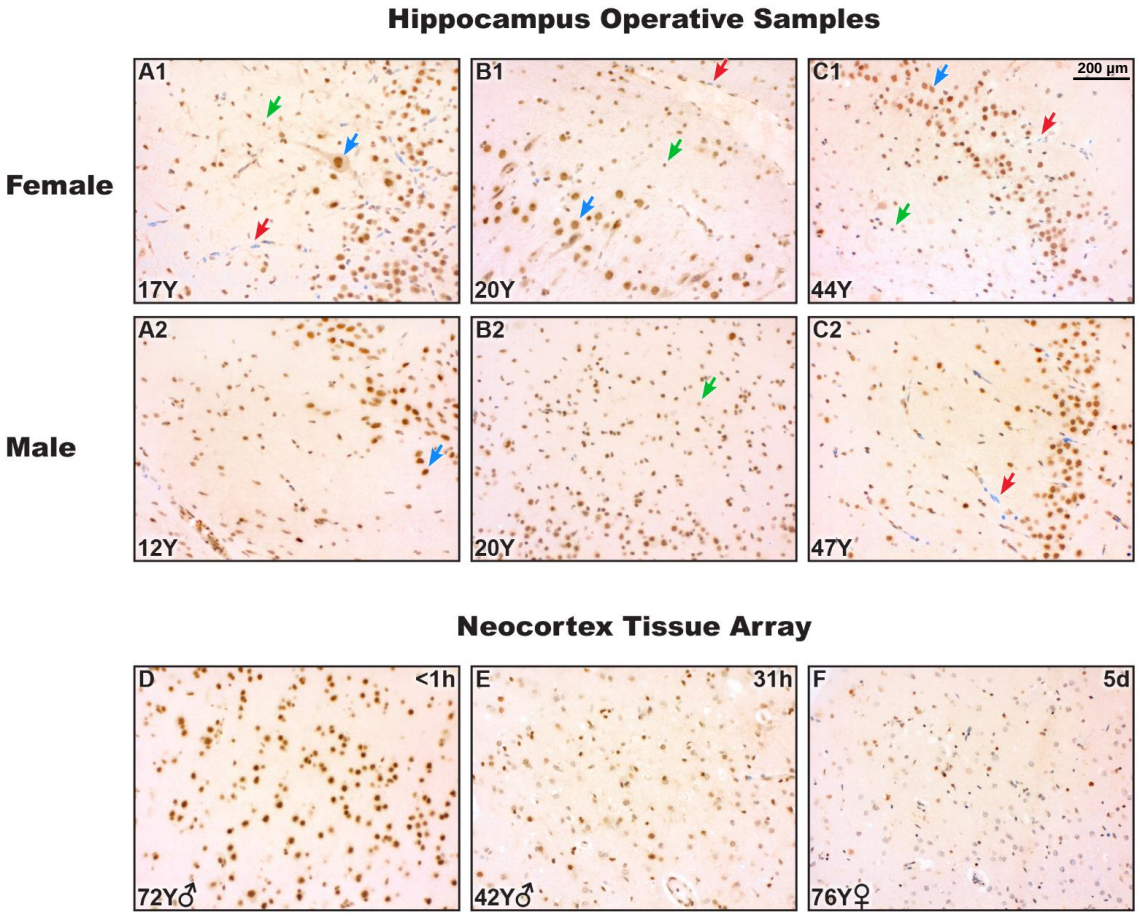

Figure 3.10 MeCP2 immunolabeling in operative samples of human hippocampus versus a tissue array of human cortex with different post mortem delays. A1-C2) Almost all brain cells (both neuronal, Blue Arrows, and glial, Green Arrows) are immunoreactive for MeCP2 in rapidly fixed operative samples excised in epilepsy patients. Endothelial cells are variable (mainly negative) in staining for MeCP2 (Red Arrows). The two sexes do not show significant differences in immunoreactivity for MeCP2 (x 200 magnification). D-F) Three samples of human brain tissue array stained for MeCP2. Human cortex with the minimum delay to fixation (<1 hour) show maximum immunoreactivity for MeCP2 (D). Delay in fixation process accompanies variable staining of similar cell groups in the studied human brain neocortex (E, F); x 200 Magnification. Scale bar shown in C1 is identical for the whole figure.

To study the impact of PMD on MeCP2 staining, next we performed MeCP2 labeling on a tissue array of human brain neocortical samples provided by our collaborator, Dr. Marc Del Bigio, who had reviewed neuropathology surgical and autopsy records in order to obtain neocortical samples that had been formalin fixed after a range of devitalization or death. Four millimetre-diameter tissue samples were punched out of representative paraffin blocks and assembled into a 5x3 array. The tissue sections on this

slide had been fixed in formalin in a range of less than one hour to 5 days. The purpose of this experiment was to investigate the PMD effects on MeCP2 immunostaining. From the 13 brain tissues on the microarray slides, 3 are shown in Figure 3.10 D-F and the rest are presented in Figure 3.12.

MeCP2 immunoreactivity in the brain tissues with minimum delay was similar to the previously studied operative samples where almost all the cells were stained positive for MeCP2 (Figure 3.10 D). Less than 24 hours delay in fixation was not associated with noticeable impact on MeCP2 immunoreactivity (Figure 3.10 E). However, more than 24-hour delay was accompanied by variable and inconsistent MeCP2 immunostaining (Figure 3.10 F). A pattern similar to our array tissues with long fixation delay had been reported in previous studies on MeCP2 labeling of post-mortem human brain tissues [29]. Table 3.1 shows that factors other than PMD might vary between different tissues on the tissue array slide. Age, medical condition prior to death such as severe hypoxia, and the fixation time with a range of 1 to 55-day storage in the formalin before slide preparation, are some of the other factors that can potentially interfere with immuno-labeling. As an example, these factors and other unknown factors that might affect immunolabeling in post-mortem tissue could be the reason behind more intense labeling in the brain tissue with a 4-day delay in fixation (Table 3.1, and Figure 3.12 L) when compared to 6h delay in another sample (Table 3.1, and Figure 3.12 C).

As part of optimization process for MeCP2 immunolabeling, we also performed IHC on normal appendix tissue fixed without delay after surgery. This operative tissue was used because of accessibility of normal appendix, as the clinical manifestations of appendicitis could be mimicked by the pathology of other organs. In addition, a previous study on human intestine had shown low detectable level of *MECP2* transcript in human colon and barely detectable amount of *MECP2* in the small intestine [23]. Our IHC study showed that parasympathetic ganglia of myenteric plexus, and vast majority of smooth muscles in muscularis mucosae and two layers of muscularis externa were positive for MeCP2. However, other cell types in mucosal and submucosal layer including epithelial and lymphoid tissue did not show nuclear labeling for MeCP2 (Figure 3.13).

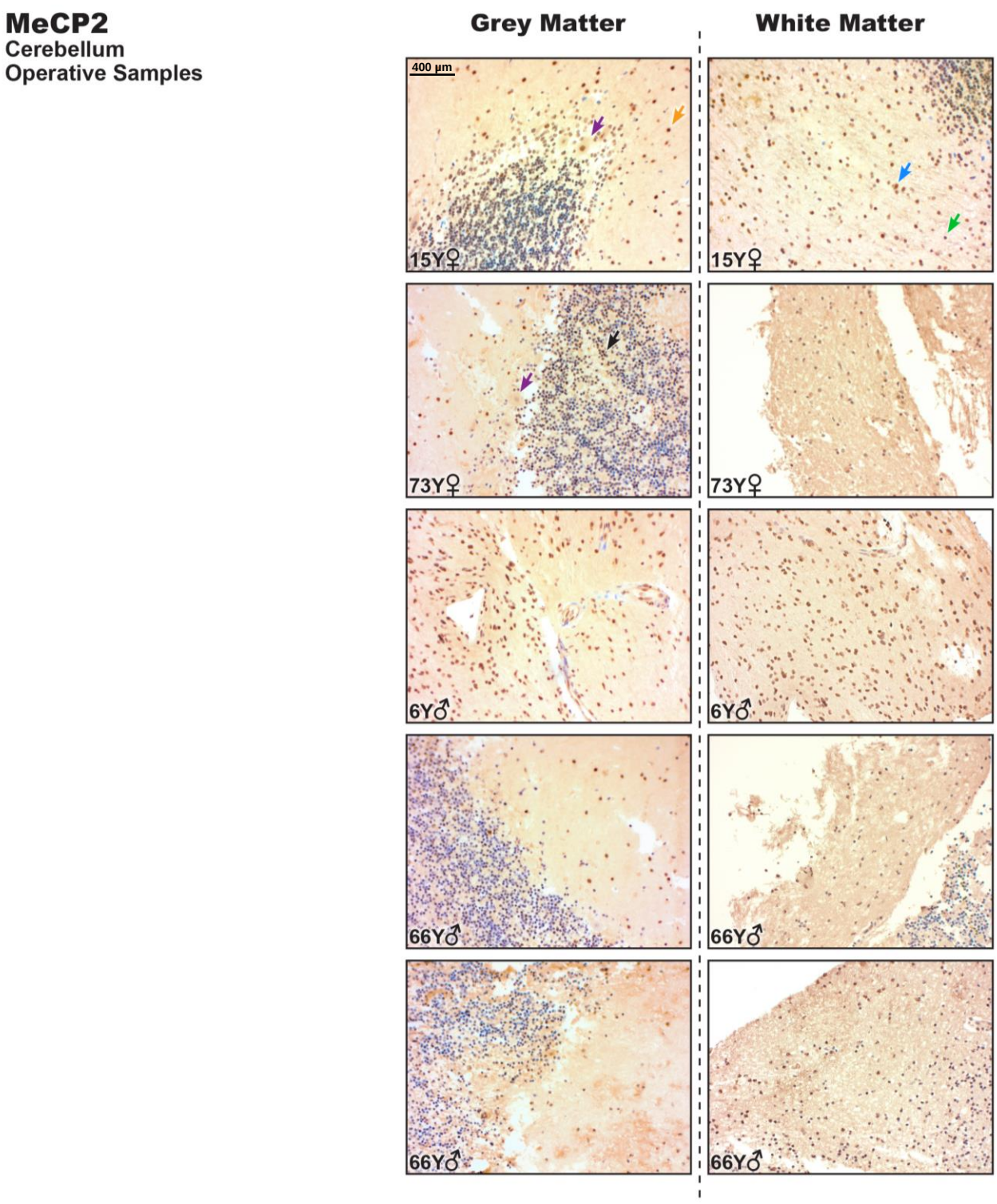

Figure 3.11 Cerebellum Operative Samples Immunostained for MeCP2. The majority of molecular layer (Orange Arrow) and white matter cells (both neuronal, Blue Arrow, and glial, Green Arrow) are immunoreactive for MeCP2 in rapidly fixed intraoperative samples excised due to brain infarct or different tumors. Purkinje (Purple Arrow) and Granular cells (Black Arrow) show sparse and weak immunoreactivity; Year old (Y); x 100 Magnification. Scale bar shown on top left is identical for the whole figure.

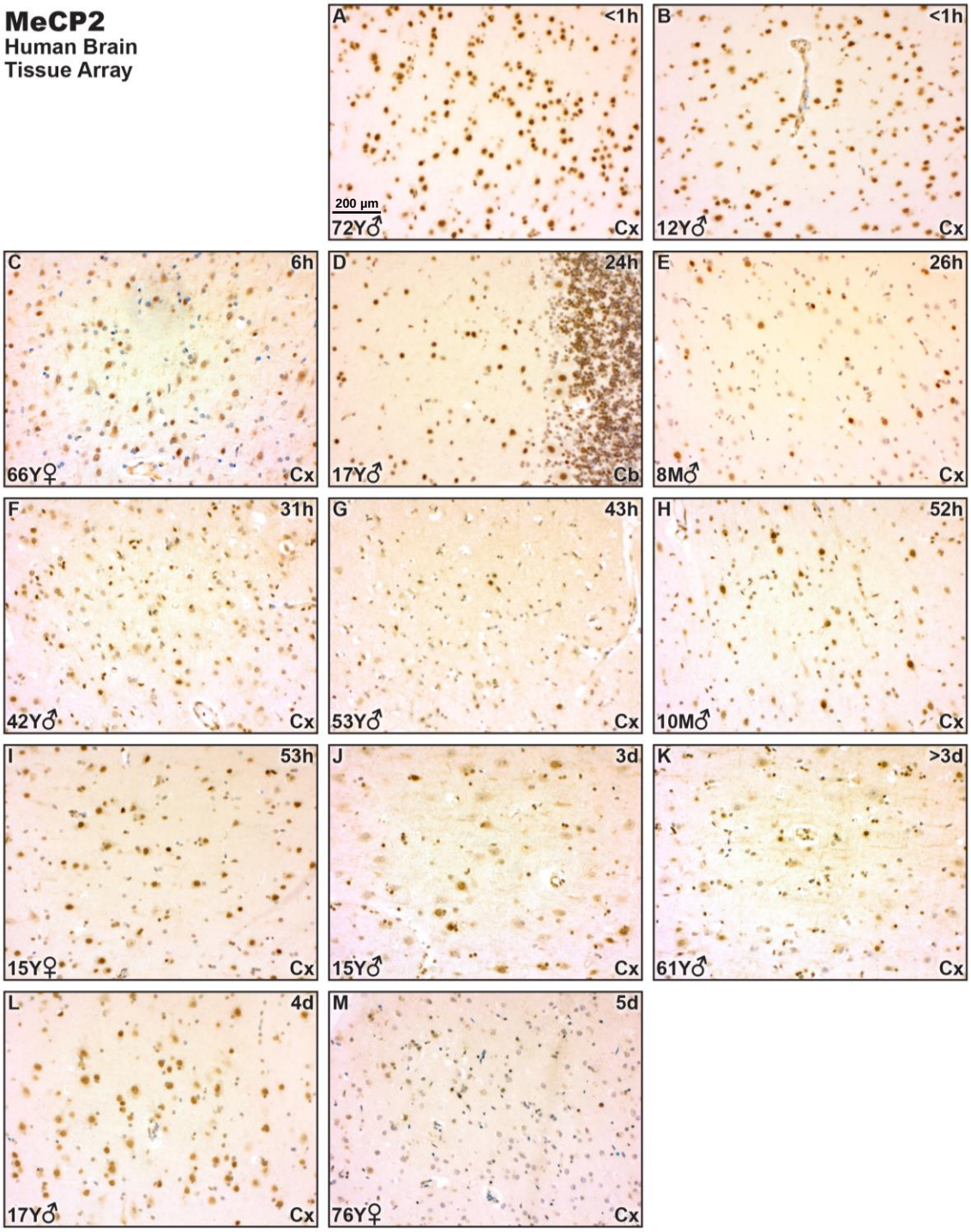

Figure 3.12 Immunostaining for MeCP2 in the human brain tissue array. Brain tissues with the minimum delay to fixation (<1 hour) show maximum immunoreactivity for MeCP2. Delay in fixation process accompanies variable staining of similar cell groups in the studied human brain microarray; hours delay in fixation (h); days delay in fixation (d); Year old (Y); Cortex (Cx); Cerebellum (Cb); x 200 Magnification. Scale bar shown in A is identical for the whole figure.

Table 3.1 Information of human brain neocortex tissue array to study post-mortem delay effects. Year old (Y); Month old (M).

Sample	Delay to fixation	Details	Age / sex	Fixation time (days)
A	<1 hour	Temporal cortex (surgical access, adjacent to tumor)	72Y, male	1
B	<1 hour	Temporal cortex (hippocampus surgery for epilepsy)	12Y, male	1
C	6 hours	Frontal cortex-normal	66Y, female	14
D	24 hours	Cerebellum (reference location)	17Y, male	4
E	26 hours	Frontal cortex-sudden unexpected death in infant (SUDI)	8M, male	8
F	31 hours	Frontal cortex-severe hypoxia+7days survival	42Y, male	19
G	43 hours	Frontal cortex-severe hypoxia+2days survival	53Y, male	19
H	52 hours	Frontal cortex-sudden unexpected death in infant (SUDI)	10M, male	2
I	53 hours	Frontal cortex-normal	15Y, female	1
J	3 days	Frontal cortex-normal	21Y, male	17
K	>3 days	Frontal cortex-decomposition, deep brain putrefaction	61Y, male	18
L	4 days	Frontal cortex-acute trauma	17Y, male	2
M	5 days	Frontal cortex-Alzheimer's disease	76Y, female	55

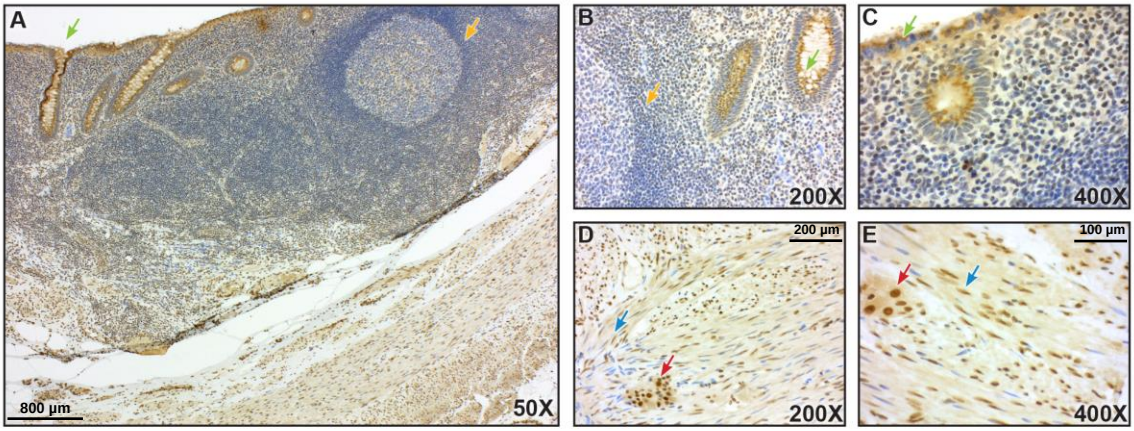

Figure 3.13 Immunostaining for MeCP2 in human normal appendix. Different cell types in mucosal layer (Green Arrow), and lymphoid follicles (Orange Arrow) do not show nuclear labeling for MeCP2 (A, B, and C). Parasympathetic ganglia of myenteric plexus are strongly positive (Red Arrow). Vast majority of smooth muscles (Blue Arrow) in muscularis mucosae and two layers of muscularis externa are immunoreactive for MeCP2 (A, D, and E). Scale bars are similar in identical magnifications.

3.4.2 MeCP2 in different brain regions of RTT patients compared to controls

Next, we performed IHC studies for MeCP2 with the DAB-labeling technique on three brain regions (cortex, hippocampus, and cerebellum) of autopsy samples from three female and one male RTT patients (cases 1-4) and their age-, and sex-matched controls. My experiments showed variable immunoreactivity with MeCP2 antibody in neurons of all studied brain samples (Figure 3.14).

This variable staining among similar neurons of both RTT and control brains was comparable with tissue array samples that were not fixed immediately. Operative samples and tissue array samples with fixation delay below one hour showed minimum variability in immunolabeling for MeCP2 (Figure 3.10, and Figure 3.12).

Unlike previous reports [29], in this study, the grey matter of studied brain regions in RTT samples was not remarkably different from the controls (Figure 3.14). However,

in the white matter of all four RTT brains, MeCP2 nuclear staining was barely detectable in the glial cells. In contrast to the abundance of MeCP2 negative glial cells, sparse neurons of the white matter were weakly to moderately MeCP2 positive (Figure 3.15). These findings were consistent for the three studied brain regions of all four pairs of RTT and control brain tissues (Figure 3.14, Figure 3.15, and Figure 3.16).

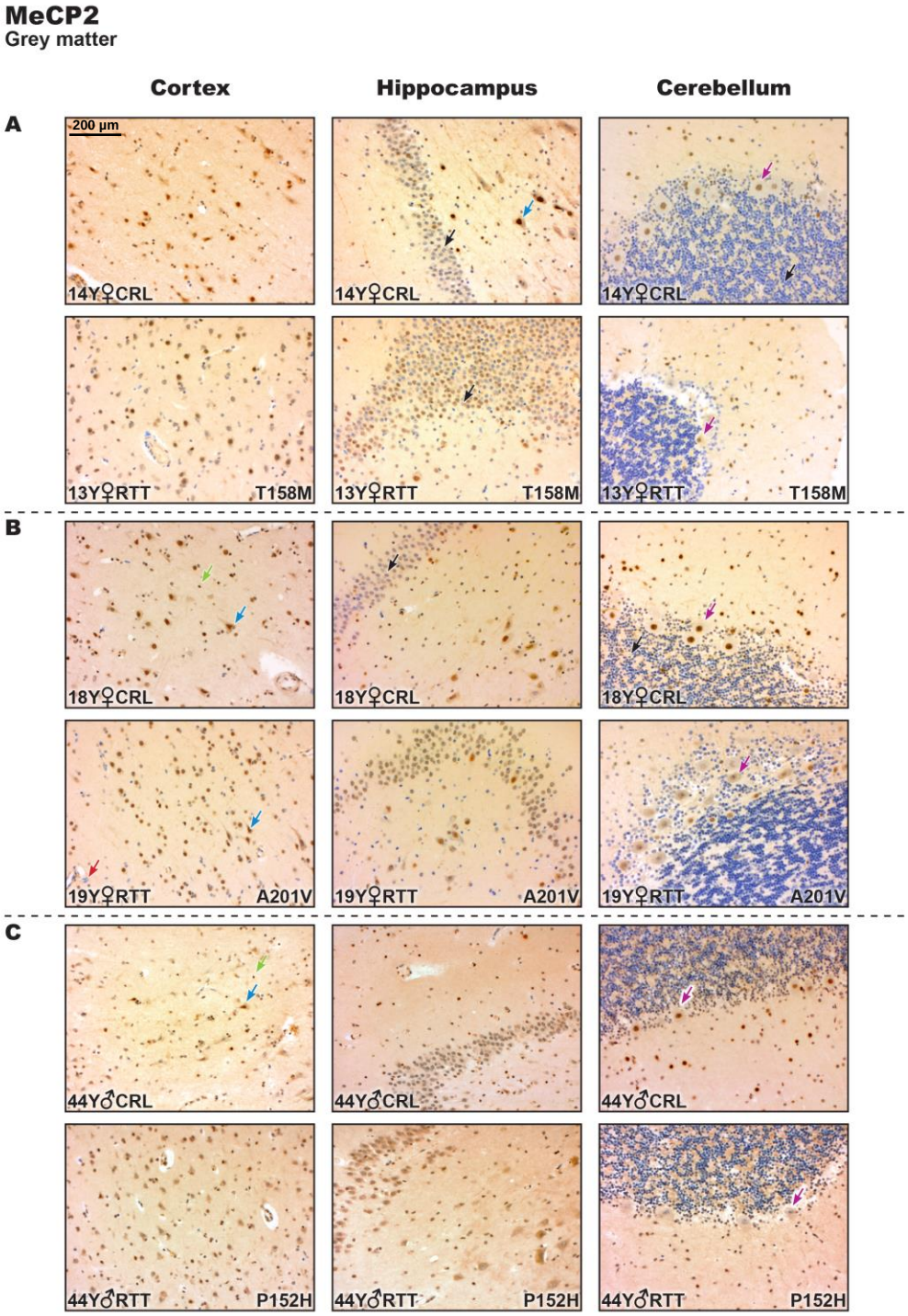

Figure 3.14 IHC studies of grey matter in three brain regions (hippocampus, cortex, and cerebellum) of three RTT patients and their sex-, and age-matched controls for MeCP2. Variable immunorecativity among brain cells is observed in both RTT, and controls. Grey matter in RTT brain is not showing significant decreased immunolabeling when compared to controls (A-C). IHC; Immunohistochemistry; Purkinje cells (Purple Arrow); Granular Layer (Black Arrow); Large Neurons (Blue Arrow); Glial Cells (Green Arrow); Endothelial Cells (Red Arrow); x 200 Magnification. Scale bar shown on top left of part A is identical for the whole figure.

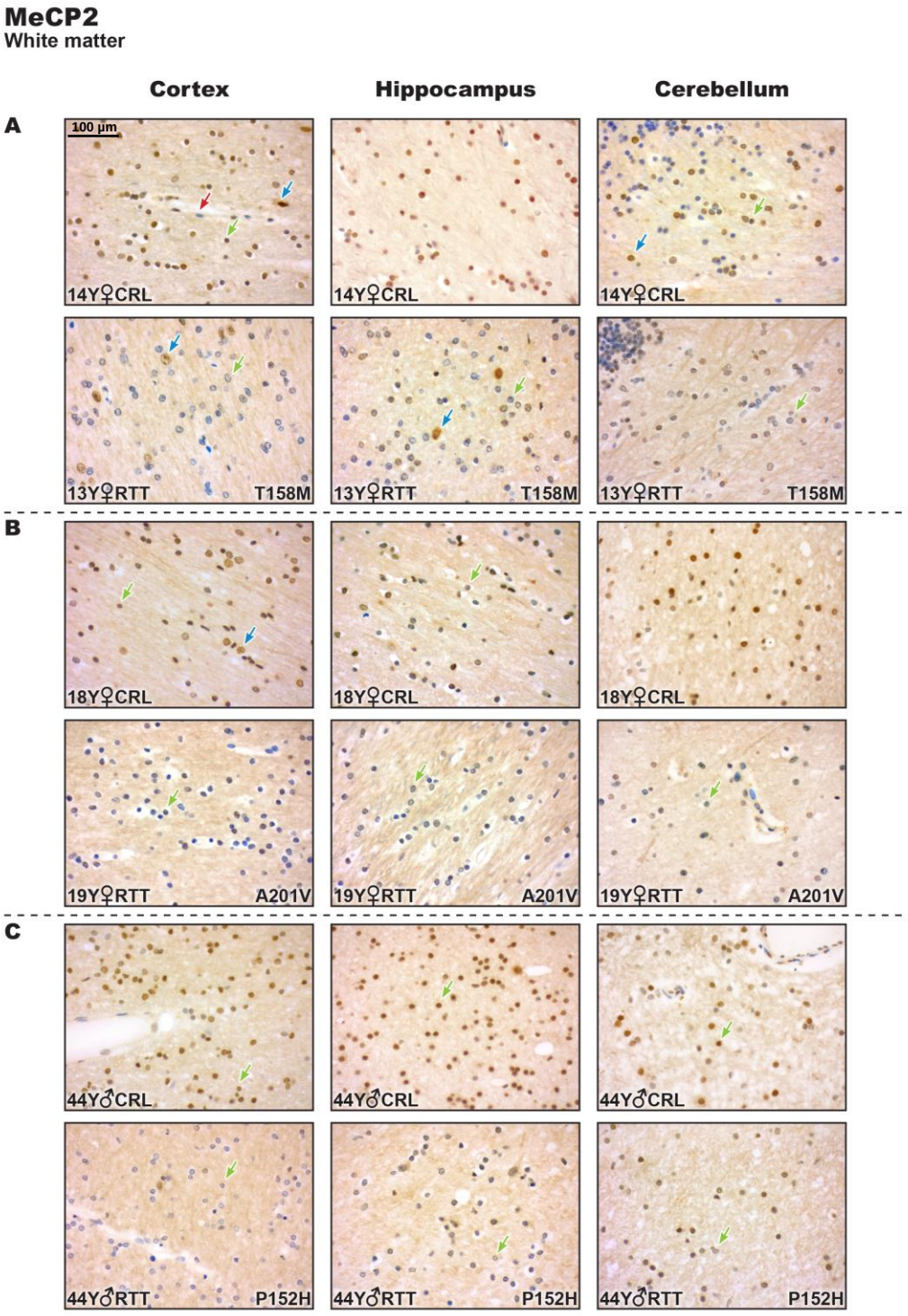

Figure 3.15 Immunohistochemistry studies of white matter in three brain regions (hippocampus, cortex, and cerebellum) of three RTT patients and their sex-, and age-matched controls for MeCP2. Significant decrease in MeCP2 nuclear staining in glial cells of white matter is the main finding of all studied RTT samples when compared to the controls (A-C). Neurons (Blue Arrow); Glial Cells (Green Arrow); Endothelial Cells (Red Arrow); x 400 Magnification. Scale bar shown on top left of part A is identical for the whole figure.

For the RTT and control brain samples received from NIH Brain Bank, NIH#4516: R255X, and NIH#5646: 20Y-old control, I had to adjust the pH of buffer for antigen retrieval (explained in Chapter 2) in order to make the IHC process possible for these overfixed tissues (>14 years of storage in fixative for NIH#4516, and > 5 years for NIH#5646, as shown in Table 2.1). The quality of staining was below what I had with other brain samples with shorter storage times. However, the pattern was similar to other RTT-control pairs (Figure 3.16).

MeCP2 staining in some neurons of RTT tissues, such as Purkinje cells of the cerebellum, was slightly weaker compared to the age and sex matched controls. Absence of MeCP2 staining in the cerebellar granular layer and variable staining of hippocampal dentate granular neurons for MeCP2 were other common findings in all RTT and controls (Figure 3.14), which could be a post-mortem artifact. The overfixed pair of RTT and control stained differently. Granular layer of cerebellum show staining for MeCP2 in RTT brain with R255X mutation, but not in its control. On the contrary, the hippocampal dentate granular neurons are positive for the control but not RTT brain (Figure 3.16).

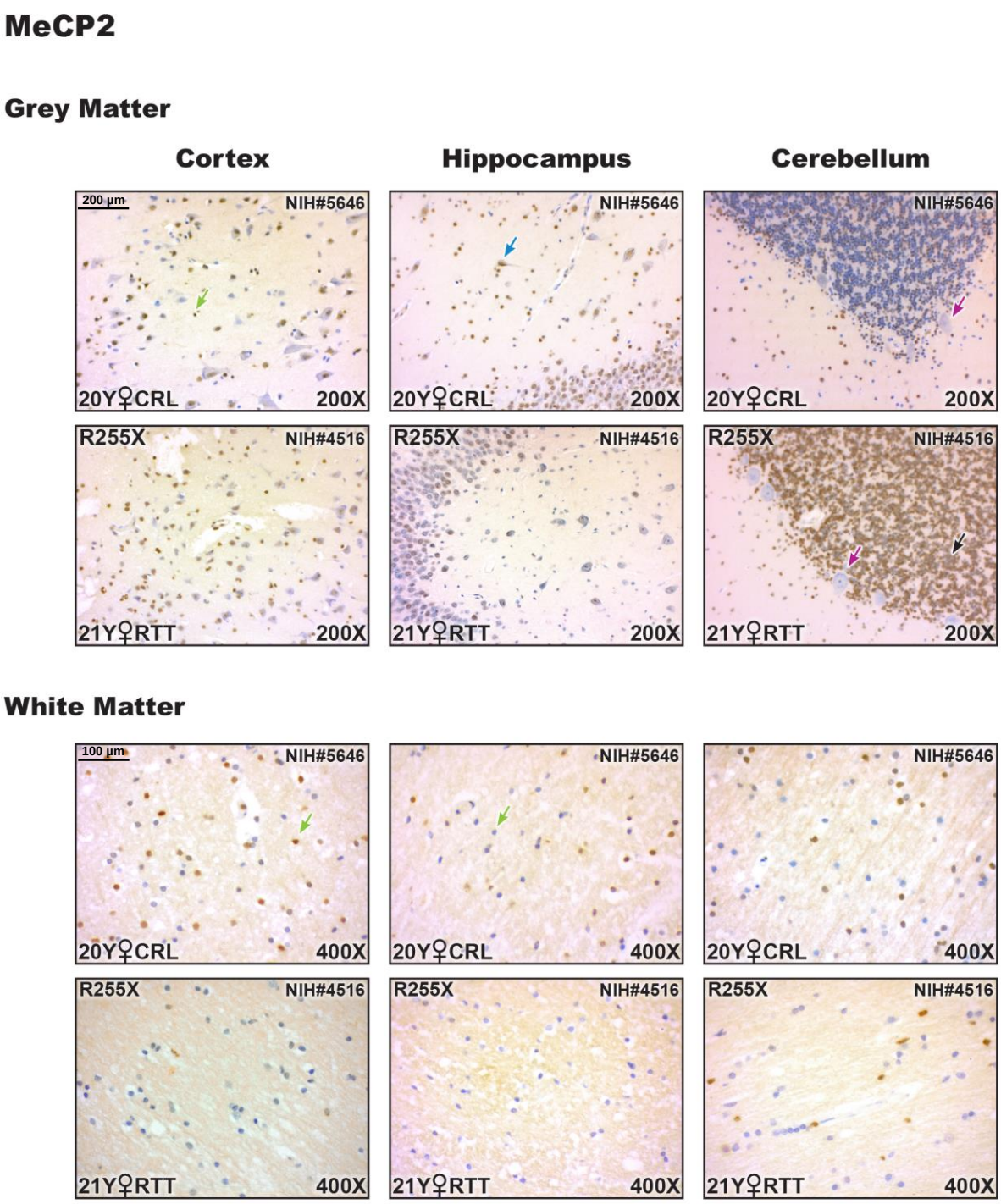

Figure 3.16 MeCP2 immunostaining of three brain regions (cortex, hippocampus and cerebellum) in the overfixed RTT and control sample (NIH#4516: R255X, and NIH#5646: 20Y-old control). After pH adjustment in antigen retrieval buffer, we had the same pattern as the other samples despite an overall lower quality of immunostaining. The only difference is that the granular layer of cerebellum was labeled for MeCP2 exclusively in RTT brain with R255X mutation (Black Arrow) and not in the rest of RTT or control brains. Purkinje cells (Purple Arrow); Neurons (Blue Arrow); Glial Cells (Green Arrow). Scale bars are similar for identical magnifications.

3.4.3 BDNF in different brain regions of RTT patients compared with controls

In order to have an insight on BDNF level and cellular distribution in RTT and control human samples, we performed IHC on these brain tissues, and labeled them with the same BDNF antibody we used for Western blot experiments. First, we investigated the impact of PMD on BDNF immunostaining. BDNF was apparently more resistant to PMD, compared to MeCP2. All the brain tissue fragments on the Tissue array slide were similar in terms of their staining pattern. Three days or more delay in the fixation was associated with a slight decrease in the intensity of labeling (Figure3.17). Other factors that potentially affected the immunolabeling such as variations in peri-sampling conditions, and fixation time among these brain samples are listed in Table 3.1.

In the next step, we compared three brain regions (cortex, hippocampus, and cerebellum) of RTT and their counterpart controls for BDNF immunolabeling. In all RTT-control pairs and in all brain regions, there was a strong cytoplasmic staining with astroglial/endothelial pattern (Figure 3.18 A-C, and Figure 3.19).

By single staining for BDNF, astrocytic endfeet were not differentiable from the adjacent endothelial cells in the sections of cerebral capillaries, and as both cell types might contain BDNF, we have referred to the staining pattern as astroglial/endothelial.

Neurons in the cortex and hippocampus were not labeled. Only Purkinje cells showed strong BDNF immunolabeling. Astroglial/endothelial BDNF staining in RTT samples was not significantly different from the controls (Figure 3.19), and more noticeably, the Purkinje cells of RTT cerebellar samples showed stronger cytoplasmic BDNF protein in all 4 RTT patients, when compared to the control brain samples (Figure 3.18, and Figure 3.19).

As explained for MeCP2 labeling for the overfixed RTT and control brain samples received from NIH Brain Bank, NIH#4516: R255X, and NIH#5646: 20Y-old control with long storage time in fixative as shown in Table 2.1, we had to adjust the pH of buffer for antigen retrieval to make the IHC process possible for these overfixed samples. The quality of staining was below what we had with other brain samples with shorter storage

times in the fixative. However, the pattern was similar to other RTT-control pairs (Figure 3.19).

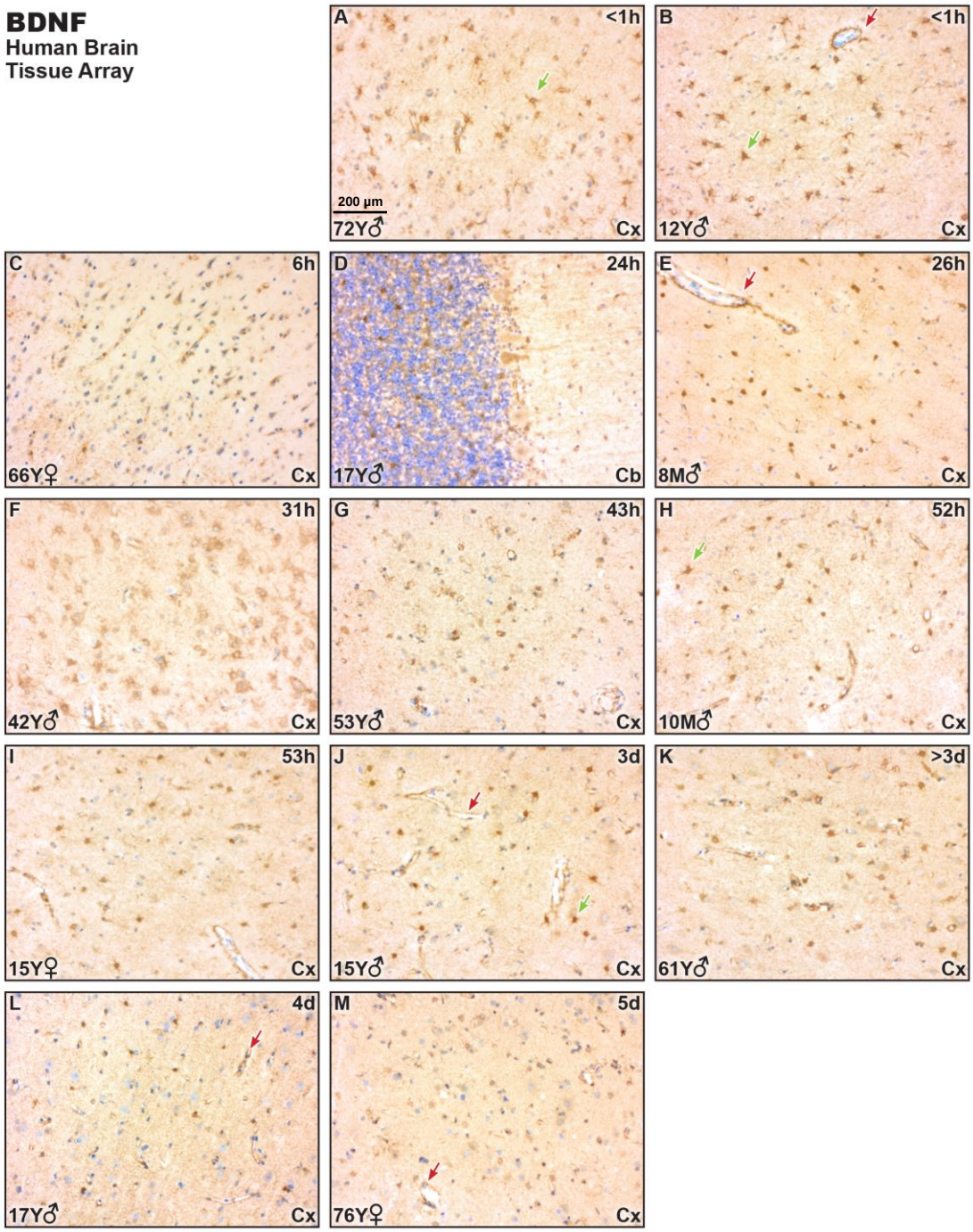

Figure 3.17 Immunostaining for BDNF in the human brain tissue array. BDNF shows higher stability with post mortem delay compared to MeCP2 (Figure 3.12). A slight decrease is observed in the intensity of staining for longer intervals (Fixation after 3 days). Glial Cells (Green Arrow); Endothelial Cells (Red Arrow); x 200 Magnification. Scale bar shown in A is identical for the whole figure.

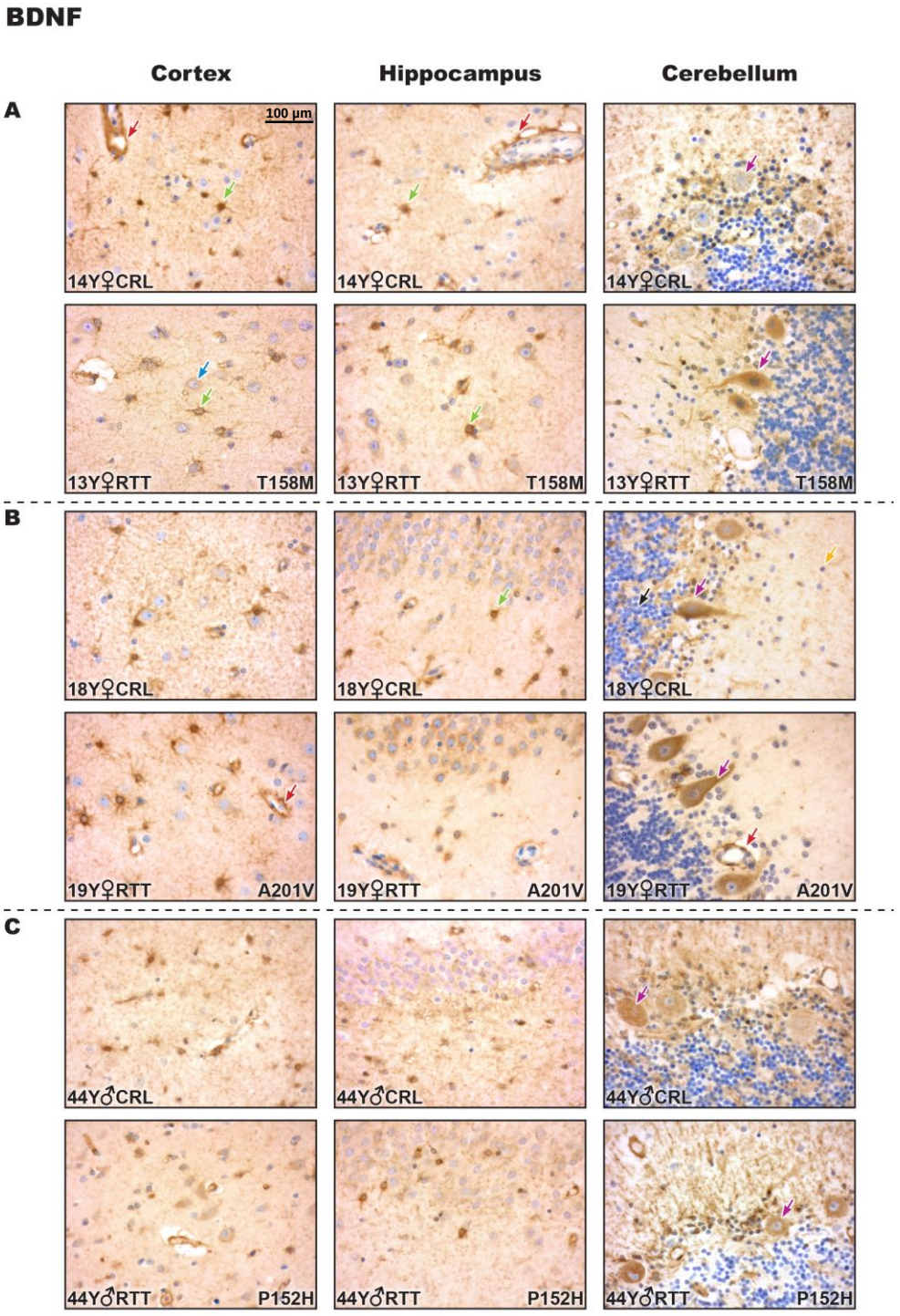

Figure 3.18 BDNF immunolabeling of three brain regions (cortex, hippocampus, and cerebellum) in three RTT patient and their sex-, and age-matched controls. Prominent astroglial/endothelial pattern in BDNF labeling is seen in both RTTs and controls without significant difference between the two groups. Purkinje cells of the cerebellum (Purple Arrow) are exceptionally positive for BDNF compared to the other neurons. They show relatively higher intensity in RTT patient. Granular layer (Black Arrow); Astroglial cells (Green Arrow); Endothelial cells (Red Arrow); Molecular layer (Orange Arrow); x 400 Magnification. Scale bar shown in A is identical for the whole figure.

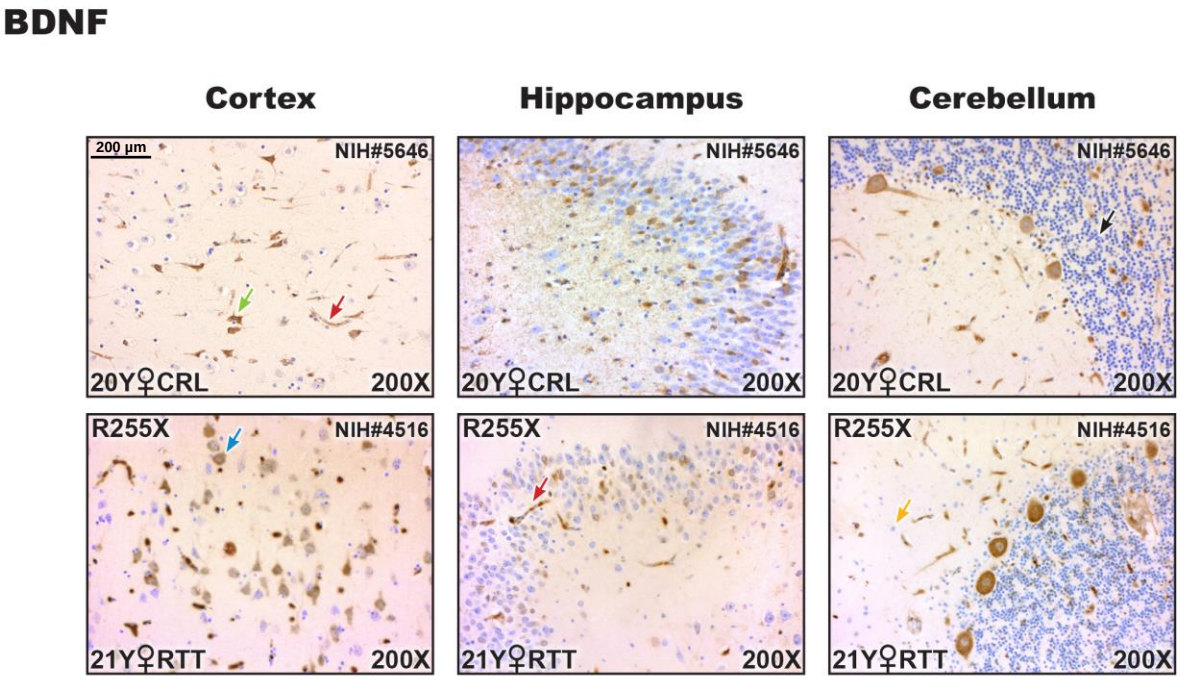

Figure 3.19 BDNF immunostaining of three brain regions (cortex, hippocampus and cerebellum) in the overfixed RTT and control sample (NIH#4516: R255X, and NIH#5646: 20Y-old control). After pH adjustment in antigen retrieval buffer, we had the same pattern as the other samples despite an overall lower quality of immunostaining. Granular layer (Black Arrow); Astroglial cells (Green Arrow); Endothelial cells (Red Arrow); Molecular layer (Orange Arrow); x 200 Magnification. Scale bar shown on top left is identical for the whole figure.

Protein fixation creates crosslinks that mask tissue antigen and limit antibody-epitope binding. Antigen retrieval restores antigenicity and enhances antibody-epitope binding by reversing protein crosslinks in tissue sections [234]. We used heat and a change in pH as the antigen retrieval method in order to improve antibody affinity for its epitope. The longer storage time in fixative for the two fixed brain samples we received from NIH (#4516, and #5646) was assumed to play a role in lower quality of immunolabeling for both studied proteins (MeCP2, and BDNF). For the rest of samples, antigen retrieval was performed in pH=9, however these two NIH samples showed better results with PH=3 for MeCP2 staining, and pH=6 for BDNF staining (Figure 3.15 and Figure 3.18).

Regarding the process of histopathological evaluation of human brain samples, the H&E slides were prepared in the Pathology and Human Anatomy and Cell Science Departments of University of Manitoba as paid services. Unstained slides of brain samples for IHC studies were also prepared in Pathology Department. We performed the IHC experiments and examined the H&E and IHC stained slides by light microscope and did the imaging. Then our neuropathologist collaborator, Dr. Marc Del Bigio, evaluated them in a blind manner. I also made a semiquantitative assessment according to the percentage of labeled cells and the intensity of peroxidase deposits ranging from light beige to dark brown, which is shown in the Table 3.2 to Table 3.6.

Table 3.2 Semiquantitative assessment of RTT brain with T158M mutation and its age-, and sex-matched control brain immunostained for MeCP2 and BDNF. The assessments are based on percentage of labeled cells and the intensity of staining.

A1		**MeCP2**			
	Cell Type	**Control (14y)**		**RTT (T158M)**	
		Positivity (Intensity)		**Positivity (Intensity)**	
Frontal Cortex	Large Neurons	80% (3+)		10% (2+)	50% (+)
	Small/Medium Neurons	50% (3+)	10% (+)	20% (2+)	40% (+)
	Neuroglial Cells (White Matter)	85% (2+)	10% (+)	<1% (+)	
	Sparse Neurons (White Matter)	Almost All (+ to 2+)		50% (Weak +)	
Temporal Cortex	Large Neurons	80% (2 to 3+)		60% (Weak to +)	
	Small/Medium Neurons	60-70% (2 to 3+)		50% (+)	5% (2+)
Hippocampus	Granular Layer (Dentate Gyrus)	10%(2+)	10% (+)	40-50% (Weak to +)	
	Large Neurons	10%(3+)	10% (2+)	30% (+)	
	Neuroglial Cells (White Matter)	90% (+ to 2+)		1% (Weak to +)	
Cerebellum	Purkinje Cells	85% (2 to 3+)	10% (+)	60% (Weak to +)	10% (2+)
	Granular Layer	Rare (+)		2% (Weak +)	
	Molecular Layer	30% (2 to 3+)	40% (+)	40% (+)	10% (2+)
	Neuroglial Cells (White Matter)	70% (+)	20% (2+)	< 5% (Weak +)	
A2		**BDNF**			
	Cell Type	**Control (14y)**		**RTT (T158M)**	
		Positivity (Intensity)		**Positivity (Intensity)**	
Frontal Cortex	Large Neurons	Rare (Weak+)		30% (Weak+)	
	Small/Medium Neurons	Rare (Weak+)		30% (Weak+)	
	Neuroglial/Endothelial Cells (Grey matter)	40% (2+ to 3+)		40% (+)	
	Endothelial Cells (White Matter)	Weak to +		Almost All (Weak to +)	
	Neuroglial Cells (White Matter)	Rare (+)		Rare (+)	
Hippocampus	Granular Layer (Dentate Gyrus)	Rare (Weak+)		Rare (+)	
	Neurons	Rare (Weak +)		70-80 % (Weak+)	
	Neuroglial/Endothelial Cells (Grey matter)	90-95% (+)		50% (+ to 3+)	
	Endothelial Cells (White Matter)	Weak +		Weak +	
	Neuroglial Cells (White Matter)	Rare (+)		Rare (Weak+)	
	Temporal Cortex Neurons	Rare (Weak+)		70-80% (Weak+)	
Cerebellum	Purkinje Cells	70% (Weak to+)		Almost All (+ to 2+)	
	Granular Layer	Rare (+)		5% (Weak to +)	
	Molecular Layer	Rare (+)		Rare (+)	
	Neuroglial Cells (White matter)	Rare (+)		Rare (+)	
	Endothelial	+		White (Rare Weak+)	Grey (+)

Table 3.3 Semiquantitative assessment of RTT brain with A201V mutation and its age-, and sex-matched control brain immunostained for MeCP2 and BDNF. The assessments are based on percentage of labeled cells and the intensity of staining.

B1		**MeCP2**	
	Cell Type	**Control (18y)**	**RTT (A201V)**
		Positivity (Intensity)	**Positivity (Intensity)**
Frontal Cortex	Large Neurons	80% (2+ to 3+)	80-90% (+ to 2+)
	Small/Medium Neurons	60-70% (2+ to 3+)	80-90% (+ to 2+)
	Neuroglial Cells (Grey Matter)	50% (Weak to +)	Scattered (Weak +)
	Neuroglial Cells (White Matter)	80-90% (+)	Rare (Weak +)
Temporal Cortex	Large Neurons	80% (2+ to 3+)	80-90%% (+ to 2+)
	Small/Medium Neurons	60-70% (2+ to 3+)	80-90%% (+ to 2+)
	Neuroglial Cells (White Matter)	80-90% (+)	Rare (weak+)
Hippocampus	Granular Layer (Dentate Gyrus)	5% (Weak+)	90% (Weak +)
	Large Neurons	40% (2+ to 3+)	Almost All (Weak to +)
	Small Neurons	Scattered (Weak +)	Scattered (Weak +)
	Neuroglial Cells (White Matter)	90-95% (+)	Rare (Weak +)
	Large Neurons of Nucleolus	+	+
Cerebellum	Purkinje Cells	Almost All (+ to 2+)	Almost All (Weak to +)
	Granular Layer	Rare (+)	Negative
	Molecular Layer	Rare (+)	80-90% (+ to 2+)
	Neuroglial Cells (White Matter)	Scattered (Weak+)	80-90% (Weak +)
	Endothelial Cells	Weak +	
B2		**BDNF**	
	Cell Type	**Control (18y)**	**RTT (A201V)**
		Positivity (Intensity)	**Positivity (Intensity)**
Frontal Cortex	Large Neurons	50% (Weak to +)	20% (Weak +)
	Small/Medium Neurons		
	Neuroglial/Endothelial Cells (Grey matter)	40-50% (2+ to 3+)	30% (1+ to 2+)
	Endothelial Cells (White Matter)	Weak to +	Weak to +
	Neuroglial Cells (White matter)	Scattered Granular (Weak +)	Rare Granular (+)
Hippocampus	Granular Layer (Dentate Gyrus)	Rare (Weak +)	40-50% (Weak to +)
	Large Neurons	Majority (+ to 2+)	Majority (Weak to +)
	Neuroglial/Endothelial Cells (Grey matter)	40% (+ to 2+)	Rare (Weak to +)
	Endothelial Cells (White Matter)	Weak +	Weak +
	Neuroglial Cells (White matter)	Scattered (Weak +)	Rare (+)
	Temporal Cortex Neurons	50% (Weak to +)	50% (Weak +)
Cerebellum	Purkinje Cells	Almost All (1+ to 2+)	Almost All (1+ to 2+)
	Granular Layer	Rare (+)	Rare (+)
	Molecular Layer	Rare (+)	Rare (+)
	Neuroglial Cells (White matter)	Rare (+)	Weak +
	Endothelial	Rare (+)	White (Weak +) | Grey (+)
	Large Neurons of Red Nucleous	Majority (Weak +)	NA

Table 3.4 Semiquantitative assessment of RTT brain with R255X mutation and its age-, and sex-matched control brain immunostained for MeCP2 and BDNF. The assessments are based on percentage of labeled cells and the intensity of staining.

C1	**MeCP2**		
	Cell Type	**Control (20y)**	**RTT (R255X)**
		Positivity (Intensity)	**Positivity (Intensity)**
Frontal Cortex	Large Neurons	30-40 % (Weak +)	30 % (Very Weak +)
	Small/Medium Neurons	80 % (+)	70 % (Weak to +)
	Neuroglial Cells (White Matter)	50 % (Weak to +)	5% (Weak +)
	Sparse Neurons (White Matter)	Weak +	Weak +
Temporal Cortex	Large Neurons	30-40 % (Weak to +)	30 % (Very Weak +)
	Small/Medium Neurons	80 % (+)	70 % (Weak to +)
	Neuroglial Cells (White Matter)	50 % (Weak to +)	Negative
Hippocampus	Granular Layer (Dentate Gyrus)	Almost All (Weak to +)	40-50% (Very Weak +)
	Large Neurons	40%-50% (Weak +)	20-30% (Very Weak +)
	Small Neurons		20-30% (Very Weak +)
	Neuroglial Cells (White matter)	50% (Weak to +)	Negative
Cerebellum	Purkinje Cells	< 1 % (+)	Negative
	Granular Layer	90 % (Weak to +)	Almost All (+)
	Molecular Layer	Almost All (1+ to 2+)	60 % (Weak to +)
	Neuroglial Cells (White matter)	50-60 % (1+ to 2+)	5 % (+)
	Sparse Neurons (White Matter)	+	Negative
C2	**BDNF**		
	Cell Type	**Control (20y)**	**RTT (R255X)**
		Positivity (Intensity)	**Positivity (Intensity)**
Frontal Cortex	Large Neurons	10% (+ to 3+)	80% (Weak to 2+)
	Small/Medium Neurons	20-30% (+ to 3+)	60-70% (Weak+)
	Neuroglial/Endothelial Cells (Grey matter)	10-20% (+)	5% Granular (Weak+)
	Endothelial Cells (White Matter)	Weak +	+
	Neuroglial Cells (White matter)	20% (Granular +)	20% (+ to 3+)
Hippocampus	Granular Layer (Dentate Gyrus)	40% (Weak to 2+)	30-40% (Weak +)
	Large Neurons	Ganglion like (Weak to 2+)	Ganglion like (30%+) 10% (+)
	Neuroglial/Endothelial Cells (Grey matter)	40%-50 (+)	10% (Weak +)
	Endothelial Cells (White Matter)	+	Weak +
	Neuroglial Cells (White matter)	30-40% (+)	Rare (+)
	Temporal Cortex Neurons	Sparse (Weak +)	Sparse (Very Weak +)
Cerebellum	Purkinje Cells	Almost All (+ to 3+)	50-60% (+ to 3+)
	Granular Layer	Rare (+)	Negative
	Molecular Layer	10% (Weak to 1+)	20-30% (Weak to 1+)
	Neuroglial Cells (White matter)	60% (Granular +)	Negative
	Endothelial	+	+

Table 3.5 Semiquantitative assessment of RTT brain with P152H mutation and its age-, and sex-matched control brain immunostained for MeCP2 and BDNF. The assessments are based on percentage of labeled cells and the intensity of staining.

D1	**MeCP2**		
	Cell Type	**Control (44y)**	**RTT (P152H)**
		Positivity (Intensity)	**Positivity (Intensity)**
Frontal Cortex	Large Neurons	< 5 % (+ to 2+)	< 1 % (Weak +)
	Small/Medium Neurons	5 % (+ to 2+)	50 % (Weak +)
	Neuroglial Cells (Grey Matter)	50 % (Weak to +)	80 % (Weak +)
	Neuroglial Cells (White Matter)	Almost All (+ to 2+)	Almost All (Negative)
	Sparse Neurons (White Matter)	Weak +	Very Weak +
Temporal Cortex	Large Neurons	< 5 % (+ to 2+)	< 1 % (+)
	Small/Medium Neurons	5 % (+ to 2+)	50% (Weak to +)
	Neuroglial Cells (Grey Matter)	50 % (+ to 2+)	50 % (Weak to +)
Hippocampus	Granular Layer (Dentate Gyrus)	Almost All Negative	Almost All Negative
	Large Neurons	Granular Staining	Granular Staining
	Neuroglial Cells (White matter)	Almost All (+ to 2+)	Almost All (Weak +)
	Sparse Neurons (White Matter)	Weak to +	50% (Weak +)
	Large Neurons of Nucleolus	Granular Staining	Granular Staining
Cerebellum	Purkinje Cells	< 5 % (+ to 2+)	1% (Weak to +)
	Granular Layer	Almost All Negative	Almost All Negative
	Molecular Layer	60 % (+ to 3+)	40-50 % (Weak to +)
	Neuroglial Cells (White matter)	60% (+ to 2+)	40 % (Weak +)
	Sparse Neurons (White Matter)	Negative to Weak	Negative
	Large Neurons of Red Nucleous	Granular Staining	Granular Staining
D2	**BDNF**		
	Cell Type	**Control (44y)**	**RTT (P152H)**
		Positivity (Intensity)	**Positivity (Intensity)**
Frontal Cortex	Large Neurons	Negative	70-80% (Granular Weak to 2+)
	Small/Medium Neurons	Rare (+)	Rare (+)
	Neuroglial/Endothelial Cells (Grey matter)	40-50% (+ to 3+)	5% (Granular+)
	Endothelial Cells (White Matter)	+	+
	Neuroglial Cells (White matter)	40-50% (Granular +)	10-20% (Granular +)
	Sparse Neurons (White Matter)	Negative	Negative
Hippocampus	Granular Layer (Dentate Gyrus)	Rare (Granular +)	Rare (Granular +)
	Large Neurons	Rare (Very Weak+)	5% (Granular Very Weak +)
	Neuroglial/Endothelial Cells (Grey matter)	40% (+ to 2+)	30% (Granular Weak to +)
	Endothelial Cells (White Matter)	+	+
	Neuroglial Cells (White matter)	20-30% (+ to 2+)	50-60% (Granular +)
	Temporal Cortex Neurons	Negative	Negative
	Large Neurons of Nucleolus	Granular +1 to 3+	Granular +1 to 2+
Cerebellum	Purkinje Cells	<10% (Weak to 2+)	Almost All (+ to 3+)
	Granular Layer	Rare (+)	Rare (+)
	Molecular Layer	Rare (+)	Rare (+)
	Neuroglial Cells/Endothelial Cells (Grey matter)	5-10% (+)	Rare (+)
	Endothelial Cells (White Matter)	+	+
	Neuroglial Cells (White matter)	30-40% (Granular + to 2+)	30% (Granular +)
	Sparse Neurons (White Matter)	+	+

Table 3.6 Semiquantitative assessment of hippocampal region of two male control brain immunostained for MeCP2 and BDNF. The assessments are based on percentage of labeled cells and the intensity of staining.

E1	**MeCP2**		
	Cell Type	**Male Control (15y)**	**Male Control (19Y)**
		Positivity (Intensity)	**Positivity (Intensity)**
Hippocampus	Granular Layer (Dentate Gyrus)	Almost All (+)	Almost All Negative
	Large Neurons	Almost All (+ to 2+)	40-50% (+ to 3+)
	Neuroglial Cells (White matter)	90% (Very Weak +)	Almost All +
	Sparse Neurons (White Matter)	Weak to +	+ to 2+
Temporal Cortex	Large Neurons	90 % (+ to 2+)	40-50 % (+ to 3+)
	Small/Medium Neurons	80 % (Weak to +)	40-50 % (+ to 3+)
E2	**BDNF**		
	Cell Type	**Male Control (15y)**	**Male Control (19Y)**
		Positivity (Intensity)	**Positivity (Intensity)**
Hippocampus	Granular Layer (Dentate Gyrus)	Almost All (Granular +)	Mostly (Very Weak) / < 5 % (+)
	Large Neurons	80 % (Granular Weak +)	Almost All (+ to 3+)
	Neuroglial Cells (White matter)	90% (Very Weak +)	20 % (Granular +)
	Endothelial Cells	+	Weak +
	Sparse Neurons (White Matter)	Rare Granular +	50 % (Weak +)
	Large Neurons of Nucleolus	80 % (Granular Weak +)	Almost All (Weak to 2+)
Temporal Cortex	Large Neurons	95 % (2+ to 3+)	Rare Weak
	Small/Medium Neurons	95 % (2+ to 3+)	Rare Weak
	Neuroglial Cells (Grey matter)	50-60 % (2+ to 3+)	30-40 % (+ to 3+)
	Endothelial Cells	+	+

4. Discussion

In this study, elements of a regulatory network suggested for MeCP2 homeostasis in rat brain [187] (Figure 1.8), were evaluated in human brain in order to test our hypothesis about conservation of this network from rodents to human. The studied elements included *miR132*, MeCP2 isoforms, and BDNF at both the transcript and protein levels. These factors were assessed in four different regions of human post-mortem brains. In order to test our hypothesis on alteration of these elements in Rett Syndrome, we evaluated the same factors in post-mortem brain samples of RTT patients. The studies were performed on frozen brain lysates for the first aim of my project, and qRT-PCR, TaqMan assay, Western Blot, and ELISA techniques were used for transcript and protein assessments.

For the second aim of my project, we evaluated two protein elements of the regulatory network (MeCP2, and BDNF) in a histological context by using formalin-fixed brain samples of RTT patients and their age- and sex-matched controls. We evaluated the histopathology of the brain samples and performed immunolabeling for the two mentioned proteins on both RTT and control brain samples. Furthermore, for the first time in this project, post-mortem delay effects on MeCP2 and BDNF immunolabeling was studied in human brain tissue.

4.1 Lessons learned from the human brain on MeCP2-BDNF-*miR132* regulatory components

I showed a lower transcript level of *MECP2* isoforms in human RTT brain (Figure 3.6), which was in agreement with previous studies on total MeCP2, that had shown decreased level of *MECP2* transcript or impaired structure and function of MeCP2 protein in neuronal [29, 41, 229], or non-neuronal RTT samples (e.g. peripheral blood) [235].

Here, I did not find a clear association between *MECP2E1/E2* transcript and MeCP2E1/E2 protein levels (Figure 3.8). BDNF and its precursor did not show any concordance with *BDNF* transcript either. Complex regulation of protein expression in the human brain has been suggested as a possible reason behind the low predictive value of transcript expression for the corresponding protein(s) in the brain [236]. Post-transcriptional control, as well as cell- or tissue-specific regulation rather than transcriptional-specific control are among other possible explanations [23].

In human post-mortem RTT brain, BDNF showed a similar pattern to *MECP2*E1/E2 with lower transcript expression (Figure 3.6), without any significant difference at the protein levels compared to controls (Figure 3.7). However, my studies on the formalin-fixed brain samples added another layer to the complexity of MeCP2-BDNF relationship. Based on my results from the BDNF immunolabeling, different cells in the brain i.e. astrocytes, endothelial cells, and neurons were labelled with the BDNF antibody, and could play a role in MeCP2 homeostasis as sources of BDNF. Therefore, it might be too simplistic to suggest one regulatory system without considering the cellular source of each protein.

In contrast to the negative regulatory role of *miR132*, suggested by experiments in rodents [187], lower transcript level of *MECP2* isoforms that I found in human RTT brains was associated with lower level of *miR132* in all brain regions except for the cerebellum (Figure 3.6). This finding does not support a conserved suppressive role for *miR132 on MECP2/*MeCP2 homeostasis in human brain. However, as explained before, cerebellum was different from the other three regions by showing similar level of *miR132* in RTT and control brains.

The inter-regional variations that I showed in the elements of the suggested regulatory network in human brain might be the result of variable number of cells and different cell types with different functions in each region, and again makes finding a unique regulatory system in the whole brain of human less probable.

4.2 Effects of post-mortem interval on MeCP2-BDNF detection in the human brain

Although transgenic animal models and *in vitro* cellular studies may provide valuable information about neurological disorders, studying human post-mortem brain tissues has an essential place in deciphering the pathophysiology of human neurologic disorders [237]. Theses valuable human brain samples from RTT as a rare disease bring challenges to this research field. Similar PMD in RTT patients studied here and their controls reduced the effect of PMD in our comparisons. However, unpredictable peri-mortem factors may also contribute in the lower level of the detected proteins in some controls. Similarly, there might be a differential degradation pattern of MeCP2 isoforms, which may influence the quantified level of each isoform at the transcript or protein level.

To our knowledge, our study of the human brain tissue array is the first effort towards addressing PMD effects on MeCP2, and BDNF in the human brain. We showed that while BDNF is stable more than 72 hours post-mortem, MeCP2 shows notable reduction in immunolabeling as soon as 24 hours. Considering other potential factors that may impact these brain samples, studying controlled model systems with different PMD would help to make a more complete picture of post-mortem changes in similar gene regulation studies.

4.3 White matter astrocytes are the major difference between RTT and control brains

An intriguing finding of this study is the absence of MeCP2 detection in almost all glial cells of the white matter in human RTT brain, whereas it appears to be widely present in glial cells of the control brain tissues. As a syndrome with mainly neurological symptoms, pathogenesis of RTT has been primarily attributed to neuronal malfunction [5, 40]. The role of the most abundant cell type of the brain (astroglial cells) has been overlooked in most studies [111]. While MeCP2 is not absent in the astrocytes as suggested earlier by researchers of this field [23, 66, 101, 116], its level has been shown to be five-fold lower in astrocytes compared to neurons [104, 111]. Despite low level of

MeCP2 in the astrocytes, its deficiency has been suggested to contribute in abnormal neurodevelopment [104].

The role of astrocytes in dendritic growth, synaptogenesis, synapse function, and plasticity has already been reported in the literature [238]. Moreover, the fact that the peak period of astrocytes generation is after birth and continues even in the adult brain is in line with postnatal onset of a neurodevelopmental disorder such as RTT. Besides that, MeCP2 loss- and gain-of-function in postnatal astrocytes can result in RTT-like phenotype in mice and subsequent rescue of most features respectively [239]. An intriguing finding of my study is the absence of MeCP2 immunoreactivity in almost all astroglial cells of the white matter in human RTT brain, whereas it appears to be ubiquitously present in astroglial cells of the control brain tissues. Noticeably, neurons in the RTT brain tissues are not significantly different from their control counterparts.

In one study, Maezawa and colleagues showed that MeCP2 protein level in the cultured astrocytes from mosaic female heterozygous *Mecp2*$^{-/+}$mice (from mating *Mecp2*$^{tm1.1Bird/+}$ mice with C57BL/6J mice of Jackson Laboratories) was 10-30% of wild type astrocytes, which was far below a balanced X-chromosome inactivation [239]. Neurons did not follow the same pattern. MeCP2 expression had been shown in 70-80% of neurons with mosaic *Mecp2*$^{-/+}$ by Maezawa and a few other researchers [240, 241]. Maezawa et al [239] showed similar results in an *in vivo* study suggesting that a non-cell autonomous effect from MeCP2^{-} astrocytes could negatively influence MeCP2 level in cells that were MeCP2^{+}. They also suggested a few candidate negative regulators including *miR132* that might transfer overtime from MeCP2^{-} to MeCP2^{+} astrocytes *via* gap junctions and result in astrocyte selective decline of MeCP2 around the time of phenotypic regression in RTT [239].

In addition to the theory of astrocytic spread of MeCP2-deficiency through connexin-mediated gap junctions, another study has shown that neural stem cells with knocked-out *MECP2* have higher tendency to differentiate into astrocytes than neurons [242]. Based on this study, from a pool of heterozygous neural stem cells, those with defective *MECP2* gene on the active X might preferentially differentiate intro astrocytes

rather than neurons. This can provide an explanation for the dominant MeCP2^{-} astrocytes in our studied RTT brain samples.

Working on post-mortem brain samples, we should also consider that a protein like MeCP2 in different cell types of the brain might react variably to peri-mortem conditions and glial cells might be more susceptible to these intervening factors.

4.4 BDNF and its cellular source in IHC studies on human brain samples

The fact that BDNF was primarily purified from the brain [146] does not mean that neurons are the main cellular source of this protein. In fact, it is almost 20 years that cell culture studies have shown that endothelial cells of the cerebral microvasculature can express BDNF [243, 244]. After being overlooked for years, more recent *in vivo* studies have shown BDNF expression by endothelial cells of adult cerebrovasculature [245, 246]. Even a 50-time higher BDNF production rate has been attributed to cerebral endothelial cells in comparison with cortical neurons [247]. Based on a few other research studies, removal of cerebral endothelial cells significantly decreases BDNF levels in the brain [248]. Furthermore, different studies have shown that glial cells such as astrocytes and oligodendrocytes synthetize and release BDNF [249, 250]. The prominent astroglial/endothelial pattern of BDNF staining in my study extends previous findings in the animal models and cell culture systems to different regions of normal as well as RTT human brain. At the same time, it adds more questions to the role of MeCP2-BDNF cross-talks in RTT pathophysiology because most model systems have focused on neurons as the main source of BDNF, which has been challenged by my results.

Apart from the cellular source of BDNF, its impairment in RTT patients is another controversy that our study has approached from a post-mortem human brain angle. Here, I showed lower *BDNF* transcript expression in RTT brain. However, BDNF protein levels (detected by WB, ELISA, and IHC) did not follow the same trend. Surprisingly, we observed higher BDNF expression in Purkinje cells of RTT cerebellar tissues. As mentioned earlier, the weak predictive value of transcript expression for corresponding

proteins is not uncommon and has been linked to complex regulation of protein expression in the human brain [236]. However, it is noticeable that the anti-BDNF antibody that we used for WB and IHC is capable of detecting pro-BDNF and the mature protein. The coating antibody of the ELISA kit also detects both mature BDNF and pro-BDNF. While WB experiment differentiate between pro-BDNF and mature BDNF by molecular size, ELISA and IHC show the combination of both protein forms.

Considering the inhibitory character of Purkinje cells as GABAergic neurons, we might relate more intense immunolabeling of these cells in RTT brains to higher level of ProBDNF, which has a reverse function compared to the mature BDNF [167]. Our WB results with lower level of mature BDNF and higher level of ProBDNF in the cerebellum are in line with IHC findings. Furthermore, BDNF immunoreactivity has been shown to increase with conditions like hypoxia or neuroinflammation [251, 252], which are part of the pathogenesis of different neurological diseases, not yet studied in RTT brain. Finally, our results are important from a therapeutic point of view. This is mainly by considering the endothelial cells as a major source of BDNF in human brain that might allow us to circumvent the blood-brain-barrier and focus on increasing BDNF levels in the brain through its non-neuronal sources.

5. Conclusion

5.1 Strength, Challenges and limitations

5.1.1 Significance and strength of this study

This study provides evidence about changes in total *MECP2*/MeCP2 and its isoforms, *BDNF*/BDNF, and *miR132* in four different regions of RTT human brain. While our data partly support previous studies on animal model neurons, as well as non-neuronal samples, major differences have been highlighted in this study. Our findings from post-mortem human brain samples were not supportive for the suppressive effect of *miR132* on MeCP2. However, inter-regional variations were also present in post-mortem human brains. For instance, cerebellum was not similar to the other regions in that regard, and its level of *miR132* had not changed in the same direction as the other studied transcripts (*MECP2* isoforms, and *BDNF*) in the RTT brain samples.

We further showed a significant reduction of MeCP2 labeling in glial cells of white matter, but not neurons in the RTT human brain. In addition, the relationship between BDNF, and MeCP2 was challenged from a cell of origin standpoint. This might add to the complexity of regulatory systems, but at the same time opens the possibility of a more achievable therapeutic approach through non-neuronal sources of BDNF.

While increasing number of studies have shown different MeCP2 roles from neurodevelopment to the function of immune system [253], and carcinogenesis [74], MeCP2 homeostasis regulatory network is still poorly understood. Our findings would help to shed some light on this regulatory network and obscurities caused by limited studies on MeCP2 in the human brain. Our results are important as an effort to translate the vast body of data from non-human models of RTT to the disease condition. Furthermore, several more common conditions such as Autism Spectrum Disorders or Fetal Alcohol

Spectrum Disorders with the evidence for the role of MeCP2 in their pathophysiology [74], would also benefit from the results of our study.

5.1.2 Limitations and challenges

While studies in RTT mouse models and different cell lines can be done in multiples to examine reproducibility, access to human RTT patient brain samples is limited. We still had access to different brain regions of four RTT brain and six human brain controls. We have also had access to three technical replicates for each RTT sample and its control in protein studies as well as, four technical replicates for transcript analysis.

Being aware of the intervening factors in studying human post-mortem brain samples, we tried to minimize their effect on the result by choosing comparable controls. Part of the study was also dedicated to evaluating the impacts of PMD as one of these intervening factors. However similar to other human post-mortem studies, unknown pre- and post-mortem factors may potentially exist that cannot be fully considered in choosing the controls and analysing the results.

Studying the frozen brain lysate gives us an overall result for different cell types with potentially variable regulatory systems in a complex organ such as the human brain. By doing IHC studies, we brought the analysis to the cellular level for the two main proteins of this study. I am mindful that IHC represents a snapshot of the location of the proteins at fixed samples and not necessarily representing information about the dynamics of their production and secretion. Of course, a functional model system would complement nicely this expression-based study.

5.2 Future directions of this study

Studying the same elements in more samples, especially different RTT samples with similar mutations, can give more significance to the analytic part of the study and can make the correlation studies possible.

In vitro studies on human cell lines (neuronal or glial) for the parameters studied in this project can clarify the observed changes at the cellular level. This can become more dynamic through chemical or molecular manipulation of the cells such as adding BDNF to the cells in culture, or Knock down/ overexpression of one factor and studying the alterations in the rest.

The study on the effects of post-mortem delay on IHC can be followed by making tissue arrays of different PMD from one single brain sample to eliminate factors other than post-mortem delay from the study.

References

1. Rett A: On a unusual brain atrophy syndrome in hyperammonemia in childhood. Wiener medizinische Wochenschrift 1946, 116(37):723-726.

2. Hagberg B, Aicardi J, Dias K, Ramos O: A progressive syndrome of autism, dementia, ataxia, and loss of purposeful hand use in girls: Rett's syndrome: report of 35 cases. Ann Neurol 1983, 14(4):471-9.

3. Lewis JD, Meehan RR, Henzel WJ, Maurer-Fogy I, Jeppesen P, Klein F, Bird A: Purification, sequence, and cellular localization of a novel chromosomal protein that binds to methylated DNA. Cell 1992, 69(6):905-14.

4. Amir RE, Van dV, Wan M, Tran CQ, Francke U, Zoghbi HY: Rett syndrome is caused by mutations in X-linked MECP2, encoding methyl-CpG-binding protein 2. Nat Genet 1999, 23:185-188.

5. Guy J, Hendrich B, Holmes M, Martin JE, Bird A: A mouse Mecp2-null mutation causes neurological symptoms that mimic rett syndrome. Nat Genet 2001, 27(3):322-326.

6. Leonard H, Cobb S, Downs J: Clinical and biological progress over 50 years in Rett syndrome. Nature reviews.Neurology 2017, 13(1):37-51.

7. Neul JL, Kaufmann WE, Glaze DG, Christodoulou J, Clarke AJ, Bahi-Buisson N, Leonard H, Bailey MES, Schanen NC, Zappella M, Renieri A, Huppke P, Percy AK, Consortium R: Rett syndrome: revised diagnostic criteria and nomenclature. Ann Neurol 2010, 68(6):944-50.

8. Nomura Y: Early behavior characteristics and sleep disturbance in Rett syndrome. Brain Dev 2005, 27 Suppl 1:S35-S42.

9. Segawa M: Early motor disturbances in Rett syndrome and its pathophysiological importance. Brain Dev 2005, 27 Suppl 1:S54-S58.

10. Weese-Mayer D, Lieske SP, Boothby CM, Kenny AS, Bennett HL, Ramirez J: Autonomic dysregulation in young girls with Rett Syndrome during nighttime in-home recordings. Pediatr Pulmonol 2008, 43(11):1045-1060.

11. Weese-Mayer D, Lieske SP, Boothby CM, Kenny AS, Bennett HL, Silvestri JM, Ramirez J: Autonomic nervous system dysregulation: breathing and heart rate perturbation during wakefulness in young girls with Rett syndrome. Pediatr Res 2006, 60(4):443-9.

12. Hagberg B: Rett syndrome: long-term clinical follow-up experiences over four decades. J Child Neurol 2005, 20(9):722-7.

13. Jian L, Nagarajan L, de Klerk N, Ravine D, Bower C, Anderson A, Williamson S, Christodoulou J, Leonard H: Predictors of seizure onset in Rett syndrome. J Pediatr 2006, 149(4):542-7.

14. Tarquinio DC, Hou W, Neul JL, Kaufmann WE, Glaze DG, Motil KJ, Skinner SA, Lee H, Percy AK: The Changing Face of Survival in Rett Syndrome and MECP2-Related Disorders. Pediatr Neurol 2015, 53(5):402-11.

15. Percy AK, Neul JL, Glaze DG, Motil KJ, Skinner SA, Khwaja O, Lee H, Lane JB, Barrish JO, Annese F, McNair L, Graham J, Barnes K: Rett syndrome diagnostic criteria: lessons from the Natural History Study. Ann Neurol 2010, 68(6):951-5.

16. Reichow B, George-Puskar A, Lutz T, Smith IC, Volkmar FR: Brief report: systematic review of Rett syndrome in males. J Autism Dev Disord 2015, 45(10):3377-83.

17. Neul JL, Fang P, Barrish J, Lane J, Caeg EB, Smith EO, Zoghbi H, Percy A, Glaze DG: Specific mutations in methyl-CpG-binding protein 2 confer different severity in Rett syndrome. Neurology 2008, 70(16):1313-21.

18. Girard M, Couvert P, Carrié A, Tardieu M, Chelly J, Beldjord C, Bienvenu T: Parental origin of de novo MECP2 mutations in Rett syndrome. European journal of human genetics: EJHG 2001, 9(3):231-6.

19. Wan M, Lee SS, Zhang X, Houwink-Manville I, Song HR, Amir RE, Budden S, Naidu S, Pereira JL, Lo IF, Zoghbi HY, Schanen NC, Francke U: Rett syndrome and beyond:

recurrent spontaneous and familial MECP2 mutations at CpG hotspots. Am J Hum Genet 1999, 65(6):1520-9.

20. Villard L, Kpebe A, Cardoso C, Chelly PJ, Tardieu PM, Fontes M: Two affected boys in a Rett syndrome family: clinical and molecular findings. Neurology 2000, 55(8):1188-93.

21. Krishnaraj R, Ho G, Christodoulou J: RettBASE: Rett syndrome database update. Hum Mutat 2017, 38(8):922-931.

22. Archer H, Evans J, Leonard H, Colvin L, Ravine D, Christodoulou J, Williamson S, Charman T, Bailey MES, Sampson J, de Klerk N, Clarke A: Correlation between clinical severity in patients with Rett syndrome with a p.R168X or p.T158M MECP2 mutation, and the direction and degree of skewing of X-chromosome inactivation. J Med Genet 2007, 44(2):148-52.

23. Shahbazian MD, Antalffy B, Armstrong DL, Zoghbi HY: Insight into Rett syndrome: MeCP2 levels display tissue-and cell-specific differences and correlate with neuronal maturation. Hum Mol Genet 2002, 11(2):115-124.

24. Renieri A, Meloni I, Longo I, Ariani F, Mari F, Pescucci C, Cambi F: Rett syndrome: the complex nature of a monogenic disease. J Mol Med 2003, 81(6):346-54.

25. Bourdon V, Philippe C, Bienvenu T, Koenig B, Tardieu M, Chelly J, Jonveaux P: Evidence of somatic mosaicism for a MECP2 mutation in females with Rett syndrome: diagnostic implications. J Med Genet 2001, 38(12):867-71.

26. Cuddapah VA, Pillai RB, Shekar KV, Lane JB, Motil KJ, Skinner SA, Tarquinio DC, Glaze DG, McGwin G, Kaufmann WE, Percy AK, Neul JL, Olsen ML: Methyl-CpG-binding protein 2 (MECP2) mutation type is associated with disease severity in Rett syndrome. J Med Genet 2014, 51(3):152-8.

27. Nan X, Tate P, Li E, Bird A: DNA methylation specifies chromosomal localization of MeCP2. Mol Cell Biol 1996, 16(1):414-21.

28. Smeets E, Terhal P, Casaer P, Peters A, Midro A, Schollen E, van Roozendaal K, Moog U, Matthijs G, Herbergs J, Smeets H, Curfs L, Schrander-Stumpel C, Fryns JP:

Rett syndrome in females with CTS hot spot deletions: a disorder profile. American journal of medical genetics.Part A 2005, 132A (2):117-20.

29. Armstrong DD: Neuropathology of Rett syndrome. J Child Neurol 2005, 20(9):747-53.

30. Reiss AL, Faruque F, Naidu S, Abrams M, Beaty T, Bryan RN, Moser H: Neuroanatomy of Rett syndrome: a volumetric imaging study. Ann Neurol 1993, 34(2):227-34.

31. Subramaniam B, Naidu S, Reiss AL: Neuroanatomy in Rett syndrome: cerebral cortex and posterior fossa. Neurology 1997, 48(2):399-407.

32. Armstrong D, Dunn JK, Antalffy B, Trivedi R: Selective dendritic alterations in the cortex of Rett syndrome. J Neuropathol Exp Neurol 1995, 54(2):195-201.

33. Jellinger K, Seitelberger F: Neuropathology of Rett syndrome. 1986, 1:259-288.

34. Belichenko PV, Hagberg B, Dahlström A: Morphological study of neocortical areas in Rett syndrome. Acta Neuropathol 1997, 93(1):50-61.

35. O'Connor T,M., O'Connell J, O'Brien D,I., Goode T, Bredin CP, Shanahan F: The role of substance P in inflammatory disease. J Cell Physiol 2004, 201(2):167-80.

36. Géranton S,M., Morenilla-Palao C, Hunt SP: A role for transcriptional repressor methyl-CpG-binding protein 2 and plasticity-related gene serum- and glucocorticoid-inducible kinase 1 in the induction of inflammatory pain states. The Journal of neuroscience: the official journal of the Society for Neuroscience 2007, 27(23):6163-73.

37. Downs J, Géranton S,M., Bebbington A, Jacoby P, Bahi-Buisson N, Ravine D, Leonard H: Linking MECP2 and pain sensitivity: the example of Rett syndrome. American journal of medical genetics.Part A 2010, 152A (5):1197-205.

38. Barney CC, Feyma T, Beisang A, Symons FJ: Pain experience and expression in Rett syndrome: Subjective and objective measurement approaches. Journal of developmental and physical disabilities 2015, 27(4):417-429.

39. LaSalle JM, Goldstine J, Balmer D, Greco CM: Quantitative localization of heterogeneous methyl-CpG-binding protein 2 (MeCP2) expression phenotypes in normal

and Rett syndrome brain by laser scanning cytometry. Hum Mol Genet 2001, 10(17):1729-40.

40. Ezeonwuka CD, Rastegar M: MeCP2-Related Diseases and Animal Models. Diseases (Basel, Switzerland) 2014, 2(1):45-70.

41. Chen RZ, Akbarian S, Tudor M, Jaenisch R: Deficiency of methyl-CpG binding protein-2 in CNS neurons results in a Rett-like phenotype in mice. Nat Genet 2001, 27(3):327-331.

42. Marchetto MCNM, Carromeu C, Acab A, Yu D, Yeo GW, Mu Y, Chen G, Gage FH, Muotri AR: A model for neural development and treatment of Rett syndrome using human induced pluripotent stem cells. Cell 2010, 143(4):527-39.

43. Li Y, Wang H, Muffat J, Cheng AW, Orlando DA, Kwok S, Feldman DA, Bateup HS, Gao Q, Mitalipova M, Lewis CA, Heiden MGV, Sur M, Young RA, Jaenisch R: Global transcriptional and translational repression in human embryonic stem cells-derived Rett Syndrome neurons. Cell Stem Cell 2013, 13(4):446-458.

44. Yazdani M, Deogracias R, Guy J, Poot RA, Bird A, Barde YA: Disease modeling using embryonic stem cells: MeCP2 regulates nuclear size and RNA synthesis in neurons. Stem Cells 2012.

45. Fyffe SL, Neul JL, Samaco RC, Chao H, Ben-Shachar S, Moretti P, McGill BE, Goulding EH, Sullivan E, Tecott LH, Zoghbi HY: Deletion of Mecp2 in Sim1-expressing neurons reveals a critical role for MeCP2 in feeding behavior, aggression, and the response to stress. Neuron 2008, 59(6):947-58.

46. Samaco RC, Mandel-Brehm C, Chao H, Ward CS, Fyffe-Maricich S, Ren J, Hyland K, Thaller C, Maricich SM, Humphreys P, Greer JJ, Percy A, Glaze DG, Zoghbi HY, Neul JL: Loss of MeCP2 in aminergic neurons causes cell-autonomous defects in neurotransmitter synthesis and specific behavioral abnormalities. Proc Natl Acad Sci U S A 2009, 106(51):21966-71.

47. Lawson-Yuen A, Liu D, Han L, Jiang ZI, Tsai GE, Basu AC, Picker J, Feng J, Coyle JT: Ube3a mRNA and protein expression are not decreased in Mecp2R168X mutant mice. Brain Res 2007, 1180:1-6.

48. Jentarra GM, Olfers SL, Rice SG, Srivastava N, Homanics GE, Blue M, Naidu S, Narayanan V: Abnormalities of cell packing density and dendritic complexity in the MeCP2 A140V mouse model of Rett syndrome/X-linked mental retardation. BMC neuroscience 2010, 11:19-19.

49. Calfa G, Percy AK, Pozzo-Miller L: Experimental models of Rett syndrome based on Mecp2 dysfunction. Exp Biol Med (Maywood) 2011, 236(1):3-19.

50. Lyst MJ, Bird A: Rett syndrome: A complex disorder with simple roots. Nature Reviews Genetics 2015, 16(5):261-274.

51. Fyffe SL, Neul JL, Samaco RC, Chao H, Ben-Shachar S, Moretti P, McGill BE, Goulding EH, Sullivan E, Tecott LH: Deletion of Mecp2 in Sim1-expressing neurons reveals a critical role for MeCP2 in feeding behavior, aggression, and the response to stress. Neuron 2008, 59(6):947-958.

52. Wang X, Lacza Z, Sun YE, Han W: Leptin resistance and obesity in mice with deletion of methyl-CpG-binding protein 2 (MeCP2) in hypothalamic pro-opiomelanocortin (POMC) neurons. Diabetologia 2014, 57(1):236-245.

53. Samaco RC, Mandel-Brehm C, Chao HT, Ward CS, Fyffe-Maricich SL, Ren J, Hyland K, Thaller C, Maricich SM, Humphreys P, Greer JJ, Percy A, Glaze DG, Zoghbi HY, Neul JL: Loss of MeCP2 in aminergic neurons causes cell-autonomous defects in neurotransmitter synthesis and specific behavioral abnormalities. Proc Natl Acad Sci U S A 2009, 106(51):21966-21971.

54. Goffin D, Brodkin ES, Blendy JA, Siegel SJ, Zhou Z: Cellular origins of auditory event-related potential deficits in Rett syndrome. Nat Neurosci 2014, 17(6):804.

55. Zhang W, Peterson M, Beyer B, Frankel WN, Zhang ZW: Loss of MeCP2 from forebrain excitatory neurons leads to cortical hyperexcitation and seizures. J Neurosci 2014, 34(7):2754-2763.

56. Ward CS, Arvide EM, Huang TW, Yoo J, Noebels JL, Neul JL: MeCP2 is critical within HoxB1-derived tissues of mice for normal lifespan. J Neurosci 2011, 31(28):10359-10370.

57. Adachi M, Autry AE, Covington HE,3rd, Monteggia LM: MeCP2-mediated transcription repression in the basolateral amygdala may underlie heightened anxiety in a mouse model of Rett syndrome. J Neurosci 2009, 29(13):4218-4227.

58. Chao H, Chen H, Samaco RC, Xue M, Chahrour M, Yoo J, Neul JL, Gong S, Lu H, Heintz N: Dysfunction in GABA signalling mediates autism-like stereotypies and Rett syndrome phenotypes. Nature 2010, 468(7321):263.

59. Gemelli T, Berton O, Nelson ED, Perrotti LI, Jaenisch R, Monteggia LM: Postnatal loss of methyl-CpG binding protein 2 in the forebrain is sufficient to mediate behavioral aspects of Rett syndrome in mice. Biol Psychiatry 2006, 59(5):468-476.

60. Katz DM, Bird A, Coenraads M, Gray SJ, Menon DU, Philpot BD, Tarquinio DC: Rett Syndrome: Crossing the Threshold to Clinical Translation. Trends Neurosci 2016, 39(2):100-113.

61. Chapleau CA, Lane J, Larimore J, Li W, Pozzo-Miller L, Percy AK: Recent Progress in Rett Syndrome and MeCP2 Dysfunction: Assessment of Potential Treatment Options. Future neurology 2013, 8(1).

62. Van Esch H, Bauters M, Ignatius J, Jansen M, Raynaud M, Hollanders K, Lugtenberg D, Bienvenu T, Jensen LR, Gecz J, Moraine C, Marynen P, Fryns J, Froyen G: Duplication of the MECP2 region is a frequent cause of severe mental retardation and progressive neurological symptoms in males. Am J Hum Genet 2005, 77(3):442-53.

63. del Gaudio D, Fang P, Scaglia F, Ward PA, Craigen WJ, Glaze DG, Neul JL, Patel A, Lee JA, Irons M, Berry SA, Pursley AA, Grebe TA, Freedenberg D, Martin RA, Hsich GE, Khera JR, Friedman NR, Zoghbi HY, Eng CM, Lupski JR, Beaudet AL, Cheung SW, Roa BB: Increased MECP2 gene copy number as the result of genomic duplication in neurodevelopmentally delayed males. Genetics in medicine: official journal of the American College of Medical Genetics 2006, 8(12):784-92.

64. Huang H, Allen JA, Mabb AM, King IF, Miriyala J, Taylor-Blake B, Sciaky N, Dutton JW, Lee H, Chen X, Jin J, Bridges AS, Zylka MJ, Roth BL, Philpot BD: Topoisomerase inhibitors unsilence the dormant allele of Ube3a in neurons. Nature 2011, 481(7380):185-9.

65. Meng L, Ward AJ, Chun S, Bennett CF, Beaudet AL, Rigo F: Towards a therapy for Angelman syndrome by targeting a long non-coding RNA. Nature 2015, 518(7539):409-12.

66. Rastegar M, Hotta A, Pasceri P, Makarem M, Cheung AYL, Elliott S, Park KJ, Adachi M, Jones FS, Clarke ID, Dirks P, Ellis J: MECP2 isoform-specific vectors with regulated expression for Rett syndrome gene therapy. PloS one 2009, 4(8):e6810-e6810.

67. Garg SK, Lioy DT, Cheval H, McGann JC, Bissonnette JM, Murtha MJ, Foust KD, Kaspar BK, Bird A, Mandel G: Systemic delivery of MeCP2 rescues behavioral and cellular deficits in female mouse models of Rett syndrome. The Journal of neuroscience: the official journal of the Society for Neuroscience 2013, 33(34):13612-20.

68. Keeling KM, Xue X, Gunn G, Bedwell DM: Therapeutics based on stop codon readthrough. Annual review of genomics and human genetics 2014, 15:371-94.

69. Brendel C, Belakhov V, Werner H, Wegener E, Gärtner J, Nudelman I, Baasov T, Huppke P: Readthrough of nonsense mutations in Rett syndrome: evaluation of novel aminoglycosides and generation of a new mouse model. J Mol Med 2011, 89(4):389-98.

70. Olson CO, Zachariah RM, Ezeonwuka CD, Liyanage VRB, Rastegar M: Brain region-specific expression of MeCP2 isoforms correlates with DNA methylation within Mecp2 regulatory elements. PLoS ONE 2014, 9(3).

71. Gadalla KKE, Bailey MES, Cobb SR: MeCP2 and Rett syndrome: reversibility and potential avenues for therapy. Biochem J 2011, 439(1):1-14.

72. Lombardi LM, Baker SA, Zoghbi HY: MECP2 disorders: from the clinic to mice and back. J Clin Invest 2015, 125(8):2914-23.

73. Delcuve GP, Rastegar M, Davie JR: Epigenetic control. J Cell Physiol 2009, 219(2):243-50.

74. Liyanage VRB, Rastegar M: Rett syndrome and MeCP2. NeuroMolecular Medicine 2014, 16(2):231-264.

75. Kobrossy L, Rastegar M, Featherstone M: Interplay between chromatin and trans-acting factors regulating the Hoxd4 promoter during neural differentiation. The Journal of biological chemistry 2006, 281(36):25926-39.

76. Segal E, Widom J: What controls nucleosome positions? Trends in genetics: TIG 2009, 25(8):335-43.

77. Rastegar M, Kobrossy L, Kovacs EN, Rambaldi I, Featherstone M: Sequential Histone Modifications at Hoxd4 Regulatory Regions Distinguish Anterior from Posterior Embryonic Compartments. Mol Cell Biol 2004.

78. Liyanage VRB, Zachariah RM, Delcuve GP, Davie JR, Rastegar M: An Epigenetic Perspective. In *New developments in chromatin research.* Edited by Simpson NM, Stewart VJ. New York: Nova Science; 2012:29-58.

79. Kouzarides T: Chromatin modifications and their function. Cell 2007, 128(4):693-705.

80. Barber BA, Rastegar M: Epigenetic control of Hox genes during neurogenesis, development, and disease. Ann Anat 2010, 192(5):261-74.

81. Liyanage, Vichithra R. B., Zachariah, Robby M., Delcuve Geneviève P., Davie, James R.,Rastegar, Mojgan: Chromatin Structure and Epigenetics. In *Advances in Genetics Researc.* Edited by Urbano KV. Nova Science; 2015:57-88.

82. Patel DJ, Wang Z: Readout of epigenetic modifications. Annu Rev Biochem 2013, 82:81-118.

83. Huisinga KL, Brower-Toland B, Elgin SCR: The contradictory definitions of heterochromatin: transcription and silencing. Chromosoma 2006, 115(2):110-22.

84. Trojer P, Reinberg D: Facultative heterochromatin: is there a distinctive molecular signature? Mol Cell 2007, 28(1):1-13.

85. Liyanage VRB, Jarmasz JS, Murugeshan N, Del Bigio M,R., Rastegar M, Davie JR: DNA modifications: function and applications in normal and disease States. Biology 2014, 3(4):670-723.

86. Rastegar M, Delcuve G, Davie JR: Epigenetic analysis of pluripotent cells. In *Human Stem Cell Technology and Biology: A Research Guide and Laboratory Manual.* Edited by

G. S. Stein, M. Borowski,M.X. Luong, M.-J. Shi,K. P. Smith, and P. Vazquez. John Wiley and Sons, Inc; 2011:273-288.

87. Patil VS, Zhou R, Rana TM: Gene regulation by non-coding RNAs. Crit Rev Biochem Mol Biol 49(1):16-32.

88. Beckedorff FC, Ayupe AC, Crocci-Souza R, Amaral MS, Nakaya HI, Soltys DT, Menck CFM, Reis EM, Verjovski-Almeida S: The intronic long noncoding RNA ANRASSF1 recruits PRC2 to the RASSF1A promoter, reducing the expression of RASSF1A and increasing cell proliferation. PLoS genetics 2013, 9(8):e1003705-e1003705.

89. Wu H, Tao J, Chen PJ, Shahab A, Ge W, Hart RP, Ruan X, Ruan Y, Sun YE: Genome-wide analysis reveals methyl-CpG-binding protein 2-dependent regulation of microRNAs in a mouse model of Rett syndrome. Proc Natl Acad Sci U S A 2010, 107(42):18161-6.

90. Guo JU, Su Y, Zhong C, Ming G, Song H: Emerging roles of TET proteins and 5-hydroxymethylcytosines in active DNA demethylation and beyond. Cell cycle (Georgetown, Tex.) 2011, 10(16):2662-8.

91. Rastegar M: Epigenetics and Cerebellar Neurodevelopmental Disorders. In *Development of the Cerebellum from Molecular Aspects to Diseases.* Edited by Marzban H. Springer International Publishing AG; 2017:197-218.

92. Defossez P, Stancheva I: Biological functions of methyl-CpG-binding proteins. Progress in molecular biology and translational science 2011, 101:377-98.

93. Li L, Chen B, Chan W: An epigenetic regulator: methyl-CpG-binding domain protein 1 (MBD1). International journal of molecular sciences 2015, 16(3):5125-40.

94. Du Q, Luu P, Stirzaker C, Clark SJ: Methyl-CpG-binding domain proteins: readers of the epigenome. Epigenomics 2015, 7(6):1051-73.

95. Lewis J, Bird A: DNA methylation and chromatin structure. FEBS Lett 1991, 285(2):155-9.

96. Boyes J, Bird A: DNA methylation inhibits transcription indirectly via a methyl-CpG binding protein. Cell 1991, 64(6):1123-34.

97. Mnatzakanian GN, Lohi H, Munteanu I, Alfred SE, Yamada T, MacLeod PJM, Jones JR, Scherer SW, Schanen NC, Friez MJ, Vincent JB, Minassian BA: A previously unidentified MECP2 open reading frame defines a new protein isoform relevant to Rett syndrome. Nat Genet 2004, 36(4):339-41.

98. Reeves R, Nissen MS: The A.T-DNA-binding domain of mammalian high mobility group I chromosomal proteins. A novel peptide motif for recognizing DNA structure. The Journal of biological chemistry 1990, 265(15):8573-82.

99. Adams VH, McBryant SJ, Wade PA, Woodcock CL, Hansen JC: Intrinsic disorder and autonomous domain function in the multifunctional nuclear protein, MeCP2. The Journal of biological chemistry 2007, 282(20):15057-64.

100. Kriaucionis S, Bird A: The major form of MeCP2 has a novel N-terminus generated by alternative splicing. Nucleic Acids Res 2004, 32(5):1818-23.

101. Zachariah RM, Olson CO, Ezeonwuka C, Rastegar M: Novel MeCP2 Isoform-Specific Antibody Reveals the Endogenous MeCP2E1 Expression in Murine Brain, Primary Neurons and Astrocytes. PLoS ONE 2012, 7(11):24-28.

102. Ballas N, Lioy DT, Grunseich C, Mandel G: Non-cell autonomous influence of MeCP2-deficient glia on neuronal dendritic morphology. Nat Neurosci 2009, 12(3):311-7.

103. Maezawa I, Jin L: Rett syndrome microglia damage dendrites and synapses by the elevated release of glutamate. The Journal of neuroscience: the official journal of the Society for Neuroscience 2010, 30(15):5346-56.

104. Yasui DH, Xu H, Dunaway KW, LaSalle JM, Jin L, Maezawa I: MeCP2 modulates gene expression pathways in astrocytes. Molecular Autism 2013, 4(1):3-3.

105. Derecki NC, Cronk JC, Lu Z, Xu E, Abbott SBG, Guyenet PG, Kipnis J: Wild-type microglia arrest pathology in a mouse model of Rett syndrome. Nature 2012, 484(7392):105-9.

106. Jones PL, Veenstra GJ, Wade PA, Vermaak D, Kass SU, Landsberger N, Strouboulis J, Wolffe AP: Methylated DNA and MeCP2 recruit histone deacetylase to repress transcription. Nat Genet 1998, 19(2):187-91.

107. Delcuve GP, Khan DH, Davie JR: Roles of histone deacetylases in epigenetic regulation: emerging paradigms from studies with inhibitors. Clinical epigenetics 2012, 4(1):5-5.

108. Lyst MJ, Ekiert R, Ebert DH, Merusi C, Nowak J, Selfridge J, Guy J, Kastan NR, Robinson ND, de LA, Rappsilber J, Greenberg ME, Bird A: Rett syndrome mutations abolish the interaction of MeCP2 with the NCoR/SMRT co-repressor. Nat Neurosci 2013, 16(7):898-902.

109. Chahrour M, Jung SY, Shaw C, Zhou X, Wong STC, Qin J, Zoghbi HY: MeCP2, a key contributor to neurological disease, activates and represses transcription. Science (New York, N.Y.) 2008, 320(5880):1224-9.

110. Mellén M, Ayata P, Dewell S, Kriaucionis S, Heintz N: MeCP2 binds to 5hmC enriched within active genes and accessible chromatin in the nervous system. Cell 2012, 151(7):1417-30.

111. Skene PJ, Illingworth RS, Webb S, Kerr ARW, James KD, Turner DJ, Andrews R, Bird AP: Neuronal MeCP2 Is Expressed at Near Histone-Octamer Levels and Globally Alters the Chromatin State. Mol Cell 2010, 37(4):457-468.

112. Georgel PT, Horowitz-Scherer R, Adkins N, Woodcock CL, Wade PA, Hansen JC: Chromatin compaction by human MeCP2. Assembly of novel secondary chromatin structures in the absence of DNA methylation. The Journal of biological chemistry 2003, 278(34):32181-8.

113. Horike S, Cai S, Miyano M, Cheng J, Kohwi-Shigematsu T: Loss of silent-chromatin looping and impaired imprinting of DLX5 in Rett syndrome. Nat Genet 2005, 37(1):31-40.

114. Zachariah RM, Rastegar M: Linking epigenetics to human disease and Rett syndrome: the emerging novel and challenging concepts in MeCP2 research. Neural Plast 2012, 2012:415825-415825.

115. Liu J, Francke U: Identification of cis-regulatory elements for MECP2 expression. Hum Mol Genet 2006, 15(11):1769-82.

116. Liyanage VRB, Zachariah RM, Rastegar M: Decitabine alters the expression of Mecp2 isoforms via dynamic DNA methylation at the Mecp2 regulatory elements in neural stem cells. Molecular autism 2013, 4(1):46-46.

117. Newnham CM, Hall-Pogar T, Liang S, Wu J, Tian B, Hu J, Lutz CS: Alternative polyadenylation of MeCP2: Influence of cis-acting elements and trans-acting factors. RNA biology 7(3):361-72.

118. Coy JF, Sedlacek Z, Bächner D, Delius H, Poustka A: A complex pattern of evolutionary conservation and alternative polyadenylation within the long 3"-untranslated region of the methyl-CpG-binding protein 2 gene (MeCP2) suggests a regulatory role in gene expression. Hum Mol Genet 1999, 8(7):1253-62.

119. Liyanage VRB, Zachariah RM, Davie JR, Rastegar M: Ethanol deregulates Mecp2/MeCP2 in differentiating neural stem cells via interplay between 5-methylcytosine and 5-hydroxymethylcytosine at the Mecp2 regulatory elements. Exp Neurol 2015, 265:102-17.

120. Bartholdi D, Klein A, Weissert M, Koenig N, Baumer A, Boltshauser E, Schinzel A, Berger W, Mátyás G: Clinical profiles of four patients with Rett syndrome carrying a novel exon 1 mutation or genomic rearrangement in the MECP2 gene. Clin Genet 2006, 69(4):319-26.

121. Nectoux J, Fichou Y, Rosas-Vargas H, Cagnard N, Bahi-Buisson N, Nusbaum P, Letourneur F, Chelly J, Bienvenu T: Cell cloning-based transcriptome analysis in Rett patients: relevance to the pathogenesis of Rett syndrome of new human MeCP2 target genes. J Cell Mol Med 2010, 14(7):1962-74.

122. Kerr B, Jessica SC, Saez M, Abrams A, Walz K, Young JI: Transgenic complementation of MeCP2 deficiency: phenotypic rescue of Mecp2-null mice by isoform-specific transgenes. European journal of human genetics: EJHG 2012, 20(1):69-76.

123. Sheikh TI, Ausió J, Faghfoury H, Silver J, Lane JB, Eubanks JH, MacLeod P, Percy AK, Vincent JB: From Function to Phenotype: Impaired DNA Binding and Clustering Correlates with Clinical Severity in Males with Missense Mutations in MECP2. Scientific Reports 2016, 6:1-13.

124. Zhou X, Liao Y, Xu M, Ji Z, Xu Y, Zhou L, Wei X, Hu P, Han P, Yang F, Pan S, Hu Y: A novel mutation R190H in the AT-hook 1 domain of MeCP2 identified in an atypical Rett syndrome. Oncotarget 2017, 8(47):82156-82164.

125. Sheikh TI, Harripaul R, Ayub M, Vincent JB: MeCP2 AT-Hook1 mutations in patients with intellectual disability and/or schizophrenia disrupt DNA binding and chromatin compaction in vitro. Hum Mutat 2018, 39(5):717-728.

126. Nan X, Ng HH, Johnson CA, Laherty CD, Turner BM, Eisenman RN, Bird A: Transcriptional repression by the methyl-CpG-binding protein MeCP2 involves a histone deacetylase complex. Nature 1998, 393(6683):386-9.

127. Hite KC, Adams VH, Hansen JC: Recent advances in MeCP2 structure and function. Biochem Cell Biol 2009, 87(1):219-27.

128. Zhou Z, Hong EJ, Cohen S, Zhao W, Ho HH, Schmidt L, Chen WG, Lin Y, Savner E, Griffith EC, Hu L, Steen JAJ, Weitz CJ, Greenberg ME: Brain-specific phosphorylation of MeCP2 regulates activity-dependent Bdnf transcription, dendritic growth, and spine maturation. Neuron 2006, 52(2):255-69.

129. Chen WG, Chang Q, Lin Y, Meissner A, West AE, Griffith EC, Jaenisch R, Greenberg ME: Derepression of BDNF transcription involves calcium-dependent phosphorylation of MeCP2. Science (New York, N.Y.) 2003, 302(5646):885-9.

130. Young JI, Hong EP, Castle JC, Crespo-Barreto J, Bowman AB, Rose MF, Kang D, Richman R, Johnson JM, Berget S, Zoghbi HY: Regulation of RNA splicing by the methylation-dependent transcriptional repressor methyl-CpG binding protein 2. Proc Natl Acad Sci U S A 2005, 102(49):17551-8.

131. Martinowich K, Hattori D, Wu H, Fouse S, He F, Hu Y, Fan G, Sun YE: DNA methylation-related chromatin remodeling in activity-dependent BDNF gene regulation. Science (New York, N.Y.) 2003, 302(5646):890-3.

132. Urdinguio RG, Fernandez AF, Lopez-Nieva P, Rossi S, Huertas D, Kulis M, Liu C, Croce CM, Calin GA, Esteller M: Disrupted microRNA expression caused by Mecp2 loss in a mouse model of Rett syndrome. Epigenetics 2010, 5(7):656-63.

133. Miyake K, Hirasawa T, Soutome M, Itoh M, Goto Y, Endoh K, Takahashi K, Kudo S, Nakagawa T, Yokoi S: The protocadherins, PCDHB1 and PCDH7, are regulated by MeCP2 in neuronal cells and brain tissues: implication for pathogenesis of Rett syndrome. BMC neuroscience 2011, 12(1):81.

134. Gibson JH, Slobedman B, Harikrishnan K, Williamson SL, Minchenko D, El-Osta A, Stern JL, Christodoulou J: Downstream targets of methyl CpG binding protein 2 and their abnormal expression in the frontal cortex of the human Rett syndrome brain. BMC neuroscience 2010, 11(1):53.

135. Peddada S, Yasui DH, LaSalle JM: Inhibitors of differentiation (ID1, ID2, ID3 and ID4) genes are neuronal targets of MeCP2 that are elevated in Rett syndrome. Hum Mol Genet 2006, 15(12):2003-2014.

136. Samaco RC, Hogart A, LaSalle JM: Epigenetic overlap in autism-spectrum neurodevelopmental disorders: MECP2 deficiency causes reduced expression of UBE3A and GABRB3. Hum Mol Genet 2004, 14(4):483-492.

137. Bothwell M: NGF, BDNF, NT3, and NT4. Handb Exp Pharmacol 2014, 220:3-15.

138. Binder DK, Scharfman HE: Brain-derived neurotrophic factor. Growth Factors 2004, 22(3):123-31.

139. Bronfman FC, Lazo OM, Flores C, Escudero CA: Spatiotemporal intracellular dynamics of neurotrophin and its receptors. Implications for neurotrophin signaling and neuronal function. Handb Exp Pharmacol 2014, 220:33-65.

140. West AE, Pruunsild P, Timmusk T: Neurotrophins: transcription and translation. Handb Exp Pharmacol 2014, 220:67-100.

141. Bathina S, Das UN: Brain-derived neurotrophic factor and its clinical implications. Archives of medical science: AMS 2015, 11(6):1164-78.

142. Aid T, Kazantseva A, Piirsoo M, Palm K, Timmusk T: Mouse and rat BDNF gene structure and expression revisited. J Neurosci Res 2007, 85(3):525-35.

143. An JJ, Gharami K, Liao G, Woo NH, Lau AG, Vanevski F, Torre ER, Jones KR, Feng Y, Lu B, Xu B: Distinct role of long 3' UTR BDNF mRNA in spine morphology and synaptic plasticity in hippocampal neurons. Cell 2008, 134(1):175-87.

144. Lau AG, Irier HA, Gu J, Tian D, Ku L, Liu G, Xia M, Fritsch B, Zheng JQ, Dingledine R, Xu B, Lu B, Feng Y: Distinct 3'UTRs differentially regulate activity-dependent translation of brain-derived neurotrophic factor (BDNF). Proc Natl Acad Sci U S A 2010, 107(36):15945-50.

145. Waterhouse EG, An JJ, Orefice LL, Baydyuk M, Liao G, Zheng K, Lu B, Xu B: BDNF promotes differentiation and maturation of adult-born neurons through GABAergic transmission. The Journal of neuroscience: the official journal of the Society for Neuroscience 2012, 32(41):14318-30.

146. Barde YA, Edgar D, Thoenen H: Purification of a new neurotrophic factor from mammalian brain. EMBO J 1982, 1(5):549-53.

147. Begni V, Riva MA, Cattaneo A: Cellular and molecular mechanisms of the brain-derived neurotrophic factor in physiological and pathological conditions. Clinical science (London, England: 1979) 2017, 131(2):123-138.

148. Radziejewski C, Robinson RC, DiStefano PS, Taylor JW: Dimeric structure and conformational stability of brain-derived neurotrophic factor and neurotrophin-3. Biochemistry (N Y) 1992, 31(18):4431-6.

149. Mowla SJ, Farhadi HF, Pareek S, Atwal JK, Morris SJ, Seidah NG, Murphy RA: Biosynthesis and post-translational processing of the precursor to brain-derived neurotrophic factor. The Journal of biological chemistry 2001, 276(16):12660-6.

150. Seidah NG, Mowla SJ, Hamelin J, Mamarbachi AM, Benjannet S, Touré, B.B., Basak A, Munzer JS, Marcinkiewicz J, Zhong M, Barale JC, Lazure C, Murphy RA, Chrétien M, Marcinkiewicz M: Mammalian subtilisin/kexin isozyme SKI-1: A widely expressed proprotein convertase with a unique cleavage specificity and cellular localization. Proc Natl Acad Sci U S A 1999, 96(4):1321-6.

151. Lee R, Kermani P, Teng KK, Hempstead BL: Regulation of cell survival by secreted proneurotrophins. Science (New York, N.Y.) 2001, 294(5548):1945-8.

152. Matsuda N, Lu H, Fukata Y, Noritake J, Gao H, Mukherjee S, Nemoto T, Fukata M, Poo M: Differential activity-dependent secretion of brain-derived neurotrophic factor from axon and dendrite. The Journal of neuroscience: the official journal of the Society for Neuroscience 2009, 29(45):14185-98.

153. Dean C, Liu H, Dunning FM, Chang PY, Jackson MB, Chapman ER: Synaptotagmin-IV modulates synaptic function and long-term potentiation by regulating BDNF release. Nat Neurosci 2009, 12(6):767-76.

154. Dieni S, Matsumoto T, Dekkers M, Rauskolb S, Ionescu MS, Deogracias R, Gundelfinger ED, Kojima M, Nestel S, Frotscher M, Barde Y: BDNF and its pro-peptide are stored in presynaptic dense core vesicles in brain neurons. J Cell Biol 2012, 196(6):775-88.

155. Nagappan G, Zaitsev E, Senatorov VV, Yang J, Hempstead BL, Lu B: Control of extracellular cleavage of ProBDNF by high frequency neuronal activity. Proc Natl Acad Sci U S A 2009, 106(4):1267-72.

156. Hempstead BL: Brain-Derived Neurotrophic Factor: Three Ligands, Many Actions. Trans Am Clin Climatol Assoc 2015, 126:9-19.

157. Santi S, Cappello S, Riccio M, Bergami M, Aicardi G, Schenk U, Matteoli M, Canossa M: Hippocampal neurons recycle BDNF for activity-dependent secretion and LTP maintenance. EMBO J 2006, 25(18):4372-80.

158. von Bartheld, C.S., and Wang X, Butowt R: Anterograde axonal transport, transcytosis, and recycling of neurotrophic factors: the concept of trophic currencies in neural networks. Mol Neurobiol 24(1-3):1-28.

159. Edelmann E, Lessmann V, Brigadski T: Pre- and postsynaptic twists in BDNF secretion and action in synaptic plasticity. Neuropharmacology 2014, 76 Pt C:610-27.

160. Chourbaji S, Brandwein C, Gass P: Altering BDNF expression by genetics and/or environment: impact for emotional and depression-like behaviour in laboratory mice. Neurosci Biobehav Rev 2011, 35(3):599-611.

161. Scalettar BA, Jacobs C, Fulwiler A, Prahl L, Simon A, Hilken L, Lochner JE: Hindered submicron mobility and long-term storage of presynaptic dense-core granules revealed by single-particle tracking. Developmental neurobiology 2012, 72(9):1181-95.

162. Bergami M, Santi S, Formaggio E, Cagnoli C, Verderio C, Blum R, Berninger B, Matteoli M, Canossa M: Uptake and recycling of pro-BDNF for transmitter-induced secretion by cortical astrocytes. J Cell Biol 2008, 183(2):213-221.

163. Chao MV: Neurotrophins and their receptors: a convergence point for many signalling pathways. Nature reviews.Neuroscience 2003, 4(4):299-309.

164. Lu Y, Christian K, Lu B: BDNF: a key regulator for protein synthesis-dependent LTP and long-term memory? Neurobiol Learn Mem 2008, 89(3):312-23.

165. Bibel M, Hoppe E, Barde YA: Biochemical and functional interactions between the neurotrophin receptors trk and p75NTR. EMBO J 1999, 18(3):616-22.

166. Teng HK, Teng KK, Lee R, Wright S, Tevar S, Almeida RD, Kermani P, Torkin R, Chen Z, Lee FS, Kraemer RT, Nykjaer A, Hempstead BL: ProBDNF induces neuronal apoptosis via activation of a receptor complex of p75NTR and sortilin. The Journal of neuroscience: the official journal of the Society for Neuroscience 2005, 25(22):5455-63.

167. Mizui T, Ishikawa Y, Kumanogoh H, Kojima M: Neurobiological actions by three distinct subtypes of brain-derived neurotrophic factor: Multi-ligand model of growth factor signaling. Pharmacological research 2016, 105:93-8.

168. Reichardt LF: Neurotrophin-regulated signalling pathways. Philosophical transactions of the Royal Society of London.Series B, Biological sciences 2006, 361(1473):1545-64.

169. Grewal SS, York RD, Stork PJ: Extracellular-signal-regulated kinase signalling in neurons. Curr Opin Neurobiol 1999, 9(5):544-53.

170. Shaywitz AJ, Greenberg ME: CREB: a stimulus-induced transcription factor activated by a diverse array of extracellular signals. Annu Rev Biochem 1999, 68:821-61.

171. Patapoutian A, Reichardt LF: Trk receptors: mediators of neurotrophin action. Curr Opin Neurobiol 2001, 11(3):272-80.

172. Minichiello L: TrkB signalling pathways in LTP and learning. Nature reviews.Neuroscience 2009, 10(12):850-60.

173. Lin G, Bella AJ, Lue TF, Lin C: Brain-derived neurotrophic factor (BDNF) acts primarily via the JAK/STAT pathway to promote neurite growth in the major pelvic ganglion of the rat: part 2. The journal of sexual medicine 2006, 3(5):821-829.

174. Ashcroft M, Stephens RM, Hallberg B, Downward J, Kaplan DR: The selective and inducible activation of endogenous PI 3-kinase in PC12 cells results in efficient NGF-mediated survival but defective neurite outgrowth. Oncogene 1999, 18(32):4586-97.

175. Kang H, Schuman EM: A requirement for local protein synthesis in neurotrophin-induced hippocampal synaptic plasticity. Science (New York, N.Y.) 1996, 273(5280):1402-6.

176. Takei N, Kawamura M, Hara K, Yonezawa K, Nawa H: Brain-derived neurotrophic factor enhances neuronal translation by activating multiple initiation processes: comparison with the effects of insulin. The Journal of biological chemistry 2001, 276(46):42818-25.

177. Castrén E, Zafra F, Thoenen H, Lindholm D: Light regulates expression of brain-derived neurotrophic factor mRNA in rat visual cortex. Proc Natl Acad Sci U S A 1992, 89(20):9444-8.

178. Bozzi Y, Pizzorusso T, Cremisi F, Rossi FM, Barsacchi G, Maffei L: Monocular deprivation decreases the expression of messenger RNA for brain-derived neurotrophic factor in the rat visual cortex. Neuroscience 1995, 69(4):1133-44.

179. Rocamora N, Welker E, Pascual M, Soriano E: Upregulation of BDNF mRNA expression in the barrel cortex of adult mice after sensory stimulation. The Journal of neuroscience: the official journal of the Society for Neuroscience 1996, 16(14):4411-9.

180. Zafra F, Hengerer B, Leibrock J, Thoenen H, Lindholm D: Activity dependent regulation of BDNF and NGF mRNAs in the rat hippocampus is mediated by non-NMDA glutamate receptors. EMBO J 1990, 9(11):3545-50.

181. Zafra F, Castrén E, Thoenen H, Lindholm D: Interplay between glutamate and gamma-aminobutyric acid transmitter systems in the physiological regulation of brain-

derived neurotrophic factor and nerve growth factor synthesis in hippocampal neurons. Proc Natl Acad Sci U S A 1991, 88(22):10037-41.

182. Zafra F, Lindholm D, Castrén E, Hartikka J, Thoenen H: Regulation of brain-derived neurotrophic factor and nerve growth factor mRNA in primary cultures of hippocampal neurons and astrocytes. The Journal of neuroscience: the official journal of the Society for Neuroscience 1992, 12(12):4793-9.

183. Isackson PJ, Huntsman MM, Murray KD, Gall CM: BDNF mRNA expression is increased in adult rat forebrain after limbic seizures: temporal patterns of induction distinct from NGF. Neuron 1991, 6(6):937-48.

184. Pruunsild P, Sepp M, Orav E, Koppel I, Timmusk T: Identification of cis-elements and transcription factors regulating neuronal activity-dependent transcription of human BDNF gene. The Journal of neuroscience: the official journal of the Society for Neuroscience 2011, 31(9):3295-308.

185. Mellios N, Huang H, Grigorenko A, Rogaev E, Akbarian S: A set of differentially expressed miRNAs, including miR-30a-5p, act as post-transcriptional inhibitors of BDNF in prefrontal cortex. Hum Mol Genet 2008, 17(19):3030-42.

186. Varendi K, Mätlik K, Andressoo J: From microRNA target validation to therapy: lessons learned from studies on BDNF. Cellular and molecular life sciences: CMLS 2015, 72(9):1779-94.

187. Klein ME, Lioy DT, Ma L, Impey S, Mandel G, Goodman RH: Homeostatic regulation of MeCP2 expression by a CREB-induced microRNA. Nat Neurosci 2007, 10(12):1513-1514.

188. Ballas N, Grunseich C, Lu DD, Speh JC, Mandel G: REST and its corepressors mediate plasticity of neuronal gene chromatin throughout neurogenesis. Cell 2005, 121(4):645-657.

189. Chang Q, Khare G, Dani V, Nelson S, Jaenisch R: The disease progression of Mecp2 mutant mice is affected by the level of BDNF expression. Neuron 2006, 49(3):341-8.

190. Li W, Calfa G, Larimore J, Pozzo-Miller L: Activity-dependent BDNF release and TRPC signaling is impaired in hippocampal neurons of Mecp2 mutant mice. Proc Natl Acad Sci U S A 2012, 109(42):17087-92.

191. Li W, Pozzo-Miller L: BDNF deregulation in Rett syndrome. Neuropharmacology 2014, 76 Pt C:737-46.

192. Gonzales ML, Adams S, Dunaway KW, LaSalle JM: Phosphorylation of distinct sites in MeCP2 modifies cofactor associations and the dynamics of transcriptional regulation. Mol Cell Biol 2012, 32(14):2894-903.

193. Katz DM: Brain-derived neurotrophic factor and Rett syndrome. In Edited by Anonymous Springer; 2014:481-495.

194. Vanhala R, Korhonen L, Mikelsaar M, Lindholm D, Riikonen R: Neurotrophic factors in cerebrospinal fluid and serum of patients with Rett syndrome. J Child Neurol 1998, 13(9):429-33.

195. Riikonen R: Neurotrophic factors in the pathogenesis of Rett syndrome. J Child Neurol 2003, 18(10):693-7.

196. Abuhatzira L, Makedonski K, Kaufman Y, Razin A, Shemer R: MeCP2 deficiency in the brain decreases BDNF levels by REST/CoREST-mediated repression and increases TRKB production. Epigenetics 2(4):214-22.

197. Deng V, Matagne V, Banine F, Frerking M, Ohliger P, Budden S, Pevsner J, Dissen GA, Sherman LS, Ojeda SR: FXYD1 is an MeCP2 target gene overexpressed in the brains of Rett syndrome patients and Mecp2-null mice. Hum Mol Genet 2007, 16(6):640-50.

198. Chahrour M, Zoghbi HY: The story of Rett syndrome: from clinic to neurobiology. Neuron 2007, 56(3):422-37.

199. Erickson JT, Conover JC, Borday V, Champagnat J, Barbacid M, Yancopoulos G, Katz DM: Mice lacking brain-derived neurotrophic factor exhibit visceral sensory neuron losses distinct from mice lacking NT4 and display a severe developmental deficit in control of breathing. The Journal of neuroscience: the official journal of the Society for Neuroscience 1996, 16(17):5361-71.

200. Conover JC, Erickson JT, Katz DM, Bianchi LM, Poueymirou WT, McClain J, Pan L, Helgren M, Ip NY, Boland P: Neuronal deficits, not involving motor neurons, in mice lacking BDNF and/or NT4. Nature 1995, 375(6528):235-8.

201. Rajman M, Schratt G: MicroRNAs in neural development: from master regulators to fine-tuners. Development 2017, 144(13):2310-2322.

202. Ha M, Kim VN: Regulation of microRNA biogenesis. Nature reviews.Molecular cell biology 2014, 15(8):509-24.

203. Winter J, Jung S, Keller S, Gregory RI, Diederichs S: Many roads to maturity: microRNA biogenesis pathways and their regulation. Nat Cell Biol 2009, 11(3):228-34.

204. Breving K, Esquela-Kerscher A: The complexities of microRNA regulation: mirandering around the rules. Int J Biochem Cell Biol 2010, 42(8):1316-29.

205. Vasudevan S, Tong Y, Steitz JA: Switching from repression to activation: microRNAs can up-regulate translation. Science (New York, N.Y.) 2007, 318(5858):1931-4.

206. Cochella L, Hobert O: Diverse functions of microRNAs in nervous system development. Curr Top Dev Biol 2012, 99:115-43.

207. Cheng HM, Papp JW, Varlamova O, Dziema H, Russell B, Curfman JP, Nakazawa T, Shimizu K, Okamura H, Impey S, Obrietan K: microRNA modulation of circadian-clock period and entrainment. Neuron 2007, 54(5):813-29.

208. Marler KJ, Suetterlin P, Dopplapudi A, Rubikaite A, Adnan J, Maiorano NA, Lowe AS, Thompson ID, Pathania M, Bordey A, Fulga T, Van Vactor D, L., Hindges R, Drescher U: BDNF promotes axon branching of retinal ganglion cells via miRNA-132 and p250GAP. The Journal of neuroscience: the official journal of the Society for Neuroscience 2014, 34(3):969-79.

209. Magill ST, Cambronne XA, Luikart BW, Lioy DT, Leighton BH, Westbrook GL, Mandel G, Goodman RH: microRNA-132 regulates dendritic growth and arborization of newborn neurons in the adult hippocampus. Proc Natl Acad Sci U S A 2010, 107(47):20382-7.

210. Remenyi J, van den Bosch M, W.M., Palygin O, Mistry RB, McKenzie C, Macdonald A, Hutvagner G, Arthur JS, Frenguelli BG, Pankratov Y: miR-132/212 knockout mice reveal roles for these miRNAs in regulating cortical synaptic transmission and plasticity. PloS one 2013, 8(4):e62509-e62509.

211. Edbauer D, Neilson JR, Foster KA, Wang C, Seeburg DP, Batterton MN, Tada T, Dolan BM, Sharp PA, Sheng M: Regulation of synaptic structure and function by FMRP-associated microRNAs miR-125b and miR-132. Neuron 2010, 65(3):373-84.

212. Jasińska M, Miłek J, Cymerman IA, Łęski S, Kaczmarek L, Dziembowska M: miR-132 Regulates Dendritic Spine Structure by Direct Targeting of Matrix Metalloproteinase 9 mRNA. Mol Neurobiol 2016, 53(7):4701-12.

213. Lee S, Chu K, Im W, Yoon H, Im J, Park J, Park K, Jung K, Lee SK, Kim M, Roh J: Altered microRNA regulation in Huntington's disease models. Exp Neurol 2011, 227(1):172-9.

214. Miller BH, Zeier Z, Xi L, Lanz TA, Deng S, Strathmann J, Willoughby D, Kenny PJ, Elsworth JD, Lawrence MS, Roth RH, Edbauer D, Kleiman RJ, Wahlestedt C: MicroRNA-132 dysregulation in schizophrenia has implications for both neurodevelopment and adult brain function. Proc Natl Acad Sci U S A 2012, 109(8):3125-30.

215. Wanet A, Tacheny A, Arnould T, Renard P: miR-212/132 expression and functions: within and beyond the neuronal compartment. Nucleic Acids Res 2012, 40(11):4742-53.

216. Zhang S, Hao J, Xie F, Hu X, Liu C, Tong J, Zhou J, Wu J, Shao C: Downregulation of miR-132 by promoter methylation contributes to pancreatic cancer development. Carcinogenesis 2011, 32(8):1183-9.

217. Calin GA, Liu C, Sevignani C, Ferracin M, Felli N, Dumitru CD, Shimizu M, Cimmino A, Zupo S, Dono M, Dell'Aquila M, L., Alder H, Rassenti L, Kipps TJ, Bullrich F, Negrini M, Croce CM: MicroRNA profiling reveals distinct signatures in B cell chronic lymphocytic leukemias. Proc Natl Acad Sci U S A 2004, 101(32):11755-60.

218. Hansen KF, Karelina K, Sakamoto K, Wayman GA, Impey S, Obrietan K: miRNA-132: a dynamic regulator of cognitive capacity. Brain structure & function 2013, 218(3):817-31.

219. Hansen KF, Sakamoto K, Wayman GA, Impey S, Obrietan K: Transgenic miR132 alters neuronal spine density and impairs novel object recognition memory. PloS one 2010, 5(11):e15497-e15497.

220. Han K, Gennarino VA, Lee Y, Pang K, Hashimoto-Torii K, Choufani S, Raju CS, Oldham MC, Weksberg R, Rakic P, Liu Z, Zoghbi HY: Human-specific regulation of MeCP2 levels in fetal brains by microRNA miR-483-5p. Genes Dev 2013, 27(5):485-90.

221. Zhang K, Jing X, Wang G: MicroRNAs as regulators of drug abuse and immunity. Central-European journal of immunology 2016, 41(4):426-434.

222. Zhang R, Huang M, Cao Z, Qi J, Qiu Z, Chiang L: MeCP2 plays an analgesic role in pain transmission through regulating CREB / miR-132 pathway. Molecular pain 2015, 11:19-19.

223. Sheikh TI, de Paz AM, Akhtar S, Ausió J, Vincent JB: MeCP2_E1 N-terminal modifications affect its degradation rate and are disrupted by the Ala2Val Rett mutation. Hum Mol Genet 2017, 26(21):4132-4141.

224. Ausió J, Martínez dP, Esteller M: MeCP2: the long trip from a chromatin protein to neurological disorders. Trends Mol Med 2014, 20(9):487-98.

225. Fichou Y, Nectoux J, Bahi-Buisson N, Rosas-Vargas H, Girard B, Chelly J, Bienvenu T: The first missense mutation causing Rett syndrome specifically affecting the MeCP2_e1 isoform. Neurogenetics 2009, 10(2):127-33.

226. Quenard A, Yilmaz S, Fontaine H, Bienvenu T, Moncla A, des Portes V, Rivier F, Mathieu M, Raux G, Jonveaux P, Philippe C: Deleterious mutations in exon 1 of MECP2 in Rett syndrome. European journal of medical genetics 49(4):313-22.

227. Zuccato C, Marullo M, Vitali B, Tarditi A, Mariotti C, Valenza M, Lahiri N, Wild EJ, Sassone J, Ciammola A: Brain-derived neurotrophic factor in patients with Huntington's disease. PLoS One 2011, 6(8):e22966.

228. Zou L, Chen Q, Quanbeck Z, Bechtold JE, Kaufman DS: Angiogenic activity mediates bone repair from human pluripotent stem cell-derived osteogenic cells. Scientific reports 2016, 6:22868.

229. Armstrong DD: Neuropathology of Rett syndrome. Ment Retard Dev Disabil Res Rev 2002, 8(2):72-6.

230. Dekaban AS: Changes in brain weights during the span of human life: relation of brain weights to body heights and body weights. Ann Neurol 1978, 4(4):345-56.

231. Remenyi J, Hunter CJ, Cole C, Ando H, Impey S, Monk CE, Martin KJ, Barton GJ, Hutvagner G, Arthur JS: Regulation of the miR-212/132 locus by MSK1 and CREB in response to neurotrophins. Biochem J 2010, 428(2):281-91.

232. Wetmore C, Cao YH, Pettersson RF, Olson L: Brain-derived neurotrophic factor: subcellular compartmentalization and interneuronal transfer as visualized with anti-peptide antibodies. Proc Natl Acad Sci U S A 1991, 88(21):9843-9847.

233. Aliaga EE, Mendoza I, Tapia-Arancibia L: Distinct subcellular localization of BDNF transcripts in cultured hypothalamic neurons and modification by neuronal activation. J Neural Transm 2009, 116(1):23-32.

234. Shi S, Shi Y, Taylor CR: Antigen retrieval immunohistochemistry: review and future prospects in research and diagnosis over two decades. Journal of Histochemistry & Cytochemistry 2011, 59(1):13-32.

235. Petel-Galil Y, Benteer B, Galil YP, Zeev BB, Greenbaum I, Vecsler M, Goldman B, Lohi H, Minassian BA, Gak E: Comprehensive diagnosis of Rett's syndrome relying on genetic, epigenetic and expression evidence of deficiency of the methyl-CpG-binding protein 2 gene: study of a cohort of Israeli patients. J Med Genet 2006, 43(12):e56-e56.

236. Bauernfeind AL, Babbitt CC: The predictive nature of transcript expression levels on protein expression in adult human brain. BMC Genomics 2017, 18(1):1-11.

237. Varlet V, Ryser E, Augsburger M, Palmiere C: Stability of postmortem methemoglobin: Artifactual changes caused by storage conditions. Forensic Sci Int 2018, 283:21-28.

238. Barres BA: The Mystery and Magic of Glia: A Perspective on Their Roles in Health and Disease. Neuron 2008, 60(3):430-440.

239. Maezawa I, Swanberg S, Harvey D, LaSalle JM, Jin L-: Rett Syndrome Astrocytes Are Abnormal and Spread MeCP2 Deficiency through Gap Junctions. Journal of Neuroscience 2009.

240. Braunschweig D, Simcox T, Samaco RC, LaSalle JM: X-chromosome inactivation ratios affect wild-type MeCP2 expression within mosaic Rett syndrome and Mecp2-/+mouse brain. Hum Mol Genet 2004, 13(12):1275-1286.

241. Young JI, Zoghbi HY: X-Chromosome Inactivation Patterns Are Unbalanced and Affect the Phenotypic Outcome in a Mouse Model of Rett Syndrome. Am J Hum Genet 2004, 74(3):511-520.

242. Lioy DT, Garg SK, Monaghan CE, Raber J, Foust KD, Kaspar BK, Hirrlinger PG, Kirchhoff F, Bissonnette JM, Ballas N, Mandel G: A role for glia in the progression of Rett's syndrome. Nature 2011, 475(7357):497-500.

243. Leventhal C, Rafii S, Rafii D, Shahar A, Goldman SA: Endothelial trophic support of neuronal production and recruitment from the adult mammalian subependyma. Mol Cell Neurosci 1999, 13(6):450-464.

244. Kallmann BA, Wagner S, Hummel V, Buttmann M, Bayas A, Tonn JC, Rieckmann P: Characteristic gene expression profile of primary human cerebral endothelial cells. Faseb Journal 2002, 16(2): NIL-NIL.

245. Quirié A, Hervieu M, Garnier P, Demougeot C, Mossiat C, Bertrand N, Martin A, Marie C, Prigent-Tessier A: Comparative Effect of Treadmill Exercise on Mature BDNF Production in Control versus Stroke Rats. PLoS ONE 2012, 7(9):1-10.

246. Navaratna D, Guo SZ, Hayakawa K, Wang X, Gerhardinger C, Lo EH: Decreased cerebrovascular brain-derived neurotrophic factor-mediated neuroprotection in the diabetic brain. Diabetes 2011.

247. Guo S, Kim WJ, Lok J, Lee S-, Besancon E, Luo B-, Stins MF, Wang X, Dedhar S, Lo EH: Neuroprotection via matrix-trophic coupling between cerebral endothelial cells and neurons. Proceedings of the National Academy of Sciences 2008, 105(21):7582-7587.

248. Monnier A, Prigent-Tessier A, Quirié A, Bertrand N, Savary S, Gondcaille C, Garnier P, Demougeot C, Marie C: Brain-derived neurotrophic factor of the cerebral

microvasculature: a forgotten and nitric oxide-dependent contributor of brain-derived neurotrophic factor in the brain. Acta Physiologica 2017, 219(4):790-802.

249. Bagayogo IP, Dreyfus CF: Regulated Release of BDNF by Cortical Oligodendrocytes is Mediated Through Metabotropic Glutamate Receptors and the PLC Pathway. ASN Neuro 2009, 1(1):AN20090006-AN20090006.

250. Jean YY, Lercher LD, Dreyfus CF: Glutamate elicits release of BDNF from basal forebrain astrocytes in a process dependent on metabotropic receptors and the PLC pathway. Neuron Glia Biology 2008, 4(1):35-42.

251. Satriotomo I, Nichols N, Dale E, Emery A, Dahlberg J, Mitchell G: Repetitive acute intermittent hypoxia increases growth/neurotrophic factor expression in non-respiratory motor neurons. Neuroscience 2016, 322:479-488.

252. Hartman W, Helan M, Smelter D, Sathish V, Thompson M, Pabelick CM, Johnson B, Prakash YS: Role of Hypoxia-Induced Brain Derived Neurotrophic Factor in Human Pulmonary Artery Smooth Muscle. PloS one 2015, 10(7):e0129489-e0129489.

253. Pan Y, Sawalha AH: Epigenetic regulation and the pathogenesis of systemic lupus erythematosus. Translational research 2009, 153(1):4-10.